Fomenko Invariants for the Main Integrable Cases of the Rigid Body Motion Equations

A. A. OSHEMKOV

Introduction

One of the best known problems of mechanics is that of a rigid body moving about a fixed point. Such great mathematicians as Euler, Lagrange, Kovalevskaya have investigated it. They have found integrable cases and have devised methods for reducing this problem to quadratures. Many papers in which integrable cases have been found are also devoted to the investigaton of different generalizations of this problem (motion of a gyrostat, motion of a rigid body in fluid, motion of a charged rigid body in a magnetic field, etc.). It is known that in the general case these problems are not integrable (see, for example, [7, 8, 10]). However, the investigation of integrable cases is important in order to understand the general laws of behavior for the solutions of these systems.

The qualitative investigation of the system is of great significance, because expressions of precise solutions are rather complicated and so do not give any visual understanding of how the body moves. One of the main results in the qualitative investigation of integrable Hamiltonian systems is Liouville's theorem, which states that the nonsingular compact level surface of first integrals of a completely integrable Hamiltonian system is the disjoint union of tori filled with almost-periodic (=quasiperiodic) trajectories.

Liouville's theorem shows how the system is arranged on the nonsingular level surfaces of the first integrals (i.e., on Liouville tori). But it says nothing about how the system behaves on the singular level surfaces of the first integrals and about the imbedding of the Liouville tori in the phase space of the system. A theory of "Morse type" for integrable Hamiltonian systems has been constructed by Fomenko [2, 3]. These articles present a complete investigation of how Liouville tori of completely integrable Hamiltonian systems transform in the neighborhood of critical level surfaces of the first integrals. An invariant for integrable Bott nonresonant Hamiltonians is constructed

and a topological classification of the isoenergy surfaces of integrable Hamiltonian systems is given in [4, 5].

The purpose of this paper is to describe this invariant (Fomenko invariant) for the problem of rigid body motion and for some of its generalizations. As a result, we obtain the topological classification of all major cases of integrability for the rigid body motion equations. Also we calculate the exact number of rough topological integrable Hamiltonians. Our results are presented in the Table which shows* the distribution of the values of the topological invariant. Integrable systems of differential equations are roughly topologically equivalent iff their invariants coincide. So we describe all topologically equivalent and all topologically nonequivalent integrable Hamiltonians (for all these famous cases of integrability).

§1. Description of equations for the problem of rigid body motion

A brief description of the different problems of rigid body dynamics is given in this section. It has been shown that all these problems are described by Euler's equations for the Lie algebra $e(3)$ of the transformation group of the 3-dimensional Euclidean space. A detailed description of these problems and the history of this question may be found, for example, in [9, 10].

The Euler-Poisson equations describing the motion of a rigid body about a fixed point in a gravitional field

$$
\begin{cases}
A_1\dot{\omega}_1 = (A_2 - A_3)\omega_2\omega_3 + P(r_3\nu_2 - r_2\nu_3), \\
A_2\dot{\omega}_2 = (A_3 - A_1)\omega_3\omega_1 + P(r_1\nu_3 - r_3\nu_1), \\
A_3\dot{\omega}_3 = (A_1 - A_2)\omega_1\omega_2 + P(r_2\nu_1 - r_1\nu_2), \\
\quad \dot{\nu}_1 = \nu_2\omega_3 - \nu_3\omega_2, \\
\quad \dot{\nu}_2 = \nu_3\omega_1 - \nu_1\omega_3, \\
\quad \dot{\nu}_3 = \nu_1\omega_2 - \nu_2\omega_1,
\end{cases}
\tag{1.1}
$$

are well known in mechanics. The phase variables of this system are the projections ω_1, ω_2, ω_3 of the angular velocity vector on the principal axes of inertia of the body and similar projections ν_1, ν_2, ν_3 of the unit vertical vector. The parameters of system (1.1) are the principal moments of inertia A_1, A_2, A_3 of the body, the weight P of the body, the projections r_1, r_2, r_3 of the vector with the fixed point as the origin, and the body's center of gravity as the terminus on the principal axes of inertia.

Introducing the diagonal matrix $A = \mathrm{diag}(A_1, A_2, A_3)$ and the vectors

$$\omega = (\omega_1, \omega_2, \omega_3), \quad \nu = (\nu_1, \nu_2, \nu_3), \quad r = (r_1, r_2, r_3),$$

one can write the Euler-Poisson equations in vector form:

$$
\begin{cases}
A\dot{\omega} = A\omega \times \omega - Pr \times \nu, \\
\quad \dot{\nu} = \nu \times \omega.
\end{cases}
\tag{1.2}
$$

*Editor's note. The Table and figures appear at the end of the article.

Here $a \times b$ denotes the vector product in $\mathbb{R}^3$.

The vector $A\omega$ in system (1.2) has the meaning of the rigid body's kinetic momentum relative to a fixed point. N. E. Zhukovskiĭ has investigated the problem of rigid body motion when the body has cavities filled with an ideal incompressible fluid performing nonvortex motion. In this case the body's kinetic momentum is $A\omega + \lambda$, where $\lambda = (\lambda_1, \lambda_2, \lambda_3)$ is a constant vector (in the coordinate system connected with the body), which characterizes the cyclic motion of the fluid in the cavities. Kinetic momentum has a similar form in the case when a fly-wheel is fixed in the body and its axis has angles $\alpha_1, \alpha_2, \alpha_3$ with the principal axes of inertia such that $(\cos \alpha_1 : \cos \alpha_2 : \cos \alpha_3) = (\lambda_1 : \lambda_2 : \lambda_3)$. Such a mechanical system is called a gyrostat. The motion of a gyrostat in a gravity field and some other problems of mechanics are described by the following system of equations:

$$\begin{cases} A\dot{\omega} = (A\omega + \lambda) \times \omega - Pr \times \nu, \\ \dot{\nu} = \nu \times \omega. \end{cases} \tag{1.3}$$

When $\lambda = 0$, system (1.3) transforms into system (1.2).

The external field is considered to be uniform (force of gravity) in the classical way of setting the problem of a rigid body's motion about a fixed point. The natural generalization of this problem consists in replacing an ordinary field by a more complicated one. The field of Newton forces is the next more complicated case that actually occurs in mechanics. The equations of motion for this case, found by Euler, have the form:

$$\begin{cases} A\dot{\omega} = A\omega \times \omega - \varepsilon^2 A\nu \times \nu - Pr \times \nu, \\ \dot{\nu} = \nu \times \omega, \end{cases} \tag{1.4}$$

where ε is some constant which depends on the gravitational force and the distance from the center of gravity.

The equations for the motion of a rigid body with fixed point in an arbitrary potential field were found by Lagrange. If this field has an axis of symmetry, then it can be considered vertical and the equations are of the form:

$$\begin{cases} A\dot{\omega} = A\omega \times \omega + \nu \times (\partial U / \partial \nu), \\ \dot{\nu} = \nu \times \omega, \end{cases} \tag{1.5}$$

where $U(\nu_1, \nu_2, \nu_3)$ is the potential function and $(\partial U / \partial \nu)$ denotes the vector with coordinates

$$(\partial U / \partial \nu_1, \partial U / \partial \nu_2, \partial U / \partial \nu_3).$$

The potential function has the form $U = P(r, \nu)$ for the gravity field, and $U = P(r, \nu) + \varepsilon^2 (A\nu, \nu)/2$ for the Newton field. Here (a, b) denotes the Euclidean scalar product in $\mathbb{R}^3$. Having substituted these expressions in (1.5), one obtains systems (1.2) and (1.4).

Having replaced the expressions for the body's kinetic momentum $A\omega$ by the kinetic momentum of a gyrostat $A\omega + \lambda$ in equations (1.5), one obtains

equations which describe the motion of the gyrostat in an axially symmetric field. This mechanical system has also been examined in many papers.

M. P. Kharlamov has obtained equations of the most general form which describe different problems of a rigid body dynamics [6]. Introducing the so-called gyroscopic forces, he has obtained the following system of equations:

$$\begin{cases} A\dot{\omega} = (A\omega + \varkappa) \times \omega + \nu \times (\partial U/\partial \nu), \\ \dot{\nu} = \nu \times \omega, \end{cases} \qquad (1.6)$$

where $\varkappa = (\varkappa_1, \varkappa_2, \varkappa_3)$ is a vector function whose components $\varkappa_i(\nu)$ are coefficients of a closed 2-form on SO(3) (the form of gyroscopic forces). Besides, the vector function $\varkappa(\nu)$ is not arbitrary, but is of the form

$$\varkappa = \lambda + (\Lambda - \operatorname{div}\lambda)\nu, \qquad (1.7)$$

where $\lambda(\nu)$ is an arbitrary vector function, $\Lambda = (\partial\lambda_i/\partial\nu_j)^T$ is the transposed Jacobi matrix,

$$\operatorname{div}\lambda = \frac{\partial\lambda_1}{\partial\nu_1} + \frac{\partial\lambda_2}{\partial\nu_2} + \frac{\partial\lambda_3}{\partial\nu_3}.$$

From the text below the reader will understand why the function $\varkappa(\nu)$ is of the form (1.7).

The systems (1.2)–(1.5) are special cases of system (1.6) if one puts either $\lambda(\nu) \equiv 0$ or $\lambda(\nu) \equiv \operatorname{const}$ in formula (1.7). Therefore, the vector $\lambda(\nu)$ in equations (1.6), (1.7) plays the role of the gyrostatic momentum. If $\lambda(\nu) = \Lambda^T\nu$, where $\Lambda^T\nu$ is a constant matrix proportional to the "electric inertia tensor", then equations (1.6) describe the motion of an electrified rigid body in a magnetic field whose intensity is constant and collinear to the symmetry axis of the force field.

The following integrals always exist for system (1.6):

$$F = (\nu, \nu) = 1 \quad \text{(geometric integral)},$$

$$E = (A\omega, \omega)/2 + U \quad \text{(energy integral)}.$$

If $\varkappa(\nu)$ is of the form (1.7), then the area integral exists:

$$G = (A\omega + \lambda, \nu),$$

where (a, b) denotes the Euclidean scalar product in $\mathbb{R}^3$.

It turns out that the system (1.6), (1.7) may be presented in the form of Euler's equations for the Lie algebra $e(3)$ of the transformation group of three-dimensional Euclidean space. These systems are Hamiltonian on 4-dimensional orbits of the coadjoint representation; for the complete integrability in sense of Liouville it is nessesary, as usual, to indicate one more integral (see, for example, [1, 11]).

S. P. Novikov was the first to note [12] that the equations of motion of a rigid body may be presented in Hamiltonian form. As shown in [6], equations (1.6), (1.7) are also Hamiltonian relative to some symplectic structure on the common level surfaces of the geometric integral and the area integral.

For convenience, we write these equations in the form of Euler's equations $\dot{f} = \{f, H\}$ for the Lie algebra $e(3)$. Let us describe the embedding of the system (1.6), (1.7) in the space $e(3)^*$ conjugate to $e(3)$.

Let S_1, S_2, S_3, R_1, R_2, R_3 be the coordinate functions on $e(3)$. Then the Poisson bracket is of the form:

$$\{S_i, S_j\} = \varepsilon_{ijk} S_k, \qquad \{R_i, R_j\} = 0,$$
$$\{S_i, R_j\} = \{R_i, S_j\} = \varepsilon_{ijk} R_k, \tag{1.8}$$

where $\{i, j, k\} = \{1, 2, 3\}$ and

$$\varepsilon_{ijk} = \begin{cases} \text{sign of the transposition } (i, j, k) \text{ if all the } i, j, k \text{ are different;} \\ 0 \text{ otherwise.} \end{cases}$$

For arbitrary functions f, g on $e(3)$, the bracket is defined by the formula:

$$\{f, g\}(x) = x([df(x), dg(x)]), \tag{1.9}$$

where $x \in e(3)^*$; $[\ ,\ ]$ is the commutator in the Lie algebra $e(3)$; $df(x)$, $dg(x) \in e(3)$ according to the natural identification of $e(3)$ and $e(3)^{**}$ (see [11]). Using the explicit form of the bracket (1.8), we can rewrite formula (1.9) in the following way:

$$\{f, g\} = \sum_{i, j, k} \varepsilon_{ijk} \left(S_k \frac{\partial f}{\partial S_i} \frac{\partial g}{\partial S_j} + R_k \frac{\partial f}{\partial S_i} \frac{\partial g}{\partial R_j} + R_k \frac{\partial f}{\partial R_i} \frac{\partial g}{\partial S_j} \right). \tag{1.10}$$

A Hamiltonian system on the space $e(3)^*$ with bracket (1.8) is, according to definition, of the form:

$$\begin{cases} \dot{S}_i = \{S_i, H\}, \\ \dot{R}_i = \{R_i, H\}, \end{cases} \tag{1.11}$$

where H, which is called the Hamiltonian, is a function on $e(3)^*$. Introducing the 3-dimensional vectors

$$S = (S_1, S_2, S_3), \qquad R = (R_1, R_2, R_3),$$

$$\frac{\partial H}{\partial S} = \left(\frac{\partial H}{\partial S_1}, \frac{\partial H}{\partial S_2}, \frac{\partial H}{\partial S_3} \right),$$

$$\frac{\partial H}{\partial R} = \left(\frac{\partial H}{\partial R_1}, \frac{\partial H}{\partial R_2}, \frac{\partial H}{\partial R_3} \right),$$

the system (1.11) may be rewritten in the form:

$$\begin{cases} \dot{S} = \dfrac{\partial H}{\partial S} \times S + \dfrac{\partial H}{\partial R} \times R, \\ \dot{R} = \dfrac{\partial H}{\partial S} \times R. \end{cases} \tag{1.12}$$

The equations (1.12) are called "Kirchhoff's equations".

It turns out that system (1.12) is equivalent to the system (1.6), (1.7) for a suitable choice of H.

STATEMENT. *The mapping* $\varphi\colon \mathbb{R}^6(\omega, \nu) \to \mathbb{R}^6(S, R)$ *defined by the formulas*

$$S_i = -(A_i\omega_i + \lambda_i),$$
$$R_i = \nu_i \qquad (i = 1, 2, 3) \tag{1.13}$$

determines an isomorphism between the system (1.6), (1.7) *and the system* (1.12) *with Hamiltonian*

$$H = \frac{(S_1 + \lambda_1)^2}{2A_1} + \frac{(S_2 + \lambda_2)^2}{2A_2} + \frac{(S_3 + \lambda_3)^2}{2A_3} + U, \tag{1.14}$$

where the parameters A_1, A_2, A_3 *and the functions* λ_1, λ_2, λ_3, U *are taken from the system* (1.6), (1.7) *but are defined on* $\mathbb{R}^3(R)$ *instead of* $\mathbb{R}^3(\nu)$.

PROOF. In order to prove the statement it suffices to show that the differential $d\varphi$ of the mapping (1.13) takes the vector field determined by system (1.6), (1.7) to the vector field determined by system (1.12), (1.14). In the chosen coordinates the differential $d\varphi$ is defined by the (6×6) matrix

$$d\varphi = \begin{pmatrix} -A & -\Lambda^T \\ 0 & E \end{pmatrix}.$$

One can see that $d\varphi$ is nondegenerate at all points (ω, ν). Thus, it is necessary to show that for any point $P \in \mathbb{R}^6(\omega, \nu)$ we have

$$\begin{pmatrix} -A & -\Lambda^T \\ 0 & E \end{pmatrix}_P \begin{pmatrix} \dot\omega \\ \dot\nu \end{pmatrix}_P = \begin{pmatrix} \dot S \\ \dot R \end{pmatrix}_{\varphi(P)}.$$

1) $\quad \dot S = \left(\dfrac{\partial H}{\partial S}\right) \times S + \left(\dfrac{\partial H}{\partial R}\right) \times R$

$\qquad = (A^{-1}(S + \lambda)) \times S + (\Lambda A^{-1}(S + \lambda)) \times R + \left(\dfrac{\partial U}{\partial R}\right) \times R \,;$

$-A\dot\omega - \Lambda^T\dot\nu = -(A\omega + \lambda + (\Lambda - \operatorname{div}\lambda)\nu) \times \omega - \nu \times \left(\dfrac{\partial U}{\partial \nu}\right) - \Lambda^T(\nu \times \omega)$

$\qquad = \omega \times (A\omega + \lambda)$

$\qquad\quad - ((\Lambda\nu) \times \omega + \Lambda^T(\nu \times \omega) - \operatorname{div}\lambda(\nu \times \omega)) + \left(\dfrac{\partial U}{\partial \nu}\right) \times \nu$

$\qquad = \omega \times (A\omega + \lambda) - (\Lambda\omega) \times \nu + \left(\dfrac{\partial U}{\partial \nu}\right) \times \nu.$

Here the formula

$$(Ca) \times b + a \times (Cb) + C^T(a \times b) = (\operatorname{tr} C)(a \times b)$$

is used; it is valid for any matrix C and any vectors $a, b \in \mathbb{R}^3$. Comparing the obtained equations and taking into consideration (1.13), one gets

$$\dot S(\varphi(P)) = (-A\dot\omega - \Lambda^T\dot\nu)(P).$$

2) Similarly for $\dot{R}$ we obtain:

$$\dot{R} = \left(\frac{\partial H}{\partial S}\right) \times R = (A^{-1}(S + \lambda)) \times R,$$

$$\dot{\nu} = \nu \times \omega.$$

Hence, $\dot{R}(\varphi(P)) = \dot{\nu}(P)$. The statement is proved.

Under the indicated isomorphism φ, the integrals $F = (\nu, \nu)$ and $G = (A\omega + \lambda, \nu)$ become invariants of the Lie algebra $e(3)$:

$$f_1 = R_1^2 + R_2^2 + R_3^2, \qquad f_2 = S_1 R_1 + S_2 R_2 + S_3 R_3 \qquad (1.15)$$

and the energy integral $E = (A\omega, \omega)/2$ becomes the Hamiltonian (1.14).

Let us note that an arbitrary Hamiltonian of the form

$$f = (AS, S) + (W(R), S) + V(R), \qquad (1.16)$$

where A is a constant symmetric matrix, $W(R)$ is an arbitrary vector function, and $V(R)$ is an arbitrary function, may be reduced to the form (1.14) by a linear coordinate transformation that preserves the bracket (1.8) in $e(3)^*$. Thus the Hamiltonian (1.14) is the most general form of quadratic function with respect to the variables S such that the quadratic part does not depend on R. Now the meaning of condition (1.7) about the form of gyroscopic forces becomes clear. It is precisely the condition that system (1.6) is equivalent to the Hamiltonian system on $e(3)^*$ with Hamiltonian of the form (1.16).

Many other problems in mechanics and physics are described by equations (1.12) with Hamiltonian (1.16). Let us enumerate some of them.

1) The motion of a rigid body in an incompressible fluid:

$$H = T(S, R) + L(S, R),$$

where $T(S, R)$ is a quadratic form with respect to variables S and R (kinetic energy of the system body-fluid) and $L(S, R)$ is a linear function that takes into account the fluid circulation in the cavities of the body and its leakage through the holes in the body (if there are no holes and cavities, then $L(S, R) \equiv 0$). Here the variables S and R have the meaning of angular momentum and momentum of the system body-fluid in the mobile coordinate system rigidly connected with the body (see [10]).

2) The spin dynamics in A-phase of the superfluid He:

$$H = \frac{d(S_1^2 + S_2^2 + S_3^2)}{2} + \lambda(S_1 h_1 + S_2 h_2 + S_3 h_3) + U(R),$$

where S is the magnetic momentum, d is the spin part of the order parameter, and (h_1, h_2, h_3) is the external magnetic field vector. For details see [12].

3) The deformation of an elastic rod. The Hamiltonian is quadratic with respect to S and linear in R. In this case equations (1.12) describe the equilibrium condition of the deformed elastic rod. Besides, the partial derivatives

of the variables S and R are taken with respect to the arc coordinate of the rod instead of time. The physical meaning of the variables S, R and of the parameters of the Hamiltonian may be found, for example, in [22].

§2. Integrable cases

The phase space of the Hamiltonian system (1.11) has dimension 6. There are always two functionally independent integrals (1.15) for the system (1.11), since the bracket (1.8) is degenerate. Nonsingular common level surfaces of the integrals (1.15)

$$\{R_1^2 + R_2^2 + R_3^2 = c \; ; \; S_1 R_1 + S_2 R_2 + S_3 R_3 = g\} \subset \mathbb{R}^6 (S, R) \qquad (2.1)$$

are symplectic manifolds homeomorphic to TS^2 (the tangent bundle of a two-dimensional sphere). The restriction of the system (1.11) to some common level surface (2.1) is a Hamiltonian system on a four-dimensional symplectic manifold (see, for example, [1]). For its complete integrability in the sense of Liouville, the existence of two functionally independent integrals on TS is necessary. Since the Hamiltonian is always an integral of the system, the integrability of system (1.11) in the sense of Liouville on some level surface (2.1) means the existence of an integral which is functionally independent of the Hamiltonian on this level surface. Let us note that an additional integral may exist only on certain level surfaces (2.1) but not on all.

Since the linear transformation $S' = S$, $R' = \gamma R$ (where $\gamma = \text{const}$) preserves the bracket (1.8), one may examine systems only on surfaces (2.1) where $c = 1$.

As shown in §1, the system of equations (1.11) with Hamiltonian of the form (1.14) describes various problems of rigid body dynamics and some other problems. Until recently, all these problems were studied separately, and for each problem integrable cases were found (i.e., an additional integral was indicated). The analogy between different mechanical problems (i.e., the existence of coordinate transformations which reduce equations to equivalent form) has been noted by different authors (on this subject see [12, 13, 15]).

The list of the main known integrable cases for equations (1.11) with Hamiltonian of the form (1.14) is given below; we indicate who, when, and for what problem has first found this integrable case. In all cases the Hamiltonian H and the additional integral K are functions of variables S, R. The physical meaning of the restrictions put on the system can be understood by expressing S and R in terms of the original variables of the problem.

1) Euler's case (1750, motion of a rigid body about a fixed point).

$$H = \frac{S_1^2}{2A_1} + \frac{S_2^2}{2A_2} + \frac{S_3^2}{2A_3},$$

$$K = S_1^2 + S_2^2 + S_3^2. \qquad (2.2)$$

2) Lagrange's case (1788, motion of a rigid body about a fixed point).

$$H = \frac{S_1^2}{2A} + \frac{S_2^2}{2A} + \frac{S_3^2}{2B} + aR_3,$$
$$K = S_3. \tag{2.3}$$

3) Kovalevskaya's case (1889, motion of a rigid body about a fixed point).

$$H = \frac{S_1^2}{2A} + \frac{S_2^2}{2A} + \frac{S_3^2}{A} + a_1R_1 + a_2R_2;$$
$$A = A_1 = A_2 = 2A_3;$$
$$K = \left(\frac{S_1^2 - S_2^2}{2A} + a_2R_2 - a_1R_1\right)^2 + \left(\frac{S_1S_2}{A} - a_1R_2 - a_2R_1\right)^2. \tag{2.4}$$

Also see formulas (3.5) and (5.1).

4) Goryachev-Chaplygin case (1899, motion of a rigid body about a fixed point).

$$H = \frac{S_1^2}{2A} + \frac{S_2^2}{2A} + \frac{2S_3^2}{A} + a_1R_1 + a_2R_2,$$
$$A = A_1 = A_2 = 4A_3,$$
$$K = S_3(S_1^2 + S_2^2) - AR_3(a_1S_1 + a_2S_2). \tag{2.5}$$

Here $\{H, K\} = (S_1R_1 + S_2R_2 + S_3R_3)(a_2S_1 - a_1S_2)$. Therefore, the system is integrable only on the surface $\{R_1^2 + R_2^2 + R_3^2 = 1; \ S_1R_1 + S_2R_2 + S_3R_3 = 0\}$.

5) Zhukovskii's case (1885, motion of a gyrostat in a gravitational field).

$$H = \frac{(S_1 + \lambda_1)^2}{2A_1} + \frac{(S_2 + \lambda_2)^2}{2A_2} + \frac{(S_3 + \lambda_3)^2}{2A_3},$$
$$K = S_1^2 + S_2^2 + S_3^2. \tag{2.6}$$

6) Sretenskii's case (1963, motion of a gyrostat in a gravitational field).

$$H = \frac{S_1^2}{2A} + \frac{S_2^2}{2A} + \frac{2(S_3 + \lambda)^2}{A} + a_1R_1 + a_2R_2,$$
$$K = (S_3 + 2\lambda)(S_1^2 + S_2^2) - AR_3(a_1S_1 + a_2S_2). \tag{2.7}$$

Here, as in the Goryachev-Chaplygin case, the system is integrable only on the surface $\{R_1^2 + R_2^2 + R_3^2 = 1; \ S_1R_1 + S_2R_2 + S_3R_3 = 0\}$.

7) Clebsch's case (1871, motion of a rigid body in a fluid).

$$H = \frac{S_1^2}{2A_1} + \frac{S_2^2}{2A_2} + \frac{S_3^2}{2A_3} + \frac{\varepsilon}{2}(A_1R_1^2 + A_2R_2^2 + A_3R_3^2),$$
$$K = S_1^2 + S_2^2 + S_3^2 - \varepsilon(A_2A_3R_1^2 + A_3A_1R_2^2 + A_1A_2R_3^2). \tag{2.8}$$

Also see formulas (3.8), (3.9), and (7.1).

8) Steklov-Lyapunov case (1893, motion of a rigid body in a fluid).

$$H = \frac{S_1^2}{2A_1} + \frac{S_2^2}{2A_2} + \frac{S_3^2}{2A_3} + \varepsilon(A_1 S_1 R_1 + A_2 S_2 R_2 + A_3 S_3 R_3)$$

$$+ \frac{\varepsilon^2}{2}(A_1(A_2^2 + A_3^2)R_1^2 + A_2(A_3^2 + A_1^2)R_2^2 + A_3(A_1^2 + A_2^2)R_3^2),$$

$$K = (S_1^2 + S_2^2 + S_3^2) - 2\varepsilon(A_2 A_3 S_1 R_1 + A_3 A_1 S_2 R_2 + A_1 A_2 S_3 R_3)$$

$$+ \varepsilon^2(A_1^2(A_2 - A_3)^2 R_1^2 + A_2^2(A_3 - A_1)^2 R_2^2 + A_3^2(A_1 - A_2)^2 R_3^2). \quad (2.9)$$

Also see formula (8.2).

Only the main cases of integrability of equations (1.12) known today are given in this list. A complete list of Hamiltonians for which an additional integral can be indicated does not yet exist. However, under some restrictions on the form of the Hamiltonian and of the additional integral, one can state that there exist no more integrable cases. On this subject see [8, 10, 14, 16].

Fomenko's invariants for the integrable cases enumerated above will be described in this work. A detailed description of Fomenko's invariant can be found in [4, 5].

As has already been noted, the system of equations (1.12) is Hamiltonian on the symplectic manifolds

$$\{f_1 = R_1^2 + R_2^2 + R_3^2 = 1; \ f_2 = S_1 R_1 + S_2 R_2 + S_3 R_3 = g\}.$$

The surface

$$Q_h = \{f_1 = 1; \ f_2 = g; \ H = h\} \subset \mathbb{R}^6(S, R) \qquad (2.10)$$

is called the *isoenergy surface* of the given Hamiltonian system with Hamiltonian H. An additional integral K is called *Bott* on Q_h, if the set of critical points of the function $\tilde{K} = K|_{Q_h}$ is the union of smooth nondegenerate critical submanifolds. The additional integral turns out to be nearly always Bott for the known integrable cases.

THEOREM. *For each Hamiltonian system* (1.11) *on the symplectic manifold* $TS^2 = \{f_1 = 1; f_2 = g\}$ *with Hamiltonian* H *in the enumerated integrable cases* (2.2)–(2.9), *the additional integral* K *is Bott on all nonsingular surfaces* $Q_h = \{f_1 = 1; f_2 = g; H = h\}$ *with the exception, perhaps, of a finite number.*

The proof of this theorem will be obtained by constructing the invariant for each integrable case. Besides, characteristics of surfaces Q_h on which the additional integral K is not Bott will become clear.

Fomenko's invariant is a graph with vertices of special form (letters-atoms linked by segments in the word-molecule, following the terminology of [5]). A graph (word-molecule) is assigned to each nonsingular surface Q_h with Bott integral $\tilde{K} = K|_{Q_h}$. Nonsingular level surfaces of the function $\tilde{K}$ are 2-dimensional Liouville tori. They are transformed in some way at critical

values of the function $\widetilde{K}$. The word-molecule which corresponds to the isoenergy surface Q_h encodes information about how Q_h is stratified into Liouville tori and how these tori bifurcate at critical values of the function $\widetilde{K}$.

All the Fomenko invariants appearing in systems investigated in this paper are enumerated in the Table (see the Supplement). The isoenergy surface (2.10) is determined by values g, h and the parameters of the Hamiltonian. Therefore, the description of invariants for different Q_h will be given in the following form: curves which separate domains with different Fomenko invariants as well as curves which separate domains with different topological type of Q_h will be shown on the plane $\mathbb{R}^2(g, h)$. The union of all these curves divide the (g, h)-plane so that for all points of one domain the isoenergy surfaces $Q_h = \{f_1 = 1 ; f_2 = g ; H = h\}$ have one and the same topological type and identical Fomenko invariants. Besides, the type of invariant is designated in figures by number from the Table (see the Supplement).

For some integrable cases, the separating curves may have qualitative differences for different values of the Hamiltonian's parameters. In this case several figures with separating curves corresponding to different ranges of the Hamiltonian's parameters are given. In the integrable cases when only a special integral exists (in Sretenskiĭ's case, for example, only when $g = 0$), the separating curves are shown on the plane $\mathbb{R}^2(\lambda, h)$, where λ is a certain parameter of the Hamiltonian.

Let us note that the figures with separating curves, presented in this paper, make it easy to understand how the Fomenko invariant changes when h changes (for fixed g or λ). One must construct the line $g = \text{const}$ (or $\lambda = \text{const}$) on the plane with separating curves and see what domains it traverses.

§3. Topological type of isoenergy surfaces

Before constructing Fomenko's invariants for integrable Hamiltonian systems, let us describe (following the outline given in §2) the curve separating domains with different topological type of isoenergy surfaces Q_h. These curves are in no way related to the integrability of the system and so can be constructed, generally speaking, for arbitrary Hamiltonians. This method of investigation of mechanical systems was first time proposed by Smale in [17]. It consists in the following.

The isoenergy surface Q_h is the common level surface of the function $f_2 = S_1 R_1 + S_2 R_2 + S_3 R_3$ and the Hamiltonian H defined on the set

$$S^2 \times \mathbb{R}^3 = \{f_1 = R_1^2 + R_2^2 + R_3^2 = 1\} \subset \mathbb{R}^6(S, R). \qquad (3.1)$$

Let us examine the mapping

$$F = f_2 \times H : S^2 \times \mathbb{R}^3 \to \mathbb{R}^2 \qquad (3.2)$$

determined by the formula

$$F(P) = (f_2(P), H(P)) \in \mathbb{R}^2(g, h),$$

where $P \in S^2 \times \mathbb{R}^3$. The image of the set of critical points of the mapping F is a certain subset Σ in $\mathbb{R}^2(g, h)$ called the bifurcation diagram. The preimage of an arbitrary point $(g, h) \notin \Sigma$ is a nonsingular surface

$$Q_h = \{f_1 = 1 \; ; \; f_2 = g \; ; \; H = h\}.$$

Besides, for all points (g, h) from one of the connected domains into which Σ divides $\mathbb{R}^2(g, h)$, the topological type of Q_h is the same. What is more, sometimes one can determine how the topological type of Q_h changes while passing through Σ if the indices of critical points which belong to the preimage $F^{-1}(y)$ for all $y \in \Sigma$ are known (see [18]).

In [19, 20, 21] the topological type of the surfaces Q_h was determined and the separating curves on the plane (g, h) were constructed for the motion of a rigid body about a fixed point in a gravitational field and a linear force field. A rather general case was investigated in these works, but we are interested only in those Hamiltonians for which an additional integral K exists. These Hamiltonians have a certain symmetry, and the separating curves for them are of simpler form than in the general case. Bifurcation diagrams and the topological type of Q_h will be described for the following Hamiltonians:

$$H = \frac{S_1^2}{2A_1} + \frac{S_2^2}{2A_2} + \frac{S_3^2}{2A_3} \quad \text{(Euler's case);} \tag{3.3}$$

$$H = \frac{S_1^2 + S_2^2 + \frac{S_3^2}{\beta}}{2} + R_3 \quad \text{(Lagrange's case);} \tag{3.4}$$

$$H = \frac{S_1^2 + S_2^2 + \beta S_3^2}{2} + R_1 \quad \text{(Kovalevskaya's case);} \tag{3.5}$$

$$H = \frac{(S_1 + \lambda_1)^2}{2A_1} + \frac{(S_2 + \lambda_2)^2}{2A_2} + \frac{(S_3 + \lambda_3)^2}{2A_3} \quad \text{(Zhukovskii's case);} \tag{3.6}$$

$$H = \frac{S_1^2 + S_2^2 + 4(S_3 + \lambda)^2}{2} + R_1 \quad \text{(Sretenskii's case);} \tag{3.7}$$

$$H = \frac{S_1^2}{2A_1} + \frac{S_2^2}{2A_2} + \frac{S_3^2}{2A_3} + \frac{(A_1 R_1^2 + A_2 R_2^2 + A_3 R_3^2)}{2} \quad \text{(Clebsch's case);} \tag{3.8}$$

$$H = \frac{S_1^2}{2A_1} + \frac{S_2^2}{2A_2} + \frac{S_3^2}{2A_3} - \frac{(A_1 R_1^2 + A_2 R_2^2 + A_3 R_3^2)}{2} \quad \text{(Clebsch's case).} \tag{3.9}$$

The critical points of the function defined on the common level surfaces of other functions must be found, and the indices of these critical points must be calculated. Let us describe one of the possible methods of calculation to be used further.

Let the functions $h_0, h_1, \ldots, h_k$ be given in $\mathbb{R}^n$, and let

$$M^{n-k} = \{h_1 = p_1, \ldots, h_k = p_k\}$$

be their common nonsingular level surface. Then the vectors

$$\operatorname{grad} h_1, \ldots, \operatorname{grad} h_k$$

are linearly independent at every point $x \in M^{n-k} \subset \mathbb{R}^n$. The point $x_0 \in M^{n-k}$ is a critical point for the function $\tilde{h}_0 = h_0|_M$ iff there is a collection of coefficients $(\lambda_1, \ldots, \lambda_k)$ such that

$$\operatorname{grad} h_0(x_0) = \sum_{i=1}^{k} \lambda_i \operatorname{grad} h_i(x_0). \tag{3.10}$$

Let us examine the matrix

$$G = G_0 - \sum_{i=1}^{k} \lambda_i G_i, \tag{3.11}$$

where G_i is the Hessian of the function h_i at the point $x_0 (i = 0, 1, \ldots, k)$ and the λ_i are taken from (3.10). The Hessian at a critical point is the symmetric matrix whose elements are the function's second partial derivatives. It transforms according to the tensor law under coordinate transformation and correctly determines a certain quadratic form on tangent vectors at the critical point. The number of negative eigenvalues of this form is called the index of the critical point, and the number of zero eigenvalues is the degeneracy index of the critical point [18]. It is easy to check that matrix (3.11) does also correctly determine a quadratic form in $\mathbb{R}^n$.

LEMMA. *Let condition* (3.10) *be valid for the point* $x_0 \in M^{n-k} \subset \mathbb{R}^n$. *Then the quadratic form determined by the Hessian of the function* $\tilde{h}_0 = h_0|_M$ *at the point* x_0 *is the restriction to the tangent space* $T_{x_0} M^{n-k}$ *of the form in* $\mathbb{R}^n$ *determined by the matrix* (3.11).

PROOF. Let $\gamma(t) \subset M^{n-k}$ be an arbitrary smooth curve such that $\gamma(0) = x_0$. Then the value of the quadratic form determined by the Hessian of the

function $\widetilde{h}_0 = h_0|_M$ on the vector $a = \dot{\gamma}(0) \in T_{x_0} M^{n-k}$ is equal to

$$
\begin{aligned}
\widetilde{G}_0(a,a) &= d^2/dt^2|_{t=0}(\widetilde{h}_0(\gamma(t))) \\
&= d^2/dt^2|_{t=0}(h_0(\gamma(t))) \\
&= G_0(a,a) + \langle \operatorname{grad} h_0(x_0), \ddot{\gamma}(0) \rangle \\
&= G_0(a,a) + \sum_{i=1}^{k} \lambda_i \langle \operatorname{grad} h_i(x_0), \ddot{\gamma}(0) \rangle \\
&= G_0(a,a) + \sum_{i=1}^{k} \lambda_i (d^2/dt^2|_{t=0}(h_i(\gamma(t))) - G_i(a,a)) \\
&= G(a,a),
\end{aligned}
$$

because $h_i(\gamma(t)) \equiv p_i$. Here by $G_i(a,a)$ we denote the value of the quadratic form with matrix G_i on the vector a and by $\langle \operatorname{grad} h_i(x_0), \ddot{\gamma}(0) \rangle$ the pairing in $\mathbb{R}^n$ of the vector $\ddot{\gamma}(0)$ and covector $\operatorname{grad} h_i(x_0)$ (i.e., the value of the covector on the vector from $\mathbb{R}^n$). The lemma is proved.

The given method of calculation is convenient, because one need not introduce local coordinates on the common level surfaces of the functions in order to find the indices of critical points. It is sufficient to choose some basis in the tangent space of this surface and calculate the value of the form (3.11) on the basis vectors.

Let us describe the topological type of Q_h for the Hamiltonians (3.3)–(3.9).

The bifurcation diagram for Hamiltonian (3.3) is of simple form (see Figure 1). It consists of three parabolas $h = g^2/2A_i (i = 1, 2, 3)$, which divide the plane into six domains. For each domain the topological type of $Q_h = \{f_1 = 1; f_2 = g; H = h\}$ for all points of the domain is given. The symbol $\varnothing$ means that for every point (g, h) from this domain, $(f_2 \times H)^{-1}(g, h) = \varnothing$. The bifurcation diagram in Figure 1 is drawn for the case $0 < A_1 < A_2 < A_3$. If $A_1 \leqslant 0 < A_2 < A_3$, then there are noncompact surfaces among the Q_h and we shall not examine this case. If $0 < A_1 = A_2 < A_3$, then the two upper parabolas merge into one. When $0 < A_1 < A_2 = A_3$, then the two lower parabolas merge. When $A_1 = A_2 = A_3$, the Hamiltonian (3.3) becomes degenerate, i.e., there exist several functionally independent integrals, for example, S_1 and S_2. Such cases will not be examined.

For the Hamiltonian (3.4), the bifurcation diagrams qualitatively differ in the following cases: (a) $0 < \beta < 1$; (b) $\beta = 1$; (c) $1 < \beta \leqslant 4/3$; (d) $\beta > 4/3$. They are shown in Figure 2. All diagrams are symmetric in the line $g = 0$ and consist of two parabolas

$$
h = \frac{g^2}{2\beta} \pm 1 \tag{3.12}
$$

and the curve (except for the case (b)) given in the following parametric form:

$$g = t + \frac{1}{(\beta - 1)t^3}, \qquad h = \frac{t^2}{2} + \frac{3}{2(\beta - 1)t^2}, \qquad t^2 \geqslant \frac{1}{|\beta - 1|}. \qquad (3.13)$$

The curve (3.13) is tangent to the parabola at the points with coordinates

$$\left(\frac{\pm\beta}{\sqrt{|1 - \beta|}}, \ \frac{3\beta - 2}{2|1 - \beta|} \right) \in \mathbb{R}^2(g, h).$$

In case (d), the curve (3.13) has two cusps with coordinates

$$\left(\pm\frac{4}{3}\sqrt[4]{\frac{3}{\beta - 1}}, \ \sqrt{\frac{3}{\beta - 1}} \right).$$

For each domain into which the plane $\mathbb{R}^2(g, h)$ is divided by the bifurcation diagram, the topological type of Q_h is given in the figure.

The bifurcation diagrams for the Hamiltonian (3.5) have the same form as for the Hamiltonian (3.4) (they are obtained by contraction with coefficient $\sqrt{\beta}$ along the axis g) but there is another topological type of surfaces Q_h in this case. We are interested in this Hamiltonian in connection with Kovalevskaya's case, so the bifurcation diagram in Figure 3 is given only for $\beta > 4/3$. When $\beta = 2$, the coordinates of points where the curve is tangent to the parabola are $(\pm\sqrt{2}, 2)$; the coordinates of the curve's cusps are $(\pm(4/3)^{3/4}, \sqrt{3})$; the coordinates of points where the curve transversally crosses the parabola are $(\pm 2\sqrt{\sqrt{2} - 1}, 2\sqrt{2} - 1)$. The topological type of Q_h is given in Figure 3. The surface denoted by K^3 may be described in the following way: it is a fiber bundle with base the sphere S^2 with three "holes" (i.e., three open disjoint two-dimensional disks removed from it), and whose fiber is the circle S^1, but the fiber is contracted to a point over every boundary point of the base. The surface K^3 may be also obtained by removing three submanifolds $D^2 \times S^1$ (from $S^1 \times S^2$) whose axes are fibers in the product $S^1 \times S^2$, and gluing them back in $S^1 \times S^2$ via the diffeomorphism that exchanges base circles on boundary tori. One can also show that K^3 is homeomorphic to the connected sum $(S^1 \times S^2) \# (S^1 \times S^2)$.

The described bifurcation diagrams for Hamiltonians (3.3)–(3.5) are well known (see, for example, [19]).

Now let us construct the bifurcation diagram for the Hamiltonian (3.6). Let $0 < A_1 < A_2 < A_3$ and $\lambda_1, \lambda_2, \lambda_3$ differ from zero. Critical points of the mapping $f_2 \times H \colon S^2 \times \mathbb{R}^3 \to \mathbb{R}^2$ are determined from the condition

$$\begin{cases} \operatorname{grad} H = \mu_1 \operatorname{grad} f_1 + \mu_2 \operatorname{grad} f_2, \\ f_1 = 1, \end{cases} \qquad (3.14)$$

where f_1, f_2 are the functions (1.15) on $\mathbb{R}^6(S, R)$ and μ_1, μ_2 are certain numbers. Introducing the vectors

$$S = (S_1, S_2, S_3), \qquad R = (R_1, R_2, R_3), \qquad \lambda = (\lambda_1, \lambda_2, \lambda_3),$$

and the matrix $A = \text{diag}(A_1, A_2, A_3)$, let us rewrite the system (3.14) in vector form:

$$\begin{cases} A^{-1}(S + \lambda) = \mu_2 R, \\ 2\mu_1 R + \mu_2 S = 0, \\ (R, R) = 1. \end{cases} \qquad (3.15)$$

If $\mu_2 = 0$, then $\mu_1 = 0$ (because $R \neq 0$). One can obtain the following solution of system (3.15):

$$S = -\lambda, \qquad (R, R) = 1, \qquad \mu_1 = \mu_2 = 0. \qquad (3.16)$$

The set (3.16) is a two-dimensional sphere in $\mathbb{R}^6(S, R)$. The Hamiltonian H vanishes and the function f_2 is equal to $g = -(\lambda, R)$ at the points of this sphere. Therefore, the image of the set (3.16) under the mapping $f_2 \times H$ is the segment $\{h = 0, |g| \leqslant \sqrt{(\lambda, \lambda)}\}$ on the coordinate axis $h = 0$ of the plane $\mathbb{R}^2(g, h)$. The preimage of every interior point of this segment is a circle, which is minimal for the function

$$\widetilde{H} = H\big|_{\{f_1 = 1, f_2 = g\}}, \quad \text{where } |g| \leqslant \sqrt{(\lambda, \lambda)}.$$

Now let $\mu_2 \neq 0$ in system (3.15). Then

$$S = -(2\mu_1/\mu_2)R. \qquad (3.18)$$

This implies

$$\begin{aligned} A^{-1}(\lambda - (2\mu_1/\mu_2)R) &= \mu_2 R, \\ (\mu_2 A + (2\mu_1/\mu_2)E)R &= \lambda, \end{aligned} \qquad (3.19)$$

where E is the 3×3 unit matrix. From (3.18) one also obtains

$$g = (S, R) = -(2\mu_1/\mu_2)(R, R) = -(2\mu_1/\mu_2).$$

Substituting $(-2\mu_1/\mu_2)$ for g in (3.19) and (3.18), one obtains a solution of system (3.15) in the following form:

$$S_i = \frac{\lambda_i g}{A_i t - g}, \qquad R_i = \frac{\lambda_i}{A_i t - g} \qquad (i = 1, 2, 3),$$
$$\mu_1 = -gt/2, \qquad \mu_2 = t, \qquad (3.20)$$

where t is some parameter and $g(t)$ is given by

$$\frac{\lambda_1^2}{(A_1 t - g)^2} + \frac{\lambda_2^2}{(A_2 t - g)^2} + \frac{\lambda_3^2}{(A_3 t - g)^2} = 1. \qquad (3.21)$$

At the points (3.20), the Hamiltonian H has values

$$h = \frac{t^2}{2}\left(\frac{\lambda_1^2 A_1}{(A_1 t - g)^2} + \frac{\lambda_2^2 A_2}{(A_2 t - g)^2} + \frac{\lambda_3^2 A_3}{(A_3 t - g)^2}\right). \qquad (3.22)$$

Thus, for any values of t and g which satisfy condition (3.21) there is only one point (3.20) at which the gradients of the functions f_2 and H are

dependent. The image of this point under the mapping $f_2 \times H$ is the point with coordinates $(g, h) \in \mathbb{R}^2$, where h is determined by formula (3.22). So it is neccessary to construct the curve $(g(t), h(t))$ implicitely determined by formulas (3.21), (3.22) on the plane $\mathbb{R}^2(g, h)$.

Let us note that for these functions the following relation is valid:

$$\frac{dh}{dt} = t\frac{dg}{dt}. \qquad (3.23)$$

This can be directly checked by differentiating equalities (3.21) and (3.22) with respect to t. As a matter of fact, it follows from the fact that parameter t is equal to the coefficient μ_2 in the presentation of $\operatorname{grad} H$ in the form of a linear combination of $\operatorname{grad} f_1$ and $\operatorname{grad} f_2$ (3.14). Actually, the set of points (3.20) can be presented as the curve $\gamma(t) \subset \mathbb{R}^6(S, R)$ at all points of which formula (3.14) with some $\mu_1(t)$, $\mu_2(t)$ is valid. Then

$$\begin{aligned}
\frac{dh}{dt} &= \frac{d}{dt}(H(\gamma(t))) = \langle \operatorname{grad} H(\gamma(t)), \dot{\gamma}(t)\rangle \\
&= \langle \mu_1(t)\operatorname{grad} f_1(\gamma(t)) + \mu_2(t)\operatorname{grad} f_2(\gamma(t)), \dot{\gamma}(t)\rangle \\
&= \mu_1(t)\frac{d}{dt}(f_1(\gamma(t))) + \mu_2(t)\frac{d}{dt}(f_2(\gamma(t))) = \mu_2(t)\frac{dg}{dt},
\end{aligned}$$

because $f_1(\gamma(t)) \equiv 1$. By $\langle\,,\,\rangle$ we denote the ordinary pairing of the covector $\operatorname{grad} f$ and the vector $\dot{\gamma}$ in $\mathbb{R}^6(S, R)$.

In this case $\mu_2(t) = t$ and so (3.23) is valid. A similar relation is valid in an even more general case. Without going into details, we note that in this paper, the following relation is always valid for the bifurcation curve given in parametric form with some parameter p:

$$\frac{dh}{dp} = \mu_2(p)\frac{dg}{dp}, \qquad (3.24)$$

where $\mu_2(p)$ is the coefficient of $\operatorname{grad} f_2$ in the decomposition of $\operatorname{grad} H$ into $\operatorname{grad} f_1$ and $\operatorname{grad} f_2$. This relation very often simplifies the investigation of the bifurcation curve.

From the above it follows that it is sufficient to construct the curve (3.21) in the plane $\mathbb{R}^2(t, g)$. After this, by using (3.23), the bifurcation diagram on the plane $\mathbb{R}^2(g, h)$ can be easily obtained. Introducing polar coordinates $t = r\cos\varphi$, $g = r\sin\varphi$, from (3.21) one obtains a relation between r and φ:

$$r = \sqrt{\frac{\lambda_1^2}{(A_1^2 + 1)\sin^2(\varphi - \varphi_1)} + \frac{\lambda_2^2}{(A_2^2 + 1)\sin^2(\varphi - \varphi_2)} + \frac{\lambda_3^2}{(A_3^2 + 1)\sin^2(\varphi - \varphi_3)}},$$

where $\tan\varphi_i = A_i$ $(i = 1, 2, 3)$. The curve determined by this relation is shown in Figure 4. It is symmetric in the origin and has asymptotes $g = A_i t \pm \lambda_i$, the dotted lines in Figure 4.

Formula (3.22) defines a mapping of this curve into the plane $\mathbb{R}^2(g, h)$. Its image, combined with the segment (3.17), is the bifurcation diagram of the examined mapping $f_2 \times H$. Taking into consideration (3.23), it becomes clear that cusps of the bifurcation curve correspond to points of local minimum and maximum of the function $g(t)$ (see Figure 4) and points of inflection of the bifurcation curve correspond to points of local minimum and maximum of the inverse function $t(g)$. If the point that moves along the curve shown in Figure 4 asymptotically approaches (as $t \to \infty$) the line $g = A_i t \pm \lambda_i$, then the image of this point on the bifurcation curve asymptotically approaches the parabola

$$ h = \frac{(g \mp \lambda_i)^2}{2A_i} + \frac{1}{2}\left(\frac{\lambda_j^2 A_j}{(A_j - A_i)^2} + \frac{\lambda_k^2 A_k}{(A_k - A_i)^2} \right), \qquad (3.25) $$

where $\{i, j, k\} = \{1, 2, 3\}$.

Summarizing all the above, one obtains the bifurcation diagram of the mapping $f_2 \times H$ for the Hamiltonian (3.6) shown in Figure 5. The diagram is symmetric in the line $g = 0$. Points where the segment is tangent to the curve have coordinates

$$ \left(\pm\sqrt{\lambda_1^2 + \lambda_2^2 + \lambda_3^2}, 0 \right) \in \mathbb{R}^2(g, h) $$

and the point where the two branches of the curve intersect has coordinates

$$ \left(0, \frac{\lambda_1^2}{2A_1} + \frac{\lambda_2^2}{2A_2} + \frac{\lambda_3^2}{2A_3} \right) \in R^2(g, h). $$

The topological type of Q_h in each domain may be defined by examining the projection of Q_h on the Poisson sphere, using the method of [17] (see also [20, 21]). The same thing may be done by another method. Let us change λ_i to $\lambda_i' = \alpha\lambda_i$, where α tends to zero. At the limit the bifurcation diagram shown in Figure 5 transforms into the bifurcation diagram for the Hamiltonian (3.3) shown in Figure 1. Further, the unbounded domains in Figure 5 for which the topological type of Q_h is $2S^3$, $S^1 \times S^2$, or $\mathbb{R}P^3$ become the corresponding domains in Figure 1. For the "triangle" near the origin (in Figure 5), the topological type of Q_h is $S^1 \times S^2$ and for its boundary domains it is S^3. This follows from Morse theory [18], because in the preimage of each point of the segment there is only one minimal circle of the function $\widetilde{H} = H|_{\{f_1 = 1, f_2 = g\}}$ and in the preimage of other boundary points of the image of TS^2 there is only one critical point.

Now let us proceed to the Hamiltonian (3.7). This is the Hamiltonian of Sretenskiĭ's case, and an additional integral exists only on the surface

$$ \{f_1 = 1, f_2 = 0\} \subset \mathbb{R}^6(S, R). $$

Therefore, one need not examine the mapping $f_2 \times H$ in order to describe Fomenko's invariants for this integrable case. The topological type of Q_h and

Fomenko's invariants in this case depend only on the value of the parameter λ and the value of h determining the isoenergy surface Q_h for the Hamiltonian (3.7). So, for Sretenskii's case we shall construct separating curves on the plane $\mathbb{R}^2(\lambda, h)$ and determine the topological type of Q_h in each domain.

The topological type of the surface $Q_h = \{f_1 = 1, f_2 = g, H = h\}$, where H is a Hamiltonian of the form (1.14), may be examined using the projection on the Poisson sphere

$$\pi : TS^2 \to S^2, \tag{3.26}$$

where $TS^2 = \{f_1 = 1, f_2 = g\} \subset \mathbb{R}^6(S, R)$ and $S^2 = \{f_1 = 1\} \subset \mathbb{R}^3(R)$. This method has been developed in [17] for certain natural mechanical systems and has been carried over in [6] to the case of systems with gyroscopic forces. Under the projection (3.26), the surface Q_h transforms into a domain on the Poisson sphere. It can be shown that this domain is distinguished by the condition

$$\varphi_g(R) \leqslant h, \tag{3.27}$$

where $\varphi_g(R)$ is the function on the Poisson sphere determined by the formula

$$\varphi_g(R) = \frac{(g + \lambda_1 R_1 + \lambda_2 R_2 + \lambda_3 R_3)^2}{2(A_1 R_1^2 + A_2 R_2^2 + A_3 R_3^2)} + U(R). \tag{3.28}$$

The function (3.28) is the analog of the reduced potential examined in [17].

The topological type of Q_h is completely determined by the form of domain (3.27). If the domain (3.27) is the entire sphere, then Q_h is homeomorphic to $\mathbb{R}P^3$. If the domain (3.27) consists of several connected components, each of which is either a two-dimensional disk D^2 or a two-dimensional disk D^2 with m holes (i.e., m disjoint open disks removed from it), then the connected component of Q_h homeomorphic to S^3 corresponds to each disk D^2 and the connected sum of m copies of $S^1 \times S^2$ corresponds to each disk D^2 with m holes. For example, the surface K^3 described in the study of the Hamiltonian (3.5) is obtained when $m = 2$.

For the Hamiltonian (3.7), the function (3.28) is of the form:

$$\varphi_0(R) = \frac{2\lambda^2 R_3^2}{4 - 3R_3^2} + R_1. \tag{3.29}$$

In order to determine the type of domain for

$$\varphi_0(R) \leqslant h, \tag{3.30}$$

let us find the critical points of the function (3.29) defined on the sphere

$$\{R_1^2 + R_2^2 + R_3^2 = 1\} \subset \mathbb{R}^3(R).$$

They are determined by the system of equations

$$\begin{cases} \dfrac{\partial \varphi_0}{\partial R_i} = 2\mu R_i & (i = 1, 2, 3), \\ R_1^2 + R_2^2 + R_3^2 = 1. \end{cases}$$

Its solutions are two critical points which exist for any value of λ:

$$R_1 = \pm 1, \qquad R_2 = R_3 = 0, \qquad \mu = \pm 1/2, \qquad (3.31)$$

and also two critical points which depend on the value of λ:

$$R_1 = 1/2\xi, \qquad R_2 = 0, \qquad R_3 = \pm\sqrt{1 - 1/4\xi^2}, \qquad \mu = \xi, \qquad (3.32)$$

$$\text{where} \qquad \lambda^2 = (4\xi^2 + 3)^2/128\xi^3, \qquad \xi \geqslant 1/2.$$

The value of the function (3.29) at the points (3.31) is equal to ± 1. Since λ is arbitrary, one obtains two lines $h = \pm 1$ on the plane $\mathbb{R}^2(\lambda, h)$ which separate domains with different topological type of Q_h. At points (3.32), the value of the function (3.29) is equal to $(16\xi^4 + 40\xi^2 - 3)/64\xi^3$. Thus, these points determine in parametric form the separating curve on the plane $\mathbb{R}^2(\lambda, h)$:

$$h = \frac{16\xi^4 + 40\xi^2 - 3}{64\xi^3}, \qquad \lambda^2 = \frac{(4\xi^2 + 3)^2}{128\xi^3}, \qquad \xi \geqslant \frac{1}{2}. \qquad (3.33)$$

Putting together the lines $h = \pm 1$ and the curve (3.33) we obtain the diagram on the plane $\mathbb{R}^2(\lambda, h)$ shown in Figure 6. It is symmetric in the line $\lambda = 0$. The coordinates of the cusps of the curve (3.33) are:

$$(\pm 1/\sqrt{3}, 7/9) \in \mathbb{R}^2(\lambda, h) ;$$

the coordinates of points where the line $h = 1$ is tangent to the curve are: $(\pm 1, 1) \in \mathbb{R}^2(\lambda, h)$. The curve (3.33) asymptotically approaches the parabola $h = \lambda^2$.

One critical point of the function (3.29) corresponds to each point of the lines $h = \pm 1$, and two critical points correspond to each point of the curve. Having calculated their indices, one can see that the index is equal to 0 for the line $h = -1$, and it is equal to 2 for the segment of the line $h = 1$ between the points where this line is tangent to the curve, and to 1 for the remaining part of the line; for the curve, the index is equal to 1 for parts between the cusp and the point where the line $h = 1$ is tangent to the curve, and it is equal to 2 for the remaining part of the curve. Knowing the indices of the critical points, it is easy to determine the domains (3.30) on the Poisson sphere. They are: $\varnothing$, the disk D^2, the annulus $S^1 \times \mathbb{R}^1$ (the disk D^2 with one hole), the disk D^2 with two holes, the entire sphere S^2. The corresponding surfaces Q_h are shown in Figure 6. We denote by K^3 the same surface as for the Hamiltonian (3.5).

Now let us construct the curves that separate domains with different topological type of Q_h for the Hamiltonians (3.8) and (3.9). Let $0 < A_1 < A_2 < A_3$. One may assume that the functions

$$f_2 = S_1 R_1 + S_2 R_2 + S_3 R_3,$$

$$H = \frac{S_1^2}{2A_1} + \frac{S_2^2}{2A_2} + \frac{S_3^2}{2A_3} + \frac{\sigma}{2}(A_1 R_1^2 + A_2 R_2^2 + A_3 R_3^2)$$

are defined on the set

$$S^2 \times \mathbb{R}^3 = \{f_1 = 1\} \subset \mathbb{R}^6(S, R),$$

where $\sigma = \pm 1$. The condition $\operatorname{grad} H - \mu_1 \operatorname{grad} f_1 - \mu_2 \operatorname{grad} f_2 = 0$, which determines critical points of the mapping $f_2 \times H : S^2 \times \mathbb{R}^3 \to \mathbb{R}^2$, may be written in the form

$$\begin{pmatrix} 1/A_1 & 0 & 0 & -\mu_2 & 0 & 0 \\ 0 & 1/A_2 & 0 & 0 & -\mu_2 & 0 \\ 0 & 0 & 1/A_3 & 0 & 0 & -\mu_2 \\ -\mu_2 & 0 & 0 & \sigma A_1 - 2\mu_1 & 0 & 0 \\ 0 & -\mu_2 & 0 & 0 & \sigma A_2 - 2\mu_1 & 0 \\ 0 & 0 & -\mu_2 & 0 & 0 & \sigma A_3 - 2\mu_1 \end{pmatrix} \begin{pmatrix} S_1 \\ S_2 \\ S_3 \\ R_1 \\ R_2 \\ R_3 \end{pmatrix} = 0.$$

$$(3.34)$$

Since $R_1^2 + R_2^2 + R_3^2 = 1$, equation (3.34) is valid only in the case when the matrix in this equation has nontrivial kernel. This matrix decomposes into three 2×2 blocks with determinants

$$D_i = \sigma - 2\mu_1/A_i - \mu_2^2 \qquad (i = 1, 2, 3). \tag{3.35}$$

If $D_i \neq 0$, then $S_i = R_i = 0$. Therefore, if only one of the conditions $D_i = 0$ is valid, then, taking into account the relation $R_1^2 + R_2^2 + R_3^2 = 1$, one obtains the following critical points:

$$(t_1, 0, 0, \pm 1, 0, 0), \quad (0, t_2, 0, 0, \pm 1, 0), \quad (0, 0, t_3, 0, 0, \pm 1)$$

$$\in \mathbb{R}^6(S, R), \tag{3.36}$$

where t_1, t_2, t_3 are certain parameters.

Calculating the value of f_2 and H at these points, one obtains three parabolas on the plane $\mathbb{R}^2(g, h)$:

$$h = \frac{g^2}{2A_i} + \frac{\sigma A_i}{2} \qquad (i = 1, 2, 3). \tag{3.37}$$

There are only two critical points of the mapping $f_2 \times H$ in the preimage of every point of the parabolas (3.37). It is easy to understand that if $\sigma = -1$, no two determinants (3.35) can be simultaneously equal to zero (because $A_i \neq A_j$ when $i \neq j$). Thus, one obtains a bifurcation diagram which consists of three disjoint parabolas (3.37) with $\sigma = -1$ for the Hamiltonian (3.9). It is shown in Figure 7.

Let us examine the case $\sigma = 1$. If two determinants (3.35) are equal to zero, then $\mu_1 = 0$, $\mu_2^2 = 1$, and so the third determinant is also equal to zero. From (3.34) the following system of equations is obtained:

$$\begin{cases} S_1 = \pm A_1 R_1, \\ S_2 = \pm A_2 R_2, \\ S_3 = \pm A_3 R_3, \\ R_1^2 + R_2^2 + R_3^2 = 1. \end{cases} \tag{3.38}$$

Equations (3.38) determine two two-dimensional spheres in $\mathbb{R}^6(S, R)$, which are completely filled with critical points of the mapping $f_2 \times H$. The values of f_2 and H on the set (3.38) are

$$g = \pm(A_1 R_1^2 + A_2 R_2^2 + A_3 R_3^2),$$
$$h = A_1 R_1^2 + A_2 R_2^2 + A_3 R_3^2.$$

Therefore, under the mapping $f_2 \times H$, the two-dimensional spheres (3.38) transform into two segments

$$\{h = |g|, A_1 \leqslant |g| \leqslant A_3\} \subset \mathbb{R}^2(g, h). \tag{3.39}$$

The preimage of every point of these segments is a set of two circles consisting of critical points.

Combining the parabolas (3.37) (when $\sigma = 1$) and the segments (3.39), we obtain the bifurcation diagram shown in Figure 8. The segments (3.39) are tangent to all three parabolas at the points $(\pm A_i, A_i) \in \mathbb{R}^2(g, h)$. The parabolas (3.37) intersect at the points $\left(\pm\sqrt{A_i A_j}, (A_i + A_j)/2\right) \in \mathbb{R}^2(g, h)$.

The topological type of $Q_h = \{f_1 = 1, f_2 = g, H = h\}$ in each domain in Figures 7 and 8 may be determined by examining the projection of Q_h on the Poisson sphere. The image of Q_h under the projection on the Poisson sphere is determined by the condition

$$g^2/z + \sigma z \leqslant 2h, \qquad A_1 \leqslant z \leqslant A_3, \tag{3.40}$$

where z denotes the expression $A_1 R_1^2 + A_2 R_2^2 + A_3 R_3^2$. The graph of the function $\varphi(z) = g^2/z + \sigma z$ is shown in Figure 9(a) for $\sigma = -1$ and in Figure 9(b) for $\sigma = 1$. When $\sigma = 1$, the function $\varphi(z)$ has a minimum at $z = g$. One of the possible versions of how g may be situated (on the z-axis) relative to A_1, A_2, A_3 is given in Figure 9(b). It is easy to investigate all the possibilities and find out in every case what form the domain (3.40) has on the Poisson sphere. After that the topological type of Q_h is determined by the standard method. The manifold $(S^1 \times S^2) \# (S^1 \times S^2) \# (S^1 \times S^2)$ is denoted by N^3 in Figure 8. Its projection on the Poisson sphere is the disk with three holes.

§4. The Euler-Zhukovskiĭ case

The Hamiltonian in the Euler case (2.2) is the special version of Zhukovskiĭ's Hamiltonian (2.6) when $\lambda_1 = \lambda_2 = \lambda_3 = 0$. The additional integral in both cases is $K = S_1^2 + S_2^2 + S_3^2$.

Bifurcation diagrams for the mapping

$$H \times K : TS^2 \to \mathbb{R}^2, \tag{4.1}$$

where $TS^2 = \{f_1 = 1, f_2 = g\} \subset \mathbb{R}^6(S, R)$, are constructed in [6]. They are of the form shown in Figure 10 when $\lambda_1, \lambda_2, \lambda_3$ differ from zero (in

Figure 10(a) when $g = 0$, in Figure 10(b)–(e) when $g \neq 0$). Under the change of g which determines the manifold TS^2 where the system is defined, the bifurcation diagram transforms in the following way: the segment of the line $k = g^2$ moves to the right and gradually "strikes off" parts of the bifurcation diagram on which cusps lie. Besides, these parts can be "struck off" in different order (this depends on the Hamiltonian's parameters A_1, A_2, A_3, λ_1, λ_2, λ_3). Therefore under the change of g one obtains either the diagrams (a) – (b) – (c) – (e) or (a) – (b) – (d) – (e) shown in Figure 10. For the domains in the plane $\mathbb{R}^2(k, h)$ whose preimage is not empty under the mapping (4.1), the number of Liouville tori in the preimage of every point of the corresponding domain is indicated. The bifurcation curve is tangent (when $g = 0$) to the line $k = 0$ at the point

$$h_0 = \frac{\lambda_1^2}{2A_1} + \frac{\lambda_2^2}{2A_2} + \frac{\lambda_3^2}{2A_3} \tag{4.2}$$

and (when $g^2 < \lambda_1^2 + \lambda_2^2 + \lambda_3^2$) to the line $h = 0$ at the point $k_0 = \lambda_1^2 + \lambda_2^2 + \lambda_3^2$. Six branches of the curve have the asymptotes

$$h \sim \frac{k}{2A_i} \pm \frac{\lambda_i \sqrt{k}}{A_i} \tag{4.3}$$

as they approach infinity.

If the point moving along the plane $\mathbb{R}^2(k, h)$ crosses the bifurcation diagram, then the Liouville tori which lie in the preimage of this point bifurcate in some way. The form of their bifurcation for Zhukovskii's case is defined in [6]. They can be described as follows. Let us examine the line $h = c$, where c is sufficiently large. Then, because (4.3) is valid, this line crosses branches of the curve in some definite order. Let us enumerate them in this order: x_1, x_2, x_3, x_4, x_5, x_6 (see Figure 11(a)) and consider the function $\widetilde{K} = K|_{Q_c}$, where $Q_c = \{f_1 = 1, f_2 = g, H = c\}$. Suppose the critical values of the function $\widetilde{K}$ are $c_1, \ldots, c_6$. The graph Γ which demonstrates how Liouville tori bifurcate along the line $h = c$ is shown in Figure 11(b). The heavily drawn vertices denote minimax circles, vertices in which three edges meet correspond to saddle circles (for a detailed definition, see [2, 4]). Thus for all points of the curve, the bifurcations of the Liouville tori are described. Only minimal circles lie in the preimage of points of the segment belonging to the line $k = g^2$.

In order to describe all possible types of Fomenko invariants, one must determine how the line $h = c$ crosses the bifurcation diagram for different c. First of all let us examine the case $g = 0$. Suppose the cusp which divides the branches x_4 and x_5 has coordinates (k_1, h_1) on the plane $\mathbb{R}^2(k, h)$ and the cusp which lies between the branches x_2 and x_3 has coordinates (k_2, h_2). It is easy to see that the Fomenko invariant has type 1 (see the

Table) when $0 < c < \min(h_1, h_2)$. It has type 4 when $c > \max(h_1, h_2)$. If $\min(h_1, h_2) < c < \max(h_1, h_2)$, then the invariant is of type 2.

We see that the form of the invariant depends on which of the cusps is "lower" on the bifurcation diagram. The case $g \neq 0$ may be examined in a similar way. Here several variants also appear, depending on the position of the points h_1, h_2, and h_0 (4.2) on the h-axis. Finally, we see that two horizontal segments ending in cusps must be added to the curves that separate domains with different topological type of Q_h in Figure 5. Then the topological type of Q_h and the Fomenko invariant will coincide for all points of one domain.

Let us draw curves separating domains with different topological type of Q_h by solid lines, and curves which divide domains with different Fomenko invariants by dotted lines. Let us indicate in each domain the pair (the topological type of Q_h—Fomenko invariant of Q_h), where the invariant is denoted by the corresponding number from the table.

PROPOSITION 1. *For the system with Hamiltonian* (2.6), *when we have* $\lambda_1, \lambda_2, \lambda_3 \neq 0$ (*Zhukovskiĭ's case*), *the separating curves on the plane* $\mathbb{R}^2(g, h)$ *for different values of the Hamiltonian's parameters are of the form shown in Figure* 12(a)–(f). *For every domain in Figure* 12 *the topological type of* Q_h *and the Fomenko invariant are indicated. The complete list* (*for different parameters of the Hamiltonian*) *consists of* 9 *pairs*:

$$S^3 - 1, \quad S^3 - 2, \quad S^3 - 4, \quad S^1 \times S^2 - 1, \quad S^1 \times S^2 - 2,$$

$$S^1 \times S^2 - 4, \quad \mathbb{R}P^3 - 1, \quad \mathbb{R}P^3 - 2, \quad \mathbb{R}P^3 - 4.$$

Invariants with numbers 2 and $2'$ appear in Figure 12. These invariants exchange places when the sign of the additional integral changes, i.e., the words-molecules for invariants 2 and $2'$ coincide but the graph Γ for the invariant $2'$ is obtained from the graph Γ for the invariant 2 by symmetry in some horizontal line. What invariant is realized for a given integral will be indicated further in the figures, but they must be considered coinciding in the list of invariants for integrable cases.

Let us note that in [6] the question: "Is the additional integral $K = S_1^2 + S_2^2 + S_3^2$ Bott?" was not examined and the Liouville tori bifurcations were obtained by another method. However, one can check that this integral is Bott on almost all

$$Q_h = \{f_1 = 1, f_2 = g, H = h\}$$

and precisely this is stated in the theorem of §2. A more exact formulation of the theorem for the Zhukovskiĭ case is that the additional integral is Bott on all nonsingular Q_h except those corresponding to points on horizontal segments that separate domains with different values of the invariant in Figure 12. So, the additional integral is Bott on

$$Q_h = \{f_1 = 1, f_2 = g, H = h\},$$

if the point (g, h) does not lie on the separating curve.

Now let us examine the Hamiltonian (2.2) obtained from the Hamiltonian (2.6) when $\lambda_1 = \lambda_2 = \lambda_3 = 0$ (Euler's case). The bifurcation diagram for the mapping (4.1) is obtained from Zhukovskiĭ's case by passing to the limit. Besides, the curve's branches shown in Figure 10 are combined pairwise: x_1 and x_2, x_3 and x_4, x_5 and x_6. As a result, we obtain the bifurcation diagram shown in Figure 13. It consists of the segment

$$\{k = g^2, \; g^2/2\max(A_1, A_2, A_3) \leqslant h \leqslant g^2/2\min(A_1, A_2, A_3)\}$$

and three rays

$$\{h = k/2A_i, \; k \geqslant g^2\}.$$

The number of Liouville tori is indicated by digits on the figure. Here the invariant changes only at critical values of the function

$$\tilde{H} = H|_{\{f_1=1, f_2=g\}},$$

and the separating curves are only those shown in Figure 1.

When branches of the bifurcation diagram for Zhukovskiĭ's case unite, critical circles transform into one level and the invariant of type 5 which does not exist for Zhukovskiĭ's case arises.

PROPOSITION 2. *For the system with Hamiltonian* (2.2) (*Euler's case*) *the separating curves on the plane* $\mathbb{R}^2(g, h)$ *are shown in Figure* 14. *The list of pairs in this case is*: S^3—1, $S^1 \times S^2$—5, $\mathbb{R}P^3$—5. *The additional integral* $K = S_1^2 + S_2^2 + S_3^2$ *is Bott on all nonsingular surfaces* Q_h.

§5. The Kovalevskaya, Goryachev-Chaplygin, and Sretenskiĭ cases

The Hamiltonian in Kovalevskaya's case (2.4) can be reduced to the form (3.5) by a linear coordinate transformation which preserves the bracket (1.8). Besides, the additional integral will be of the form

$$K = \left(\frac{S_1^2}{2} - \frac{S_2^2}{2} - R_1\right)^2 + (S_1 S_2 - R_2)^2. \tag{5.1}$$

Curves which separate domains with different topological type of Q_h for the Hamiltonian (3.5) are described in §3 (see Figure 3). In order to describe all separating curves in Kovalevskaya's case, one must add to the curves in Figure 3 curves that separate domains with different Fomenko invariants. Therefore, it is necessary to determine how the invariant of the isoenergy surface

$$Q_h = \{f_1 = 1, \; f_2 = g, \; H = h\},$$

changes when h changes and g is fixed. This may be done easily by examining the bifurcation diagrams for the mapping

$$K \times H : TS^2 \to \mathbb{R}^2(k, h), \tag{5.2}$$

where H is the Hamiltonian (3.5) and K is the integral (5.1), both defined on

$$TS^2 = \{f_1 = 1, f_2 = g\} \subset \mathbb{R}^6(S, R).$$

Bifurcation diagrams for the mapping (5.2) are constructed in [6]. Bifurcations of Liouville tori at critical values of the mapping (5.2) are also described there. The form of the bifurcation diagrams for the mapping (5.2) depends on the value g. Qualitatively different diagrams are obtained in the following cases :

   (a) $0 < |g| < 1$;
   (b) $1 < |g| < (4/3)^{(3/4)}$;
   (c) $(4/3)^{(3/4)} < |g| < \sqrt{2}$;
   (d) $|g| > \sqrt{2}$.

They are presented in Figure 15. The bifurcation diagrams consist of the ray

$$\{k = 0, h \geqslant g^2\}, \tag{5.3}$$

part of the parabola

$$\left\{k = (h - g^2)^2, \frac{g^2}{2} - 1 \leqslant h \leqslant g^2 + \frac{1}{2g^2}\right\} \tag{5.4}$$

and the curve given in parametric form by

$$h = \frac{t^2}{2} - \frac{g}{t}, \qquad k = 1 + tg + \frac{t^4}{4}, \qquad t \in \,]-\infty, 0[\,\cup\,[g, +\infty[\,. \tag{5.5}$$

The cusp of the curve (5.5), when $|g| \leqslant (4/3)^{(3/4)}$, has coordinates

$$\left(1 - \frac{3g^{(4/3)}}{4}, \frac{3g^{(2/3)}}{2}\right) \in \mathbb{R}^2(k, h), \tag{5.6}$$

the point where the curve is tangent to parabola has coordinates

$$\left(\frac{1}{4g^4}, g^2 + \frac{1}{2g^2}\right) \in \mathbb{R}^2(k, h). \tag{5.7}$$

Bifurcations of Liouville tori at critical values of the mapping (5.2) are also given in Figure 15. If the point which moves along the plane $\mathbb{R}^2(k, h)$ crosses the corresponding branch of the bifurcation diagram in the direction marked by the arrow, then the bifurcation of Liouville tori in the preimage of this point is described by the letter-atom written near the corresponding arrow (for the description of letters-atoms, see [5]). The bifurcation diagrams (a), (b), (c), (d) in Figure 15 transform one into another when the parameter g changes continuously. The parts of the bifurcation diagram which transform one into another when g changes determine the same bifurcations of Liouville tori.

Knowing the bifurcations of the Liouville tori for all points of the bifurcation diagram, one can describe the Fomenko invariant of the surface Q_h

for all fixed g and h. In order to do this, we must construct the line $h = c$ and examine how Liouville tori bifurcate at the preimage of the point which moves along this line. Let us change the parameter c that determines this line. Then the Fomenko invariant which corresponds to the surface Q_h will change in some way. From the explicit form of the bifurcation diagram, one can easily undestand for what values of c the invariant will change. This happens in the following cases:

(1) when c is a critical value of the function $\widetilde{H} = H|_{TS^2}$ (in this case the topological type of Q_h also changes);

(2) when the line $h = c$ passes either through the cusp of the curve (5.5) or through the point where the curve is tangent to the parabola or through the origin of the ray (5.3).

The images of critical points of the function $\widetilde{H}$ are heavily drawn points in Figure 15. The separating curves corresponding to them have been already constructed (see Figure 3). Taking into account (5.3), (5.6), and (5.7), one obtains equations of the remaining separating curves on the plane $\mathbb{R}^2(g, h)$:

$$h = g^2 \quad \text{(origin of the ray)},$$

$$h = \frac{3g^{(2/3)}}{2}, \quad |g| \leqslant \left(\frac{4}{3}\right)^{(3/4)} \quad \text{(the cusp on the curve)},$$

$$h = g^2 + \frac{1}{2g^2} \quad \text{(the point where the curve is tangent to the parabola)}.$$

$$(5.8)$$

Having combined the curves (5.8) with those shown in Figure 3, we obtain a complete collection of separating curves for Kovalevskaya's case.

PROPOSITION 3. *For the system with Hamiltonian* (2.4) *(the Kovalevskaya case) the separating curves on the plane* $\mathbb{R}^2(g, h)$ *are shown in Figure 16. For all points* (g, h) *which do not lie on the separating curves, the additional integral is Bott on the surface*

$$Q_h = \{f_1 = 1, f_2 = g, H = h\}.$$

For each domain in the plane $\mathbb{R}^2(g, h)$, *the pair (topological type of* Q_h, *Fomenko invariant) is given. The list of invariants in this case consists of* 10 *pairs*:

$$S^3 - 1, S^3 - 2, S^3 - 4, S^3 - 6, S^1 \times S^2 - 2, S^1 \times S^2 - 6,$$
$$K^3 - 6, \mathbb{R}P^3 - 6, \mathbb{R}P^3 - 7, \mathbb{R}P^3 - 8.$$

Now let us pass to Sretenskiĭ's case. The Hamiltonian of Sretenskiĭ's case (2.7) is taken to the form (3.7) by the linear coordinate transformation which preserves the bracket (1.8) in $\mathbb{R}^6(S, R)$. Besides, the additional integral K is of the form:

$$K = (S_3 + 2\lambda)(S_1^2 + S_2^2) - S_1 R_3. \tag{5.9}$$

The Goryachev-Chaplygin case is obtained from the Sretenskiĭ case when $\lambda = 0$.

Bifurcation diagrams of the mapping $H \times K : TS^2 \to \mathbb{R}^2(h, k)$ are constructed in [6]. Here H is the Hamiltonian (3.7) and K is the integral (5.9) both defined on

$$TS^2 = \{f_1 = 1, f_2 = 0\} \subset \mathbb{R}^6(S, R).$$

The bifurcation diagrams for different values of parameter λ are shown in Figure 17:

(a) $\lambda = 0$;
(b) $-1/\sqrt{3} < \lambda < 0$;
(c) $-1 < \lambda < -1/\sqrt{3}$;
(d) $\lambda < -1$.

When λ is changed to $-\lambda$, the bifurcation diagrams reflect in the line $k = 0$. The bifurcation diagrams consist of the ray $\{k = 0, h \geqslant -1\}$ and of the following curves in parametric form:

$$h = \frac{3t^2}{2} + 4\lambda t + 2\lambda^2 \pm 1, \qquad k = t^3 + 2\lambda t^2.$$

Bifurcations of Liouville tori are shown in Figure 17 in the same way as in Kovalevskaya's case. The notation (A^*, B) means that the two bifurcations of Liouville tori corresponding to the letters-atoms A^* and B occur simultaneously. The notation (A, A') means that there are one minimal and one maximal circles of the integral K in the preimage of these points of the bifurcation diagram.

As in Kovalevskaya's case, having found the projections of cusps and tangency points of bifurcation curves on the h axis, one obtains equations for the separating curves on the plane $\mathbb{R}^2(\lambda, h)$:

$$h = 1 - \frac{2\lambda^2}{3} \text{ (cusp)},$$

$$h = 2\lambda^2 \pm 1 \text{ (points of tangency)}.$$

Combining them with the curves shown in Figure 6, we get the answer for Sretenskiĭ's case.

PROPOSITION 4. *For the system with Hamiltonian* (2.7) *(Sretenskiĭ's case) the separating curves are shown in Figure* 18. *The additional integral is Bott for all* (λ, h) *not on the separating curves. The list of invariants for the given case consists of* 8 *pairs*:

$$S^3 - 1, S^3 - 3, S^3 - 10, S^1 \times S^2 - 2, S^1 \times S^2 - 11,$$

$$\mathbb{R}P^3 - 9, \mathbb{R}P^3 - 11, K^3 - 10.$$

When $\lambda = 0$ (Goryachev-Chaplygin case) the additional integral is Bott for all nonsingular surfaces Q_h. The list of invariants for this case consists of 2 pairs: $S^3 - 3$, $\mathbb{R}P^3 - 9$.

Let us note that the Fomenko invariant for the point $(-\lambda, h)$ coincides with that for the point (λ, h), but the graph Γ (see Supplement) "flips" in this case as shown in Figure 18 (for example, observe 10 and $10'$).

§6. Lagrange case

The classical Lagrange case is a system with Hamiltonian (2.3). Under a coordinate transformation in $\mathbb{R}^6(S, R)$, this Hamiltonian may be reduced to the form (3.4). Different generalizations of the Lagrange case are known. For example, the Hamiltonian with quadratic potential may be examined

$$H = \frac{S_1^2 + S_2^2 + S_3^2/\beta}{2} + R_3^2, \tag{6.1}$$

or the gyrostatic momentum may be added

$$H = \frac{S_1^2 + S_2^2 + S_3^2/\beta}{2} + \lambda S_3 + R_3. \tag{6.2}$$

We shall examine the Hamiltonian

$$H = \frac{1}{2}(S_1^2 + S_2^2 + S_3^2/\beta) + V(R_3), \tag{6.3}$$

where V is a certain smooth function. For the Hamiltonian (6.3) the additional integral is $K = S_3$ as in the classical Lagrange case.

Let us consider the momentum mapping $H \times K : TS^2 \to \mathbb{R}^2(h, k)$, where H is the Hamiltonian (6.3), $K = S_3$, and describe critical points of this mapping. Fixing the value $S_3 = k$, we look for critical points of the function $\tilde{H} = H|_{P^3}$, where

$$P^3 = \{f_1 = 1, f_2 = g, K = k\}. \tag{6.4}$$

The surface P^3 is nonsingular when $k \neq \pm g$ (for a while, we exclude the case $k = \pm g$ from our examination). Critical points of the function $\tilde{H}$ can be found from the conditions

$$\operatorname{grad} H = \lambda_1 \operatorname{grad} f_1 + \lambda_2 \operatorname{grad} f_2 + \lambda_3 \operatorname{grad} K, \tag{6.5}$$
$$f_1 = 1, \qquad f_2 = g, \qquad K = k.$$

Denoting R_3 by x, let us express all the unknowns of system (6.5). We obtain:

$$R_1 = \sqrt{1 - x^2} \cos(t), \quad R_2 = \sqrt{1 - x^2} \sin(t), \quad R_3 = x,$$
$$S_1 = \frac{g - kx}{\sqrt{1 - x^2}} \cos(t), \quad S_2 = \frac{g - kx}{\sqrt{1 - x^2}} \sin(t), \quad S_3 = k, \tag{6.6}$$
$$\lambda_1 = -\frac{(g - kx)^2}{2(1 - x^2)^2}, \quad \lambda_2 = \frac{g - kx}{1 - x^2}, \quad \lambda_3 = \frac{k}{\beta} - \frac{x(g - kx)}{1 - x^2},$$

where t is some parameter and x is determined from the condition:

$$V'(x) + \frac{(g - kx)(gx - k)}{(1 - x^2)^2} = 0, \qquad |x| < 1. \tag{6.7}$$

The derivative of function V at the point x is denoted by $V'(x)$.

Conditions (6.6) determine just one critical circle of the function $\widetilde{H} = H|_{P^3}$ for every fixed point x satisfying (6.7). The value of the function $\widetilde{H}$ at points of this circle is

$$h = \frac{(g - kx)^2}{2(1 - x^2)} + \frac{k^2}{2\beta} + V(x).$$

Let us introduce the function

$$W(x) = \frac{(g - kx)^2}{2(1 - x^2)} + \frac{k^2}{2\beta} + V(x).$$

Then $h = W(x)$ and condition (6.7) can be rewritten in the form

$$W'(x) = 0, \qquad |x| < 1. \tag{6.8}$$

Therefore, critical circles of the function $\widetilde{H}$ are parametrized by critical points of the function $W(x)$. The function $W(x)$ is the analog of the reduced potential, and the projections of Liouville tori on the Poisson sphere are determined in this case by the condition $W(R_3) \leqslant h$.

Now let us define the indices of critical circles (6.6) of the function $\widetilde{H}$. In order to do this, we follow the outline sketched in §3 (see the Lemma), write out the matrix $G_\lambda = G_H - \lambda_1 G_1 - \lambda_2 G_2 - \lambda_3 G_3$, and then restrict the form determined by this matrix to the space orthogonal to $\operatorname{grad} f_1$, $\operatorname{grad} f_2$, $\operatorname{grad} K$. The matrix G_λ is of the following form in this case:

$$\begin{pmatrix} 1 & 0 & 0 & -\lambda_2 & 0 & 0 \\ 0 & 1 & 0 & 0 & -\lambda_2 & 0 \\ 0 & 0 & 1/\beta & 0 & 0 & -\lambda_2 \\ -\lambda_2 & 0 & 0 & -2\lambda_1 & 0 & 0 \\ 0 & -\lambda_2 & 0 & 0 & -2\lambda_1 & 0 \\ 0 & 0 & -\lambda_2 & 0 & 0 & V''(x) - 2\lambda_1 \end{pmatrix}, \tag{6.9}$$

where

$$\lambda_1 = -\frac{(g - kx)^2}{2(1 - x^2)^2}, \qquad \lambda_2 = \frac{g - kx}{1 - x^2},$$

and $V''(x)$ is the second derivative of the function $V(x)$ at the point x. The gradients of the functions f_1, f_2, K at the critical points (6.6) are equal to

$$\operatorname{grad} f_1 = (0, 0, 0, 2y\cos(t), 2y\sin(t), 2x),$$

$$\operatorname{grad} f_2 = \left(y\cos(t), y\sin(t), x, \frac{g - kx}{y}\cos(t), \frac{g - kx}{y}\sin(t), k \right),$$

$$\operatorname{grad} K = (0, 0, 1, 0, 0, 0),$$

where y denotes the expression $\sqrt{1 - x^2}$. The basis in the space orthogonal to these gradients can be chosen, for example, in the form:

$$e_1 = (\sin(t), -\cos(t), 0, 0, 0, 0),$$

$$e_2 = (0, 0, 0, \sin(t), -\cos(t), 0),$$

$$e_3 = \left(\frac{k - gx}{1 - x^2} \cos(t), \frac{k - gx}{1 - x^2} \sin(t), 0, x\cos(t), x\sin(t), -y \right).$$

Calculating $G_\lambda(e_i, e_j)$, one obtains the following matrix:

$$\widetilde{G}_\lambda = \begin{pmatrix} 1 & \dfrac{kx - g}{1 - x^2} & 0 \\ \dfrac{kx - g}{1 - x^2} & \dfrac{(kx - g)^2}{(1 - x^2)^2} & 0 \\ 0 & 0 & (1 - x^2)W''(x) \end{pmatrix}.$$

Its eigenvalues are:

$$\mu_1 = 0, \qquad \mu_2 = 1 + \frac{(kx - g)^2}{(1 - x^2)^2}, \qquad \mu_3 = (1 - x^2)W''(x).$$

The zero eigenvalue corresponds to the fact that the Hessian of the function $\widetilde{H}$ is degenerate along the direction tangent to the critical circle. The eigenvalue μ_2 is always positive, and the sign of the eigenvalue μ_3 coincides with the sign of $W''(x)$ (because $|x| < 1$). This means that critical circles of the function $\widetilde{H} = H|_{P^3}$ may be either saddle or minimal. Since critical circles are determined by condition (6.8), local maxima correspond to saddle circles, and local minima of the function $W(x)$ on the segment $[-1, 1]$ correspond to minimal circles. This gives us the opportunity to describe bifurcation diagrams for an arbitrary Hamiltonian of the form (6.3). Only the case when the function $V(x)$ in the Hamiltonian (6.3) has nonnegative second derivative on the segment $[-1, 1]$ will be examined in this work.

It is easy to check that if $V''(x) \geqslant 0$ for all $x \in [-1, 1]$, then $W''(x) > 0$ on the segment $[-1, 1]$ for any values of the constants g, k, β. This implies that the function $W(x)$ has only one local minimum and has no local maxima on the segment $[-1, 1]$. Thus for any value of the constant k (other than possibly $k = \pm g$ that we have not yet examined) the functon $\widetilde{H}$ determined on the surface (6.4) has only one minimal critical circle. Therefore, every line $k = \mathrm{const}$ intersects the bifurcation diagram of the mapping $H \times K \colon TS^2 \to \mathbb{R}^2(h, k)$ at precisely one point. The preimage of this line is the surface (6.4). An approximate picture of the bifurcation diagram is presented in Figure 19. The images of two critical points $(0, 0, \pm g, 0, 0, \pm 1) \in \mathbb{R}^6(S, R)$ for the functions $H|_{TS^2}$ and $K|_{TS^2}$ are the heavily drawn points in Figure 19. They may not lie on the bifurcation curve (see Figure 20). The preimage of every point (h, k) which lies to the

right of the bifurcation curve is a two-dimensional torus T^2, the preimage of every point (h, k) which lies to the left of the bifurcation curve is $\varnothing$.

So in case when $V''(x) \geqslant 0$, Fomenko's invariant is of a simple form.

PROPOSITION 5. *For the system with Hamiltonian* (6.3) *in the case when* $V''(R_3)$ *is nonnegative, Fomenko's invariant for any connected component of the surface*

$$Q_h = \{f_1 = 1, f_2 = g, H = h\}$$

is of type 1. *The additional integral* $K = S_3$ *is Bott on all nonsingular surfaces* Q_h.

COROLLARY. *For the system with Hamiltonian*

$$H = \frac{(S_1^2 + S_2^2 + S_3^2/\beta)}{2} + \lambda S_3 + V(R_3), \tag{6.10}$$

in the case when $V''(R_3) \geqslant 0$, *the additional integral* $K = S_3$ *is Bott on all nonsingular surfaces* Q_h, *and the Fomenko invariant is of type* 1.

The proof of the Corollary can be easily obtained if one takes into account the fact that the Hamiltonian (6.10) is a linear combination of the Hamiltonian (6.3) and the integral $K = S_3$. Thus the momentum mapping $H \times K$ for the Hamiltonian (6.10) is the composition of the momentum mapping $H \times K$ for the Hamiltonian (6.3) and the linear mapping of the plane $\mathbb{R}^2(h, k)$ into itself with matrix

$$\begin{pmatrix} 1 & \lambda \\ 0 & 1 \end{pmatrix}.$$

The Hamiltonian (3.4) for the ordinary Lagrange case is a special case of the Hamiltonian (6.3) when $V(R_3) = R_3$. Besides, $V''(R_3) \equiv 0$, i.e., the assumption of Proposition 5 is valid. Therefore, in Figure 2 a complete collection of separating curves for Lagrange's case is given. Fomenko's invariant for all domains in Figure 2 is of type 1. In Figure 20 several possible (under different values of g and β) bifurcation diagrams of the momentum mapping $H \times K$ for Hamiltonian (3.4) are given.

§7. Clebsch's case

Four parameters $A_1, A_2, A_3, \varepsilon$ appear in the Hamiltonian in Clebsch's case (2.8). Putting $A_i' = \sqrt{|\varepsilon|} A_i$, and dividing the Hamiltonian by $\sqrt{|\varepsilon|}$, we obtain the Hamiltonian in Clebsch's case with parameters A_1', A_2', A_3', and $\varepsilon = \pm 1$. So one can examine only the Hamiltonians (3.8) and (3.9) for which the curves on the plane $\mathbb{R}^2(g, h)$ separating domains with different topological type of Q_h have already been constructed in §3.

As has already been mentioned, if we know the bifurcation diagrams of the momentum mapping $H \times K: TS^2 \to \mathbb{R}^2(h, k)$, we can easily obtain the bifurcation diagram for the system with Hamiltonian $H' = \alpha H + \beta K$, where α, β are constants. It is obtained from the original diagrams by a

certain linear nondegenerate transformation of the plane $\mathbb{R}^2(h, k)$. We are interested only in how the Liouville tori bifurcate when the point moves along the line $h = \mathrm{const}$. Thus, Fomenko's invariant for the Hamiltonian H' can be described by defining how the line $\alpha h + \beta k = \mathrm{const}$ intersects the bifurcation diagram of the mapping $H \times K$.

All the Hamiltonians in Clebsch's case may be obtained, for example, in the form of a linear combination $\alpha H_0 + \beta K_0$ of the following commuting functions:

$$H_0 = (S_1^2 + S_2^2 + S_3^2) + (c_1 R_1^2 + c_2 R_2^2 + c_3 R_3^2),$$
$$K_0 = (c_1 S_1^2 + c_2 S_2^2 + c_3 S_3^2) - (c_1^2 R_1^2 + c_2^2 R_2^2 + c_3^2 R_3^2),$$
(7.1)

where $c_1 + c_2 + c_3 = 0$. What Hamiltonians in Clebsch's case are obtained for different values of α, β is shown in Figure 21. If the line $\alpha h + \beta k = 0$ lies in the domain I, then $\alpha H_0 + \beta K_0$ is the Hamiltonian of the form (3.8); if it lies in the domain II, then $\alpha H_0 + \beta K_0$ is the Hamiltonian of the form (3.9). If the line lies in the shaded domain, then there are noncompact surfaces among the isoenergy surfaces Q_h. These linear combinations are not examined.

Bifurcation diagrams for Clebsch's case were constructed and studied in [23–25]. They are shown in Figure 22 for the mapping

$$H_0 \times K_0 \colon TS^2 \to \mathbb{R}^2(h, k).$$

Three qualitatively different cases are possible:

$$\text{(a)} g^2 > p_2; \qquad \text{(b)} p_1 < g^2 < p_2; \qquad \text{(c)} g^2 < p_1,$$

where p_1 and p_2 are certain constants depending on the parameters c_1, c_2, and c_3 of the Hamiltonian H_0. When $f_2 = g$ and $f_2 = -g$ the diagrams coincide completely. The three lines

$$k = c_1 h + c_2 c_3, \qquad k = c_2 h + c_3 c_1, \qquad k = c_3 h + c_1 c_2$$

are asymptotes of the bifurcation curve. The three heavily drawn points in Figure 22 are images of points at which $\mathrm{grad}\, H_0$ and $\mathrm{grad}\, K_0$ vanish on TS^2. Their coordinates are

$$(g^2 + c_i,\, c_i(g^2 - c_i)) \in \mathbb{R}^2(h, k) \qquad (i = 1, 2, 3). \tag{7.2}$$

The bifurcations of the Liouville tori are shown in Figure 22.

Examining different lines $\alpha h + \beta k = c$, one can define the Fomenko invariant for the Hamiltonians $\alpha H_0 + \beta K_0$ for different c. The invariant may change either when c is a critical value of the function $\alpha H_0 + \beta K_0$ or when the line $\alpha h + \beta k = c$ passes through a cusp of the curve. Having constructed the separating curve corresponding to cusps of the bifurcation diagram, one obtains a description of the Fomenko invariant for Clebsch's case (which of the two Hamiltonian (3.8) or (3.9) is obtained for different α, β is indicated in Figure 21).

PROPOSITION 6. *The separating curves and the Fomenko invariants for the Hamiltonians in Clebsch's case* (3.8) *and* (3.9) *are indicated in Figure* 23,(a), (b). *The additional integral is Bott on all surfaces*

$$Q_h = \{f_1 = 1, f_2 = g, H = h\}$$

if the point (g, h) *does not belong to separating curves. The list of invariants for Clebsch's case consists of* 10 *pairs*:

$$S^3 - 1, S^3 - 2, S^1 \times S^2 - 1, S^1 \times S^2 - 2, S^1 \times S^2 - 5,$$
$$S^1 \times S^2 - 12, \mathbb{R}P^3 - 5, \mathbb{R}P^3 - 12, N^3 - 5, N^3 - 12.$$

REMARK. The dotted curve (which separates domains with different Fomenko invariants) may be of "lesser size" and hence intersect a lesser number of curves separating domains with different topological type of Q_h. In Figure 23, (a) and (b), the case when the dotted curve intersects the largest possible number of curves separating domains with different topological type of Q_h is shown.

§8. Steklov's case

There are four parameters A_1, A_2, A_3, ε in the Hamiltonian for Steklov's case (2.9). Let us examine the following functions:

$$\begin{aligned}
H_0 &= a_1 S_1^2 + a_2 S_2^2 + a_3 S_3^2 + 2(a_1^2 S_1 R_1 + a_2^2 S_2 R_2 + a_3^2 S_3 R_3) \\
&\quad + a_1^3 R_1^2 + a_2^3 R_2^2 + a_3^3 R_3^2, \\
K_0 &= S_1^2 + S_2^2 + S_3^2 - 2(a_1 S_1 R_1 + a_2 S_2 R_2 + a_3 S_3 R_3) \\
&\quad - 3(a_1^2 R_1^2 + a_2^2 R_2^2 + a_3^2 R_3^2),
\end{aligned} \tag{8.1}$$

where $a_1 + a_2 + a_3 = 0$. As in Clebsch's case, the arbitrary Hamiltonian H in Steklov's case can be represented in the form:

$$H = \alpha H_0 + \beta K_0 + \gamma f_1 + \delta f_2, \tag{8.2}$$

where

$$3a_1 = \varepsilon(2A_2 A_3 - A_3 A_1 - A_1 A_2), \quad 3a_2 = \varepsilon(2A_3 A_1 - A_1 A_2 - A_2 A_3),$$
$$3a_3 = \varepsilon(2A_1 A_2 - A_2 A_3 - A_3 A_1), \quad \beta = \frac{1}{6A_1} + \frac{1}{6A_2} + \frac{1}{6A_3},$$
$$\alpha = \frac{1}{2\varepsilon A_1 A_2 A_3}, \quad \gamma = \varepsilon^2 \left(\frac{2(A_1 A_2 + A_2 A_3 + A_3 A_1)^3}{27 A_1 A_2 A_3} - A_1 A_2 A_3 \right),$$
$$\delta = \frac{\varepsilon}{9} \left(5(A_1 + A_2 + A_3) - 2 \left(\frac{A_2 A_3}{A_1} + \frac{A_3 A_1}{A_2} + \frac{A_1 A_2}{A_3} \right) \right).$$

In this section bifurcation diagrams of the mapping

$$K_0 \times H_0 : TS^2 \to \mathbb{R}^2(k, h) \tag{8.3}$$

will be constructed; here H_0 and K_0 are defined on

$$TS^2 = \{f_1 = 1, f_2 = g\} \subset \mathbb{R}^6(S, R).$$

Knowing the bifurcation diagrams of the mapping (8.3), we can describe the Fomenko invariant for the Hamiltonian (8.2), determining how the Liouville tori bifurcate in the preimage of the point moving along the line $\alpha h + \beta k = $ const. Let us assume that the parameters a_1, a_2, a_3 contained in expression (8.1) satisfy the condition:

$$a_1 < 0 \leqslant a_2 < a_3. \tag{8.4}$$

The general case can be reduced to this one by a coordinate transformation. Besides, $a_1 + a_2 + a_3 = 0$. Let us find critical points of the function K_0 on TS^2. Solving the system

$$\begin{cases} \operatorname{grad} K_0 = \lambda_1 \operatorname{grad} f_1 + \lambda_2 \operatorname{grad} f_2, \\ R_1^2 + R_2^2 + R_3^2 = 1, \\ S_1 R_1 + S_2 R_2 + S_3 R_3 = g, \end{cases}$$

we see that for any g six critical points exist:

$$\begin{aligned} (\pm g, 0, 0, \pm 1, 0, 0), & (0, \pm g, 0, 0, \pm 1, 0), \\ & (0, 0, \pm g, 0, 0, \pm 1) \in \mathbb{R}^6(S, R). \end{aligned} \tag{8.5}$$

Besides, for different values of g the following critical points exist:

$$(0, (a_1 - a_3)u_1, (a_1 - a_2)v_1, 0, u_1, v_1) \in \mathbb{R}^6(S, R),$$

where $\quad u_1^2 = \dfrac{g + a_2 - a_1}{a_2 - a_3}, \quad v_1^2 = \dfrac{g + a_3 - a_1}{a_3 - a_2}, \quad a_1 - a_3 \leqslant g \leqslant a_1 - a_2;$

$$((a_2 - a_3)v_2, 0, (a_2 - a_1)u_2, v_2, 0, u_2) \in \mathbb{R}^6(S, R),$$

where $\quad u_2^2 = \dfrac{g + a_3 - a_2}{a_3 - a_1}, \quad v_2^2 = \dfrac{g + a_1 - a_2}{a_1 - a_3}, \quad a_2 - a_3 \leqslant g \leqslant a_2 - a_1;$

$$((a_3 - a_2)u_3, (a_3 - a_1)v_3, 0, u_3, v_3, 0) \in \mathbb{R}^6(S, R), \tag{8.6}$$

where $\quad u_3^2 = \dfrac{g + a_1 - a_3}{a_1 - a_2}, \quad v_3^2 = \dfrac{g + a_2 - a_3}{a_2 - a_1}, \quad a_3 - a_2 \leqslant g \leqslant a_3 - a_1.$

The number of critical points of the function K_0 on TS^2 for different values of g is indicated in Figure 24.

Now let us find points $(S, R) \in TS^2 \subset \mathbb{R}^6(S, R)$ at which

$$\operatorname{grad} H_0 = \mu \operatorname{grad} K_0 + \mu_1 \operatorname{grad} f_1 + \mu_2 \operatorname{grad} f_2, \tag{8.7}$$

where μ_1, μ_2, and μ are certain coefficients. Condition (8.7) can be rewritten in the form:

$$\begin{cases} G_\mu \begin{pmatrix} S \\ R \end{pmatrix} = 0, \\ f_1(S, R) = 1, \\ f_2(S, R) = g, \end{cases} \tag{8.8}$$

where G_μ is a 6×6 matrix. The matrix G_μ consists of two blocks,

$$G_\mu = (AB), \tag{8.9}$$

$$A = \begin{pmatrix} a_1 - \mu & 0 & 0 \\ 0 & a_2 - \mu & 0 \\ 0 & 0 & a_3 - \mu \\ a_1^2 + \mu a_1 - \mu_2/2 & 0 & 0 \\ 0 & a_2^2 + \mu a_2 - \mu_2/2 & 0 \\ 0 & 0 & a_3^2 + \mu a_3 - \mu_2/2 \end{pmatrix},$$

$$B = \begin{pmatrix} a_1^2 + \mu a_1 - \mu_2/2 & 0 & 0 \\ 0 & a_2^2 + \mu a_2 - \mu_2/2 & 0 \\ 0 & 0 & a_3^2 + \mu a_3 - \mu_2/2 \\ a_1^3 + 3\mu a_1^2 - \mu_1 & 0 & 0 \\ 0 & a_2^3 + 3\mu a_2^2 - \mu_1 & 0 \\ 0 & 0 & a_3^3 + 3\mu a_3^2 - \mu_1 \end{pmatrix}.$$

The system (8.8) has nontrivial solutions only when $\det G_\mu = 0$. This is equivalent to one or more of the following three conditions:

$$(a_1^3 + 3\mu a_1^2 - \mu_1)(a_1 - \mu) - \left(a_1^2 + \mu a_1 - \frac{\mu_2}{2}\right)^2 = 0,$$

$$(a_2^3 + 3\mu a_2^2 - \mu_1)(a_2 - \mu) - \left(a_2^2 + \mu a_2 - \frac{\mu_2}{2}\right)^2 = 0, \tag{8.10}$$

$$(a_3^3 + 3\mu a_3^2 - \mu_1)(a_3 - \mu) - \left(a_3^2 + \mu a_3 - \frac{\mu_2}{2}\right)^2 = 0.$$

If only one of the conditions (8.10) is valid, then the solutions of system (8.8) will be the points (8.5). If exactly two of the conditions (8.10) are valid, then the points (8.6) are solutions of system (8.8). Thus only the case when all three conditions (8.10) are fulfilled is left to examine.

It is easy to show that all three conditions (8.10) hold iff:

$$\mu_1 = 4\mu^3, \qquad \mu_2 = 4\mu^2. \tag{8.11}$$

For the time being, assume that $\mu \neq a_1, a_2, a_3$. Then, substituting the expression (8.11) in the system (8.8), we obtain:

$$\begin{cases} S_1 = -(a_1 + 2\mu)R_1, \\ S_2 = -(a_2 + 2\mu)R_2, \\ S_3 = -(a_3 + 2\mu)R_3, \\ R_1^2 + R_2^2 + R_3^2 = 1, \\ S_1 R_1 + S_2 R_2 + S_3 R_3 = g. \end{cases} \tag{8.12}$$

Equations (8.12) determine a two-dimensional sphere $S^2 \subset TS^2$, completely filled with critical points of the mapping (8.3). This sphere is mapped into

the curve on the plane $\mathbb{R}^2(k, h)$ defined in parametric form as follows:

$$k = -8\mu g - 12\mu^2, \qquad h = -4\mu^2 g - 8\mu^3,$$
$$-(g + a_3) \leqslant 2\mu \leqslant -(g + a_1). \tag{8.13}$$

Now let us examine the case when $\mu = a_1$, $\mu = a_2$, or $\mu = a_3$ and (8.11) is valid. Suppose, for example, that $\mu = a_1$, $\mu_1 = 4a_1^3$, $\mu_2 = 4a_1^2$. Then the system (8.8) is equivalent to the system

$$\begin{cases} S_2 = (a_3 - a_1)R_2, \\ S_3 = (a_2 - a_1)R_3, \\ R_1^2 + R_2^2 + R_3^2 = 1, \\ S_1 R_1 + S_2 R_2 + S_3 R_3 = g. \end{cases}$$

Transforming this system, we obtain:

$$\begin{cases} S_2 = (a_3 - a_1)R_2, \\ S_3 = (a_2 - a_1)R_3, \\ R_2^2 = \dfrac{t_1 R_1 + (a_3 - a_1)R_1^2 + a_2 - a_1 - g}{a_2 - a_3}, \\ R_3^2 = \dfrac{t_1 R_1 + (a_2 - a_1)R_1^2 + a_3 - a_1 - g}{a_3 - a_2}, \end{cases} \tag{8.14}$$

where t_1 denotes the expression $(S_1 + 3a_1 R_1)$.

The system of equations (8.14) determines a certain two-dimensional subset in $TS^2 \subset \mathbb{R}^6(S, R)$ consisting of critical points of the mapping (8.3). Calculating the values of the functions K_0 and H_0 at these points, we get:

$$k = t_1^2 - 12a_1^2 - 8ga_1,$$
$$h = a_1 t_1^2 - 8a_1^3 - 4ga_1^2. \tag{8.15}$$

Thus the momentum mapping $H_0 \times K_0$ takes the set (8.14) to a subset of the line $h = a_1 k + 4a_1^3 + 4ga_1^2$. In order to understand what part of this line is the image of the set (8.14), it is neccessary to determine the values of t_1 for which system (8.14) has a solution. It is evident that (8.14) has a solution iff

$$\begin{cases} \dfrac{t_1 R_1 + (a_3 - a_2)R_1^2 + a_2 - a_1 - g}{a_2 - a_3} \geqslant 0, \\ \dfrac{t_1 R_1 + (a_2 - a_3)R_1^2 + a_3 - a_1 - g}{a_3 - a_2} \geqslant 0. \end{cases} \tag{8.16}$$

The domains in the plane (R_1, t_1) determined by condition (8.16) are shown in Figure 27 (they are shaded in the figure). Different figures correspond to different values of g. The range of g for each of the figures 27, (a)–(f), is shown in Figure 25. The equations of the curves shown in Figure 27 are obtained by replacing the inequality in (8.16) by an equality sign.

They are hyperbolas with asymptotes $t_1 = (a_1 - a_2)R_1$ and $t_1 = (a_1 - a_3)R_1$, and common asymptote $R_1 = 0$. Intersection points of the hyperbolas have the following coordinates

$$(\pm 1, \pm(g + 3a_1)) \in \mathbb{R}^2(R_1, t_1).$$

Let the image of the shaded domain under the orthogonal projection on the axis $R_1 = 0$ be the set $\{t_1 : |t_1| \geqslant T\}$, where T is nonnegative. Then the image of the set (8.14) under the momentum mapping $H_0 \times K_0$ is the ray

$$\{h = a_1 k + 4a_1^3 + 4ga_1^2; k \geqslant T^2 - 12a_1^2 - 8ga_1\} \subset \mathbb{R}^2(k, h). \qquad (8.17)$$

Using Figure 27 it is easy to determine the form of the set of critical points of the mapping (8.3) in the preimage of each point of the ray. Actually, the shaded domain in Figure 27 is the image of the set (8.14) under the projection π on the plane $\mathbb{R}^2(R_1, t_1)$. From explicit formulas (8.14) for R_2^2 and R_3^2, it is easy to understand that precisely four points belong to the preimage of every interior point of the shaded domain under this projection. If the point y moves in the shaded domain and reaches its boundary, then four points in the preimage $\pi^{-1}(y)$ combine into two points (pairwise). Besides, for different hyperbolas different pairs of points combine. Some examples of how the set (8.14) maps into the shaded domain under the projection π for different segments $t_1 = \mathrm{const}$ are shown in Figure 26.

Examining all the other cases in a similar way, one can understand how the stratification of the set (8.14) on the circle $t_1 = \mathrm{const}$ is arranged. From this it is easy to determine the form of function K_0 on the set of critical points (8.14). This form may be conveniently described with the help of the same graphs Γ that code bifurcations of Liouville tori (see [2, 4]). But in this case the graph Γ codes bifurcations of circles instead of bifurcations of tori. The corresponding graphs Γ are shown in Figure 28. Since the set (8.14) is noncompact and K_0 unboundedly increases on it, there are no heavily drawn points (notation for the function's maximum) among the end points of the upward edges of the graph Γ.

We have examined system (8.8) under the condition that (8.11) is valid and $\mu_1 = a_1$. The cases $\mu = a_2$ and $\mu = a_3$ are examined in the same way. Two more rays on the plane $\mathbb{R}^2(k, h)$ are obtained as a result. In these cases one can also determine how the circles bifurcate in the preimage of point moving along these rays. The result for all three rays is given in the table (Figure 29). The ranges of g are shown above the table.

Now bifurcation diagrams of the mapping (8.3) can be described. From the above it follows that the bifurcation diagram for any g is the union of the curve (8.13) and three rays belonging to the lines

$$h = a_i k + 4a_i^3 + 4ga_i^2 \qquad (i = 1, 2, 3).$$

The curve (8.13) is of the form given in Figure 30:

(a) $g < -3a_3$;
(b) $-3a_3 < g < -3a_2$;
(c) $-3a_2 < g < -3a_1$;
(d) $g > -3a_1$.

The curve (8.13) is defined in parametric form with parameter μ. For the point of the curve marked by the digit i ($i = 1, 2, 3$) in Figure 30, the value of the parameter μ is equal to $-(g + a_i)/2$. This is the intersection point of the curve and the line $h = a_i k + 4a_i^3 + 4ga_i^2$. For the cusp of the curve we have

$$\mu = -g/3 \qquad (\text{when} \quad -3a_3 < g < -3a_1).$$

Besides, at all points of the curve the relation

$$dh/d\mu = \mu dk/d\mu \qquad (8.18)$$

is valid, where $h(\mu)$ and $k(\mu)$ are functions from (8.13) (this is a special case of relation (3.24)). Let us also note that the "angles" in Figure 26 (the points $R_1 = \pm 1$, $t_1 = \pm(g + 3a_1)$) correspond to the intesection of the curve (8.13) with the ray (8.17). The situation is analogous for the other two rays. Points of local extremum of the function $t_1(R_1)$ (and the similar functions $t_2(R_2)$ and $t_3(R_3)$) correspond to the intersection of rays on the bifurcation diagram. The ray is tangent to the curve when the graph Γ corresponding to this ray is either Γ_4, or Γ_5, or Γ_6 (see Figure 28). The parameter μ is equal to a_i at the point where the ray is tangent to the curve.

Summarizing all the above, we obtain the bifurcation diagrams shown in Figure 31. Cases (a)–(j) in Figure 31 correspond to values of g indicated in Figure 29 (below the table). In order to simplify the figures, the coordinate axes (k, h) are not shown. Liouville tori bifurcations indicated in Figure 31 will be defined below.

Let us now calculate the indices of critical circles of the function $\tilde{H}_0 = H_0|_{Q_k}$, where

$$Q_k = \{f_1 = 1, f_2 = g, K_0 = k\}.$$

Critical cicles which lie in the preimage of the curve (8.13) are determined by the system of equations (8.12). In addition, $k = -8\mu g - 12\mu^2$. Let us examine the vectors

$$e_1 = (0, (a_1 - a_3)R_3, (a_2 - a_1)R_2, 0, R_3, -R_2),$$
$$e_2 = ((a_3 - a_2)R_3, 0, (a_2 - a_1)R_1, -R_3, 0, R_1),$$
$$e_3 = ((a_3 - a_2)R_2, (a_1 - a_3)R_1, 0, R_2, -R_1, 0)$$

in $\mathbb{R}^6(S, R)$. It is easy to check that these vectors form a basis in the tangent space to

$$Q_k = \{f_1 = 1, f_2 = g, K_0 = -8\mu g - 12\mu^2\}$$

at all points determined by the system (8.12), except at critical points (8.5) of the function K_0 on TS^2.

Let us examine the matrix

$$G_\mu = G_H - \mu G_K - \mu_1 G_1 - \mu_2 G_2 = G_H - \mu G_K - 4\mu^3 G_1 - 4\mu^2 G_2,$$

where G_H, G_K, G_1, G_2 are the Hessians of the functions H_0, K_0, f_1, f_2. We must restrict the form with matrix G_μ to the tangent space to Q_k. In the basis (e_1, e_2, e_3), the matrix of the restriction of this form is $\widetilde{G}_\mu$, where $(\widetilde{G}_\mu)_{ij} = G_\mu(e_i, e_j)$. The matrix $\widetilde{G}_\mu$ always has a zero eigenvalue, because the vector which is tangent to the critical circle belongs to its kernel. Calculating, we see that the product of other two eigenvalues is equal to

$$\Delta(\mu) = 16(g + 3\mu)(\mu - a_1)(\mu - a_2)(\mu - a_3)$$
$$\times ((\mu - a_1)^2 R_1^2 + (\mu - a_2)^2 R_2^2 + (\mu - a_3)^2 R_3^2),$$

and their sum is equal to

$$\operatorname{tr}\widetilde{G}_\mu = -4(8\mu^3 + 3g\mu^2 + a_1 a_2 a_3 + (g + 2\mu)(a_1 a_2 + a_2 a_3 + a_3 a_1)).$$

Taking into account that $\mu = -g/3$ corresponds to the cusp of the curve, and $\mu = a_i$ corresponds to the point where the curve is tangent to the line

$$h = a_i k + 4a_i^3 + 4g a_i^2,$$

it is easy to determine signs of the eigenvalues of the matrix $\widetilde{G}_\mu$ (and thus the indices of critical circles of the function $\widetilde{H}_0$) at all points of the curve.

Now let us examine critical points of the function $\widetilde{H}_0$ in the preimage of the line $h = a_1 k + 4a_1^3 + 4g a_1^2$. They are determined by the system

$$\begin{cases} S_1 = t_1 - 3a_1 R_1, \\ S_2 = (a_3 - a_1) R_2, \\ S_3 = (a_2 - a_1) R_3, \\ R_1^2 + R_2^2 + R_3^2 = 1, \\ S_1 R_1 + S_2 R_2 + S_3 R_3 = g. \end{cases}$$

The basis in the tangent space to the surface

$$Q_k = \{f_1 = 1, f_2 = g, K_0 = t_1^2 - 12a_1^2 - 8g a_1\}$$

may be chosen, for example, in the form:

$$e_1 = (0, (a_1 - a_3) R_3, (a_2 - a_1) R_2, 0, R_3, -R_2),$$
$$e_2 = ((a_3 - a_2) R_3, 0, (a_2 - a_1) R_1 + t_1, -R_3, 0, R_1),$$
$$e_3 = ((a_3 - a_2) R_2, (a_1 - a_3) R_1 - t_1, 0, R_2, -R_1, 0).$$

Restricting the form with matrix

$$G_{a_1}(t_1) = G_H - a_1 G_K - 4a_1^3 G_1 - 4a_1^2 G_2$$

to the tangent space to Q_k, we obtain the matrix $\widetilde{G}_{a_1}(t_1)$. Calculating, we obtain that the product of two nonzero eigenvalues of the matrix $\widetilde{G}_{a_1}(t_1)$ is equal to

$$\Delta(t_1) = t_1^2(a_3 - a_1)(a_2 - a_1)(t_1^2 + 4(a_2 - a_1)^2 R_2^2 + 4(a_3 - a_1)^2 R_3^2),$$

and their sum is equal to

$$\operatorname{tr}\widetilde{G}_{a_1}(t_1) = 4(a_2 - a_1)(a_3 - a_1)((a_2 - a_1)R_2^2 + (a_3 - a_1)R_3^2) - 3a_1 t_1^2.$$

From the expressions for $\Delta(t_1)$ and $\operatorname{tr}\widetilde{G}_{a_1}(t_1)$ it follows that eigenvalues are always positive in this case except when $t_1 = 0$ (in this case one special eigenvalue is zero and the other is positive). Making analogous calculations for the two other rays, we finally conclude that the index of the critical circle of the function $\widetilde{H}_0$ which lies in the preimage of the line

$$h = a_i k + 4a_i^3 + 4g a_i^2$$

is equal to $i - 1$.

Thus, we have defined indices of all critical circles of the mapping $H_0 \times K_0$. Moreover, we have proved that all critical circles are nondegenerate, except those which lie in the preimage of a cusp of the curve and points where the curve is tangent to rays. Now it is not hard to determine the Liouville tori bifurcations at the critical values of the mapping (8.3). It is evident that the letter-atom which encodes the bifurcation corresponding to those parts of the diagrams for which the index of the critical circle is equal to 0 or 2 is A (see [5]). Knowing these bifurcations, it is easy to determine the number of Liouville tori in the preimage of every point which does not lie on the bifurcation diagram. It remains to determine the type of bifurcations arising from saddle circles.

Let us examine, say, Figure 31(g). This bifurcation diagram is shown in more detail in Figure 32. The digits in Figure 32 indicate the number of Liouville tori, the number of saddle circles (for example, $4s$) and the number of minimax circles (for example, $2m$). Bifurcations along the arrows I and II are bifurcations of two Liouville tori into four tori on two saddle circles. There exists only one bifurcation with these properties (see the list in [5]). This bifurcation is coded by two letters-atoms B. The bifurcation of tori along the arrow III has the same form as the bifurcation of critical circles in the preimage of a point which moves along the arrow III$'$ (see A. V. Bolsinov's paper in this volume). The graph Γ_3 corresponds to the ray along which the arrow III$'$ is directed (see Figures 28 and 29). Thus the bifurcation along arrow III is coded by two letters-atoms C_2. When the value of g changes, the bifurcation diagram is deformed; for sufficiently large g it has the form shown in Figure 31, (j). Besides, the rays are transformed into corresponding rays. Therefore, the bifurcation along the arrow IV has the same type as the bifurcation which occurs at the intersection of the middle

ray in Figure 31, (j). It has type C_2 and can be obtained in the same way as the bifurcation along the arrow III. Examining all the other cases in the same way, one can determine all bifurcations of Liouville tori. The answer is shown in Figure 31.

PROPOSITION 7. *Let the Hamiltonian* (2.9) *(Steklov's case) be represented in the form* (8.2). *Then the bifurcation diagrams of the momentum mapping* $H \times K : TS^2 \to \mathbb{R}^2$ *are obtained from the bifurcation diagrams shown in Figure* 31 *via a nondegenerate linear transformation of the plane* $\mathbb{R}^2(k, h)$. *The additional integral is Bott on all nonsingular isoenergy surfaces*

$$Q_c = \{ f_1 = 1 , f_2 = g , H = c \},$$

with the exception of those for which the line

$$\alpha h + \beta k = c - \gamma - \delta g$$

on the plane $\mathbb{R}^2(k, h)$ *passes through the point where the ray is tangent to the curve or through a cusp of the curve (for the diagram in Figure* 31). *Bifurcations of Liouville tori at critical values of the momentum mapping* $H \times K$ *are shown in Figure* 31. *The list of all possible Fomenko invariants for Steklov's case (for different* α, β, g, h*) consists of* 6 *words-molecules of type* 1, 2, 5, 12, 13, *and* 17 *from the Table (see the Supplement).*

§9. Four-dimensional rigid body

As we showed in §1, different generalizations of the classical problem of rigid body motion (introducing the gyrostatic momentum, changing the potential, and so on) are described by Euler's equations (1.11) for the Lie algebra $e(3)$. Analogous equations may also be examined for other Lie algebras. In this section Euler's equations for the Lie algebra $so(4)$ with quadratic Hamiltonian will be examined.

Elements of the Lie algebra $so(4)$ are represented as skew-symmetric matrices X with the ordinary commutator

$$[X, Y] = XY - YX. \tag{9.1}$$

Let the matrix X be of the form:

$$X = \begin{pmatrix} 0 & -M_3 & M_2 & p_1 \\ M_3 & 0 & -M_1 & p_2 \\ -M_2 & M_1 & 0 & p_3 \\ -p_1 & -p_2 & -p_3 & 0 \end{pmatrix}.$$

Then the Poisson bracket on $so(4)^*$ corresponding to the commutator (9.1) is of the form:

$$\{M_i, M_j\} = \varepsilon_{ijk} M_k, \qquad \{M_i, p_j\} = \varepsilon_{ijk} p_k, \qquad \{p_i, p_j\} = \varepsilon_{ijk} M_k. \tag{9.2}$$

The Hamiltonian system for the Lie algebra $so(4)$ is written in the form of the Euler equations

$$\dot{M}_i = \{M_i, H\},$$
$$\dot{p}_i = \{p_i, H\}, \tag{9.3}$$

where the function $H(M, p)$ is the Hamiltonian.

The bracket (9.2) in $\mathbb{R}^6(M, p)$ is degenerate. Invariants of the Lie algebra $so(4)$

$$f_1 = M_1^2 + M_2^2 + M_3^2 + p_1^2 + p_2^2 + p_3^2,$$
$$f_2 = M_1 p_1 + M_2 p_2 + M_3 p_3 \tag{9.4}$$

commute with all functions $f(M, p)$. The common level surfaces of the functions f_1 and f_2 are the orbits of the coadjoint representation:

$$O(d_1, d_2) = \{f_1 = d_1, f_2 = d_2\} \subset \mathbb{R}^6(M, p). \tag{9.5}$$

The restriction of the Poisson bracket (9.2) to these orbits is nondegenerate. The orbits are nonsingular when $d_1 > |2d_2|$. They are homeomorphic to $S^2 \times S^2$. When $d_1 = |2d_2|$, singular orbits homeomorphic to S^2 are obtained. If $d_1 < |2d_2|$, then $O(d_1, d_2) = \varnothing$. Therefore, the bracket (9.2) determines a symplectic structure on the orbits $S^2 \times S^2$. The system (9.3) determines a Hamiltonian system with two degrees of freedom on these orbits. Its complete integrability in the sense of Liouville is equivalent to the existence of one additional integral K, which is functionally independent with the Hamiltonian H on the orbits.

Let us examine the Hamiltonian of the form

$$H = a_1 M_1^2 + a_2 M_2^2 + a_3 M_3^2 + c_1 p_1^2 + c_2 p_2^2 + c_3 p_3^2. \tag{9.6}$$

In [26] it was shown that an additional quadratic integral for the Hamiltonian (9.6) exists only in the case when the parameters of the Hamiltonian satisfy the relation

$$a_1 c_1(a_2 + c_2 - a_3 - c_3) + a_2 c_2(a_3 + c_3 - a_1 - c_1)$$
$$+ a_3 c_3(a_1 + c_1 - a_2 - c_2) = 0. \tag{9.7}$$

Let us note that the Hamiltonian (9.6) satisfying condition (9.7) is the Hamiltonian of the normal series for $so(4)$ (see [1]). The equations (9.3) with Hamiltonian (9.6), (9.7) are sometimes said to be the equations of 4-dimensional rigid body motion (it is the analog of the ordinary Euler case). Some problems of physics and mechanics are also described by these equations (see, for example, [1, Supplement 2]).

Let us examine relation (9.7). It is easy to show that it is equivalent to one of the following two conditions:

$$a_1 + c_1 = a_2 + c_2 = a_3 + c_3 \tag{9.8}$$

or

$$\begin{cases} a_1 c_1 = q + r(a_1 + c_1), \\ a_2 c_2 = q + r(a_2 + c_2), \\ a_3 c_3 = q + r(a_3 + c_3), \end{cases} \tag{9.9}$$

where q and r are certain constants. If the first condition (9.8) is valid, then the Hamiltonian (9.6) is of the form

$$H_0 = b_1 M_1^2 + b_2 M_2^2 + b_3 M_3^2 - (b_1 p_1^2 + b_2 p_2^2 + b_3 p_3^2). \qquad (9.10)$$

The second condition (9.9) may be rewritten as:

$$\begin{cases} (r - a_1)(r - c_1) = r^2 + q, \\ (r - a_2)(r - c_2) = r^2 + q, \\ (r - a_3)(r - c_3) = r^2 + q. \end{cases} \qquad (9.11)$$

If $r^2 + q = 0$, then at least three of the coefficients a_i, c_i $(i = 1, 2, 3)$ are equal to zero. Then a linear coordinate transformation in $\mathbb{R}^6(M, p)$, preserving the bracket (9.2), reduces the Hamiltonian (9.6) to one of the following:

$$H_1 = b_1 M_1^2 + b_2 M_2^2 + b_3 M_3^2, \qquad (9.12)$$

$$H_2 = b_1 p_1^2 + b_2 p_2^2 + b_3 p_3^2. \qquad (9.13)$$

Let $r^2 + q \neq 0$. Then the Hamiltonian (9.6) may be written in the form

$$H = A H_3 + r f_1, \qquad (9.14)$$

where

$$H_3 = b_1 M_1^2 + b_2 M_2^2 + b_3 M_3^2 + b_2 b_3 p_1^2 + b_3 b_1 p_2^2 + b_1 b_2 p_3^2, \qquad (9.15)$$

$$b_1 = \frac{(c_2 - r)(c_3 - r)}{r^2 + q}, \qquad b_2 = \frac{(c_3 - r)(c_1 - r)}{r^2 + q}, \qquad b_3 = \frac{(c_1 - r)(c_2 - r)}{r^2 + q},$$

$$A = \frac{(a_1 - r)(a_2 - r)(a_3 - r)}{r^2 + q}.$$

The equation (9.14) easily follows from (9.11). Since the addition of the invariant f_1 to the Hamiltonian does not change the system (9.3), we see that the Hamiltonian (9.6) is transformed to Hamiltonian of the form (9.15) if (9.11) is valid and $r^2 + q \neq 0$.

Thus, we have proved that an arbitrary Hamiltonian of the form (9.6), (9.7) is equivalent to one of the Hamiltonians H_0, H_1, H_2, H_3, each of which depends only on three parameters b_1, b_2, b_3 (in fact we can assume that H_0, H_1, H_2 depend on two parameters only, because multiplication by constant does not change their form).

Now let us examine the Hamiltonian H_0. The function

$$K_0 = (b_1 + b_2)(b_1 + b_3)p_1^2 + (b_2 + b_3)(b_2 + b_1)p_2^2 + (b_3 + b_1)(b_3 + b_2)p_3^2 \qquad (9.16)$$

may be taken as an integral which is functionally independent of H_0 on the orbits (9.5). It is easy to check that all the Hamiltonians (9.6), (9.7),

except Hamiltonians of the form (9.12), can be represented as the linear combination

$$H = \alpha H_0 + \beta K_0 + \gamma f_1, \qquad (9.17)$$

where α, β, and γ are some coefficients. Further, one may assume that

$$0 < b_1 < b_2 < b_3.$$

Therefore, the bifurcation diagrams for an arbitrary Hamiltonian (9.6), (9.7) are obtained from bifurcation diagrams of the mapping

$$H_0 \times K_0 \colon S^2 \times S^2 \to \mathbb{R}^2(h_0, k_0)$$

under a nondegenerate linear transformation of the plane $\mathbb{R}^2(h_0, k_0)$ (see §§7 and 8).

The case $H = H_1$ differs from all other cases. The integral in this case is

$$K_1 = M_1^2 + M_2^2 + M_3^2.$$

It is evident that the Hamiltonian system (9.3) with Hamiltonian (9.12) determines exactly the same phase flow as in the ordinary Euler case (coordinate transformation: $S = M$, $R = p$). The bifurcation diagram for the momentum mapping

$$K_1 \times H_1 \colon S^2 \times S^2 \to \mathbb{R}^2(k_1, h_1)$$

is shown in Figure 33. It consists of five segments which lie on the lines

$$h_1 = b_i k_1 \quad (i = 1, 2, 3), \qquad 2k_1 = d_1 \pm \sqrt{d_1^2 - 4d_2^2},$$

where d_1, d_2 determine the orbit (9.5).

The bifurcation diagram of the mapping

$$f_2 \times H_1 \colon S^5 \to \mathbb{R}^2(d_2, h_1),$$

where

$$S^5 = \{f_1 = d_1\} \subset \mathbb{R}^6(M, p),$$

is shown in Figure 34. It consists of three ellipses and two vertical segments

$$\{2d_2 = \pm d_1, \quad b_1 d_1 < 2h < b_3 d_1\},$$

which are tangent to all three ellipses (we assume that $0 < b_1 < b_2 < b_3$). This is the complete collection of separating curves for this case. The topological type and Fomenko invariant of Q_h are indicated for each domain in Figure 34.

Now let us examine the Hamiltonian H_0. Bifurcation diagrams of the mapping $H_0 \times K_0$ are presented in [27]. Let us describe their construction. We assume that the coefficients of H_0 satisfy the condition

$$0 < b_1 < b_2 < b_3. \qquad (9.18)$$

Cases when there are negative values among the b_i are reduced to (9.18) by a linear coordinate transformation in $\mathbb{R}^6(M, p)$ which preserves the bracket (9.2).

The orbit (9.5) is determined by two parameters d_1 and d_2. When $|2d_2| < d_1$, the orbit is homeomorphic to $S^2 \times S^2$. Critical points of the function $\widetilde{H}_0 = H_0|_{S^2 \times S^2}$ are obtained from the condition

$$\begin{cases} \operatorname{grad} H_0 = \lambda_1 \operatorname{grad} f_1 + \lambda_2 \operatorname{grad} f_2, \\ f_1(M, p) = d_1, \\ f_2(M, p) = d_2. \end{cases} \tag{9.19}$$

Twelve critical points are the solution of the system (9.19):

$$(\pm A, 0, 0, \pm B, 0, 0), (\pm B, 0, 0, \pm A, 0, 0),$$
$$(0, \pm A, 0, 0, \pm B, 0), (0, \pm B, 0, 0, \pm A, 0), \tag{9.20}$$
$$(0, 0, \pm A, 0, 0, \pm B), (0, 0, \pm B, 0, 0, \pm A) \in \mathbb{R}^6(M, p),$$

where $2A = \sqrt{d_1 + 2d_2} + \sqrt{d_1 - 2d_2}$, $2B = \sqrt{d_1 + 2d_2} - \sqrt{d_1 - 2d_2}$.

Let us now find the critical points of the function $\widetilde{K}_0 = K_0|_{Q_c}$, where

$$Q_c = \{f_1 = d_1, f_2 = d_2, H = c\},$$

and c is a noncritical value of $\widetilde{H}_0$. As in Steklov's case (see §8) let us write the condition

$$\operatorname{grad} K_0 = \mu_1 \operatorname{grad} f_1 + \mu_2 \operatorname{grad} f_2 + \mu \operatorname{grad} H_0$$

in the form

$$\begin{cases} G_\mu \begin{pmatrix} M \\ p \end{pmatrix} = 0, \\ f_1(M, p) = d_1, \\ f_2(M, p) = d_2, \end{cases} \tag{9.21}$$

where $G_\mu = G_{K_0} - \mu G_{H_0} - \mu_1 G_1 - \mu_2 G_2$ is the matrix obtained as the linear combination of the Hessians of the functions f_1, f_2, H_0, K_0. From the explicit form of G_μ it is easy to determine that the dimension of the kernel of the matrix G_μ is equal to 1 or 3. In the case when the kernel of G_μ is one-dimensional, only points (9.20) are solutions of the system (9.21). If the kernel is three-dimensional, then the system (9.21) may be transformed to the following form:

$$\begin{cases} \mu_1 = -\mu^2 - \mu(b_1 + b_2 + b_3), \\ \mu_2^2 = 4\mu(\mu + b_1 + b_2)(\mu + b_2 + b_3)(\mu + b_3 + b_1), \\ \mu_2 p_1 = 2\mu(\mu + b_2 + b_3)M_1, \\ \mu_2 p_2 = 2\mu(\mu + b_3 + b_1)M_2, \\ \mu_2 p_3 = 2\mu(\mu + b_1 + b_2)M_3, \\ M_1^2 + M_2^2 + M_3^2 + p_1^2 + p_2^2 + p_3^2 = d_1, \\ M_1 p_1 + M_2 p_2 + M_3 p_3 = d_2, \end{cases} \tag{9.22}$$

where $d_2 \neq 0$. The case when $d_2 = 0$ will be examined separately.

While solving the system (9.22), three qualitatively different cases appear:

(a) $\varepsilon_1 < D < 1$;

(b) $\varepsilon_2 < D < \varepsilon_1$;

(c) $0 < D < \varepsilon_2$,

where $|2d_2|/d_1$ is denoted by D, and ε_1, ε_2 are some constants which depend only on the parameters b_1, b_2, b_3 of the Hamiltonian. The second equation from system (9.22) determines the curve on the plane (μ, μ_2) which is shown in Figure 35. The system (9.22) has solutions iff the point (μ, μ_2) lies on the heavily drawn segments of the curve in Figure 35. Cases (a), (b), and (c) in Figure 35 correspond to different ranges of D indicated above.

If the point (μ, μ_2) lies on the heavily drawn segments of the curve and does not coincide with any of heavily drawn points denoted in Figure 35 by numbers, then the solution of system (9.22) consists of only two circles in $\mathbb{R}^6(M, p)$. Under the mapping $H_0 \times K_0$, both these circles transform into the point

$$(h_0(\mu), k_0(\mu)) \in \mathbb{R}^2(h_0, k_0),$$

where

$$
\begin{aligned}
h_0(\mu) &= d_1(2\mu + b_1 + b_2 + b_3) - d_2 d\mu_2/d\mu, \\
k_0(\mu) &= d_1\mu^2 + d_2(\mu_2 - \mu d\mu_2/d\mu).
\end{aligned}
\tag{9.23}
$$

Here $\mu_2(\mu)$ is the function which is determined by the second equation from (9.22). So we obtain the mapping (9.23) of heavily drawn segments of the curve into the plane $\mathbb{R}^2(h_0, k_0)$. The image of this mapping is the bifurcation diagram of the mapping $H_0 \times K_0 : S^2 \times S^2 \to \mathbb{R}^2(h_0, k_0)$.

Bifurcation diagrams given in Figure 36 (cases (a), (b), and (c) correspond to cases (a), (b), and (c) in Figure 35). The fact that they are of the form shown in Figure 36 can be proved in the following way. Points marked in Figure 35 by numbers transform into points marked by the same numbers in Figure 36 under the mapping (9.23). These points are the images of points (9.20) under the mapping $H_0 \times K_0$. Their coordinates on the plane $\mathbb{R}^2(h_0, k_0)$ are

$$
\left(\pm b_i \sqrt{d_1^2 - 4d_2^2}, \; (b_i + b_j)(b_i + b_k) \frac{d_1 \mp \sqrt{d_1^2 - 4d_2^2}}{2} \right),
\tag{9.24}
$$

$$\{i, j, k\} = \{1, 2, 3\}.$$

Thus, the bifurcation diagram is "glued" from segments of the curve shown in Figure 35. The relation

$$dk_0/d\mu = \mu \, dh_0/d\mu$$

is valid for functions $h_0(\mu)$ and $k_0(\mu)$ which define the mapping (9.23) (see (3.24)). It is easy to deduce convexity of each segment of the bifurcation diagram from this fact. It remains to determine when the bifurcation diagram

has cusps. The existence of a cusp on the bifurcation curve for some $\mu = \varepsilon$ is equivalent to the condition

$$\frac{dh_0}{d\mu}(\varepsilon) = 0.$$

Using the explicit expression (9.23) for the function $h_0(\mu)$, one can show that cusps appear only in case (c) and are situated as shown in Figure 36, (c).

As in Steklov's case, one can determine the indices of critical circles and the bifurcations of Liouville tori.

PROPOSITION 8. *For the Hamiltonian system* (9.3) *with Hamiltonian* (9.6), (9.7) *the bifurcation diagram of the momentum mapping*

$$H \times K \colon S^2 \times S^2 \to \mathbb{R}^2$$

is obtained from diagrams shown in Figure 36 *under the nondegenerate linear transformation of the plane* $\mathbb{R}^2(h_0, k_0)$. *The additional integral is Bott on all nonsingular*

$$Q_h = \{f_1 = d_1, f_2 = d_2, H = h\},$$

with the exception of those for which the line $\alpha h_0 + \beta k_0 = h - \gamma d_1$ *passes through a cusp of the bifurcation curve (here* α, β, γ *are the coefficients from* (9.17)). *Bifurcations of Liouville tori at critical values of the mapping* $H \times K$ *are shown in Figure* 36.

While constructing bifurcation diagrams of the mapping $H_0 \times K_0$, we have assumed that $d_2 \neq 0$. Now let us examine the case when $d_2 = 0$. For the mapping $H_0 \times K_0 \colon \{f_1 = d_1, f_2 = 0\} \to \mathbb{R}^2(h_0, k_0)$ the bifurcation diagram simplifies considerably. It consists of four segments and the part of parabola which is tangent to all these segments (see Figure 37). The equations of lines on which these segments lie are

$$k_0 = (b_i + b_j)(b_k d_1 - h_0), \qquad \{i, j, k\} = \{1, 2, 3\}. \tag{9.25}$$

The equation of the parabola is

$$4d_1 k_0 = (h_0 - d_1(b_1 + b_2 + b_3))^2.$$

When $d_2 \to 0$, the segment of the bifurcation curve between the cusps (see Figure 36,(c)) "approaches" the segment of the curve with end-points 1, 6, and when $d_2 = 0$, it "combines" with it.

Let us transfer the lines which contain segments of bifurcation diagram (for $d_2 = 0$) to the origin (see Figure 38). They divide the plane $\mathbb{R}^2(h_0, k_0)$ into domains. The type of the Hamiltonian (9.6), (9.7) represented in the form (9.17) depends on the domain where the line $\alpha h_0 + \beta k_0 = 0$ appears (here α and β are taken from (9.17)). Up to the sign, the following types

of Hamiltonians correspond to the domains in Figure 38:

$$H_4 = \frac{M_1^2}{A_1} + \frac{M_2^2}{A_2} + \frac{M_3^2}{A_3} + A_1 p_1^2 + A_2 p_2^2 + A_3 p_3^2,$$

$$H_5 = \frac{M_1^2}{A_1} + \frac{M_2^2}{A_2} + \frac{M_3^2}{A_3} - A_1 p_1^2 - A_2 p_2^2 - A_3 p_3^2, \qquad (9.26)$$

$$H_6 = \frac{M_1^2}{A_1} + \frac{M_2^2}{A_2} - \frac{M_3^2}{A_3} + A_1 p_1^2 + A_2 p_2^2 - A_3 p_3^2,$$

where $A_1, A_2, A_3 > 0$.

In fact, if the Hamiltonian H is represented in the form (9.17), then it can be written in the following way:

$$H = \frac{\alpha^2}{\beta}(y_1 M_1^2 + y_2 M_2^2 + y_3 M_3^2 + y_2 y_3 p_1^2 + y_3 y_1 p_2^2 + y_1 y_2 p_3^2) +$$

$$+ (\alpha(b_1 + b_2 + b_3) - \alpha^2/\beta + \gamma) f_1, \qquad (9.27)$$

where $y_1 = 1 - \frac{\beta}{\alpha}(b_2 + b_3)$, $y_2 = 1 - \frac{\beta}{\alpha}(b_3 + b_1)$, $y_3 = 1 - \frac{\beta}{\alpha}(b_1 + b_2)$, and b_1, b_2, b_3 are coefficients in H_0 and K_0. Therefore, if α and β differ from zero, then the Hamiltonian $H = \alpha H_0 + \beta K_0 + \gamma f_1$ is equivalent to a Hamiltonian of the form H_3 (see (9.15)). Suppose that y_1, y_2, y_3 are not equal to zero. Let us put

$$A_1 = \sqrt{\left|\frac{y_2 y_3}{y_1}\right|}, \qquad A_2 = \sqrt{\left|\frac{y_3 y_1}{y_2}\right|}, \qquad A_3 = \sqrt{\left|\frac{y_1 y_2}{y_3}\right|}. \qquad (9.28)$$

Substituting the expressions (9.28) into (9.27) and dividing by a constant, we see that the Hamiltonian (9.27) is equivalent to

$$H = \sigma_1 \frac{M_1^2}{A_1} + \sigma_2 \frac{M_2^2}{A_2} + \sigma_3 \frac{M_3^2}{A_3} + \sigma_2 \sigma_3 A_1 p_1^2 + \sigma_3 \sigma_1 A_2 p_2^2 + \sigma_1 \sigma_2 A_3 p_3^2, \quad (9.29)$$

where $\sigma_i = \mathrm{sgn}(y_i)$ $(i = 1, 2, 3)$. The Hamiltonian (9.29) may be reduced to the form (9.26) by a coordinate change of the form

$$M_1' = M_1, \quad M_2' = p_2, \quad M_3' = p_3, \quad p_1' = p_1, \quad p_2' = M_2, \quad p_3' = M_3,$$

$$(A_2' = 1/A_2, \qquad A_3' = 1/A_3),$$

which preserves the bracket (9.2).

Comparing the expressions (9.27) for y_1, y_2, y_3 and the equations of lines (9.25) (and also taking into account the fact that $0 < b_1 < b_2 < b_3$) one obtains domains corresponding to the Hamiltonians H_4, H_5, H_6 shown in Figure 38. If $\beta = 0$ in formula (9.17), then the Hamiltonian H is equivalent to the Hamiltonian H_0. In Figure 38, the vertical line $h_0 = 0$ corresponds to this Hamiltonian. If either $\alpha = 0$ or one of the y_i is equal to zero in the expression (9.27), then the Hamiltonian H is equivalent to

the Hamiltonian H_2 (see (9.13)). The four lines which separate domains in Figure 38 correspond to these Hamiltonians.

Now let us describe the curves on the plane $\mathbb{R}^2(d_2, h)$ which separate domains of different topological type, and the Fomenko invariant of

$$Q_h = \{f_1 = d_1, f_2 = d_2, H = h\},$$

where H is any Hamiltonian of the form H_0, H_2, H_4, H_5, H_6. The curves which separate domains with different topological type of Q_h are the images of critical points of the mapping

$$f_2 \times H: S^5 \rightarrow \mathbb{R}^2(d_2, h), \qquad (9.30)$$

where

$$S^5 = \{f_1 = d_1\} \subset \mathbb{R}^6(M, p).$$

Calculating, one sees that for any of the examined Hamiltonians, the critical points of the mapping (9.30) fill two 2-spheres:

$$\{p_1^2 + p_2^2 + p_3^2 = d_1/2, M_1 = \pm p_1, M_2 = \pm p_2, M_3 = \pm p_3\}$$
$$\subset S^5 \subset \mathbb{R}^6(M, p) \qquad (9.31)$$

and three circles

$$\{M_2 = M_3 = p_2 = p_3 = 0, M_1^2 + p_1^2 = d_1\},$$
$$\{M_3 = M_1 = p_3 = p_1 = 0, M_2^2 + p_2^2 = d_1\}, \qquad (9.32)$$
$$\{M_1 = M_2 = p_1 = p_2 = 0, M_3^2 + p_3^2 = d_1\} \subset S^5 \subset \mathbb{R}^6(M, p).$$

Besides, for the Hamiltonians H_4 and H_6, one obtains two more 2-dimensional spheres:

$$\{(1 + A_1^2)p_1^2 + (1 + A_2^2)p_2^2 + (1 + A_3^2)p_3^2 = d_1, M_1 = \pm A_1 p_1,$$
$$M_2 = \pm A_2 p_2, M_3 = \pm \sigma A_3 p_3\} \subset S^5 \subset \mathbb{R}^6(M, p), \qquad (9.33)$$

where $\sigma = 1$ for the Hamiltonian H_4 and $\sigma = -1$ for the Hamiltonian H_6.

The critical points (9.32) transform under the mapping (9.30) into three ellipses for which the line $d_2 = 0$ is an axis of symmetry and lines $d_2 = \pm d_1/2$ are common tangents. The 2-dimensional spheres (9.31) (they are singular orbits of the coadjoint representation) are mapped into two segments which lie on the lines $d_2 = \pm d_1/2$. The spheres (9.33) are mapped into two other segments which lie on the lines $h = \pm 2d_2$, which are also common tangents to ellipses. As a result one obtains separating curves shown in Figure 39. Cases (a)–(f) in Figure 39 correspond to different Hamiltonians: (a) H_4; (b) H_6; (c) H_5; (d) H_2, where b_1, b_2, b_3 have the same sign; (e) H_2, where b_1, b_2, b_3 have different signs; (f) H_0. The dotted line in Figures 39(a)–39(f) separates domains with different Fomenko invariants. As in Clebsch's case (see Figure 23), it may intersect a different number of domains. This curve can be constructed if one determines coordinates of cusps of the bifurcation diagram shown in Figure 36. The type of the Fomenko invariant is given by numbers in brackets in Figures 39.

PROPOSITION 9. *Any Hamiltonian of the form* (9.6), (9.7) (*a 4-dimensional rigid body*) *is equivalent to one of the Hamiltonians of type* H_0, H_1, H_2, H_4, H_5, H_6. *Separating curves and types of Fomenko invariants for these Hamiltonians are given in Figures* 39 *and* 34. *The additional integral in this case is Bott on* $Q_h = \{f_1 = d_1, f_2 = d_2, H = h\}$ *if the point* (d_2, h) *does not lie on the separating curve. The complete list of Fomenko invariants for all Hamiltonians of the form* (9.6), (9.7) *consists of* 9 *invariants of the type* 1, 2, 5, 9, 12, 13, 14, 15, 16 (*see the Supplement*).

Let us note the connection between Clebsch's case and the Hamiltonian system on $so(4)^*$ just examined. Let us consider another bracket $\{\ ,\ \}'$ in $\mathbb{R}^6(M, p)$:

$$\{M_i, M_j\}' = \varepsilon_{ijk} M_k, \qquad \{M_i, p_j\}' = \varepsilon_{ijk} p_k,$$
$$\{p_i, p_j\}' = \varepsilon_{ijk} M_k / N^2. \tag{9.34}$$

The bracket (9.34) is obtained from the bracket (9.2) by multiplying every p_i by some constant N, and this is equivalent to changing the basis in $so(4)$. Taking this into account, one can see that the kernel of bracket (9.34) is generated by the functions

$$f_1(N) = \frac{M_1^2 + M_2^2 + M_3^2}{N^2} + p_1^2 + p_2^2 + p_3^2, \tag{9.35}$$
$$f_2 = M_1 p_1 + M_2 p_2 + M_3 p_3.$$

The condition of integrability for the Hamiltonian (9.6) with respect to the bracket (9.34) is obtained from (9.7):

$$a_1 c_1 (a_2 - a_3) + a_2 c_2 (a_3 - a_1) + a_3 c_3 (a_1 - a_2)$$
$$+ \frac{a_1 c_1 (c_2 - c_3) + a_2 c_2 (c_3 - c_1) + a_3 c_3 (c_1 - c_2)}{N^2} = 0. \tag{9.36}$$

It is evident that as $N \to \infty$ the bracket (9.34) becomes the bracket (1.8) on $e(3)^*$, and functions (9.35) transform into invariants of the Lie algebra $e(3)$ (1.15). The relation (9.36) as $N \to \infty$ transforms into Clebsch's condition of integrability for the Hamiltonian

$$H = a_1 S_1^2 + a_2 S_2^2 + a_3 S_3^2 + c_1 R_1^2 + c_2 R_2^2 + c_3 R_3^2 \quad \text{on} \quad e(3)^*.$$

This contraction of $so(4)$ to $e(3)$ is described in [12].

Let us note that the Hamiltonians H_2, H_4, H_5, H_6 satisfy the relation (9.36) for any N. Thus the bifurcation diagrams for any N are obtained from the bifurcation diagrams shown in Figure 36 by a nondegenerate linear transformation of the plane $\mathbb{R}^2(h_0, k_0)$. This linear transformation depends on N. When $N \to \infty$, the following happens: the points denoted in Figure 36 by numbers 4, 5, 6 "go to infinity", and in the limit one obtains the bifurcation diagrams for Clebsch's case (see Figure 22).

A similar situation occurs for separating curves. For the bracket (9.34), separating curves are also of the form shown in Figure 39, but the vertical segments tangent to the ellipses lie on the lines $d_2 = \pm d_1 N/2$. As $N \to \infty$, these segments also "go to infinity", and in the limit the separating curves for Clebsch's case are obtained (see Figure 23). Cases (a) and (c) in Figure 23 correspond to cases (a) and (b) in Figure 39. For Figure 39(c) there is no analog in Clebsch's case, because some isoenergy surfaces Q_h become noncompact under the contraction.

Supplement (List of Fomenko invariants)

The Fomenko invariants for the isoenergy surfaces Q_h of integrable Hamiltonian systems investigated in this work are listed in the Table (after references). For each invariant graph Γ, the word-molecule and the complexity of the invariant (for the precise definition see [5]) are indicated.

For the letters-atoms B and C_2 the opposite segments-links which originate at these atoms correspond to Liouville tori which lie on the same level surface of an additional integral. This allows us to distinguish different Fomenko invariants which have "topologically equivalent" words-molecules (for example, invariants 4 and 9).
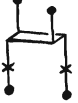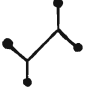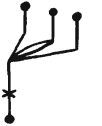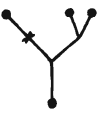
References

1. A. T. Fomenko *Symplectic geometry: methods and applications*, Izdat. Moskov. Univ., Moscow, 1988; English transl. of a first draft, in two halves, *Symplectic geometry*, Gordon and Breach, New York, 1988, and *Integrability and nonintegrability in geometry and mechanics*, Kluwer, Dordrecht, 1988.

2. _____, *The topology of surfaces of constant energy of integrable Hamiltonian systems and obstructions to integrability*, Izv. Akad. Nauk SSSR Ser. Mat. **50** (1986), 1276–1307; English transl. in Math. USSR Izv. **29** (1987), 629–658.

3. _____, *Morse theory of integrable Hamiltonian systems*, Dokl. Akad. Nauk SSSR **287** (1986), 1071–1075; English transl. in Soviet Math. Dokl. **33** (1986), 502–506.

4. _____, *Topological invariants of Hamiltonian systems integrable in the sense of Liouville*, Funktsional. Anal. i Prilozhen. **22** (1988), no. 4, 38–51; English transl. in Functional Anal. Appl. **22** (1988).

5. A. V. Bolsinov, S. V. Matveev, and A. T. Fomenko, *Topological classification of integrable Hamiltonian systems with two degrees of freedom. List of systems of small complexity*, Uspekhi Mat. Nauk **45** (1990), no. 2, 49–77; English transl. in Russian Math. Surveys **45** (1990), no. 2, 59–94.

6. M. P. Kharlamov, *Topological analysis of integrable cases in dynamics of rigid body*, Izdat. Leningrad. Univ., Leningrad, 1988. (Russian)

7. V. V. Kozlov, *Methods of qualitative analysis in the dynamics of a rigid body*, Izdat. Moskov Univ., Moscow, 1980. (Russian)

8. _____, *Integrability and nonintegrability in Hamiltonian mechanics*, Uspekhi Mat. Nauk **38** (1983), no. 1, 3–67; English transl. in Russian Math. Surveys **38** (1983), no. 1, 1–76.

9. G. V. Gorr, L. V. Kudryashova, and L. A. Stepanova, *Classical problems in the dynamics of a solid body*, "Naukova Dumka", Kiev, 1978. (Russian)

10. V. I. Arnold, V. V. Kozlov, and A. I. Neĭshtadt, *Mathematical aspects of classical and celestial mechanics*, Current Problems in Math. Fundamental Directions, vol. 3, Itogi Nauki i Tekhniki, VINITI, Moscow, 1985; English transl., Encyclopaedia of Math. Sci., vol. 3, Springer, Berlin and New York, 1988.

11. V. V. Trofimov and A. T. Fomenko, *Geometric and algebraic mechanisms for the integration of Hamiltonian systems on homogeneous spaces and Lie algebras*, Current Problems in Math. Fundamental Directions, vol. 16, Itogi Nauki i Tekhniki, VINITI, Moscow, 1987, pp. 227–299. (Russian).

12. S. P. Novikov, *The Hamiltonian formalism and many-valued analogue of Morse theory*, Uspekhi Mat. Nauk **37** (1982), no. 5, 3–49; English transl. in Russian Math. Surveys **37** (1982), no. 5, 1–56.

13. L. N. Oreshkina, *Isomorphism of two problems of mechanics*, Dokl. Akad. Nauk SSSR **291** (1986), 1080–1082; English transl. in Soviet Phys. Dokl. **21** (1986).

14. _____, *Necessary and sufficient conditions for the existence of a fourth quadratic integral in some problems of the dynamics of a rigid body*, Mekh. Tverd. Tela no. 20, **1988**, 18–29. (Russian)

15. E. I. Kharlamova and L. A. Stepanova, *On the isomorphism of some classical problems of the dynamics of a rigid body and on attempts at constructing new solutions by a change of variables*, Mekh. Tverd. Tela no. 20, **1988**, 1–13. (Russian.

16. V. V. Kozlov and D. A. Onishchenko, *Nonintegrability of Kirkhoff's equations*, Dokl. Akad. Nauk SSSR **266** (1982), 1298-1300; English transl. in Soviet Phys. Dokl. **27** (1982).

17. S. Smale, *Topology and mechanics*, Invent. Math. **10** (1970), 305–331.

18. J. Milnor, *Morse theory*, Princeton Univ. Press, Princeton, NJ, 1963.

19. S. B. Katok, *Bifurcation sets and integral manifolds in rigid body problem*, Uspekhi Mat. Nauk **27** (1972), no. 2, 126–132; English transl. in Russian Math. Surveys **27** (1972), no. 2.

20. Ya. V. Tatarinov, *On the investigation of the phase topology of compact configurations with symmetry*, Vestnik Moskov. Univ. Ser. I Mat. Mekh. **1973**, no. 5, 70–77. (Russian)

21. _____, *Portraits of the classical integrals of the problem of the rotation of a rigid body about a fixed point*, Vestnik Moskov. Univ. Ser. I Mat. Mekh. **1974**, no. 6, 99–105. (Russian)

22. A. A. Ilyukhin, *Three-dimensional problems in the nonlinear theory of elastic rods*, "Naukova Dumka", Kiev, 1979. (Russian)

23. T. I. Pogosyan, *Construction of bifurcation sets in a problem of rigid body dynamics*, Mekh. Tverd. Tela no. 12, **1980**, 9–16. (Russian)

24. _____, *Domains of possible motion in the Clebsch problem. Critical case*, Mekh. Tverd. Tela no. 15, **1983**, 3–23. (Russian)

25. _____, *Critical integral surfaces of the Clebsch problem*, Mekh. Tverd. Tela no. 16, **1984**, 19–24. (Russian)

26. A. P. Veselov, *On integrability conditions of Euler equations on so(4)*, Dokl. Akad. Nauk SSSR **270** (1983), 1298-1300; English transl. in Soviet Math. Dokl. **27** (1983), 740–742.

27. A. A. Oshemkov, *The topology of surfaces of constant energy and bifurcation diagrams for integrable cases of the dynamics rigid body on SO(4)*, Uspekhi Mat. Nauk **42** (1987), no. 6, 199-200; English transl. in Russian Math. Surveys **42** (1987), no. 6, 241–242.

Translated by THE AUTHOR

A. A. OSHEMKOV

TABLE

##	Graph Γ	Word-molecule	Complexity
1		$A - A$	(2, 1)
2		$A - B - A$ $\|$ A	(4, 3)
3		$A - A^* - A$	(3, 2)
4		$A - B - A$ $\|$ $A - B - A$	(6, 5)
5		A $\|$ $A - C_2 - A$ $\|$ A	(6, 4)
6		$A \quad A \quad A$ $\| \quad \| \quad \|$ $B - B - B$ $\| \qquad \|$ $A \qquad A$	(8, 7)
7		$A - A^* - B - A^* - A$ $\|$ A	(6, 5)
8		A $\|$ $A - A^* - C_2 - A^* - A$ $\|$ A	(8, 6)
9		$A - B - B - A$ $\| \quad \|$ $A \quad A$	(6, 5)
10		A $/$ $A - A^* - D_1 - A$ $\backslash$ A	(7, 5)
11		$A \quad A$ $\| \quad \|$ $A - A^* - B - B$ $\|$ A	(7, 6)

(Table continued)

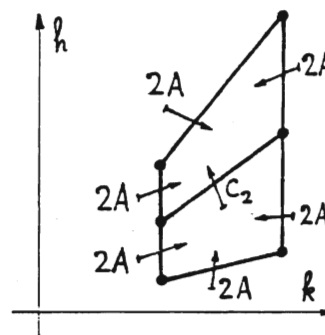| ##	Graph Γ	Word-molecule	Complexity
12		$\begin{array}{ccc} A & A & A \\ | & | & | \\ B & - C_2 - & B \\ | & | & | \\ A & A & A \end{array}$	(10, 8)
13		$A - B \quad \begin{array}{c} A \\ | \\ B \\ \ulcorner \quad \urcorner \\ \\ \llcorner \quad \lrcorner \\ B \\ | \\ A \end{array} \quad B - A$	(8, 8)
14		$A - C_2 - A \qquad A - C_2 - A$	(8, 6)
15		$A - C_2 - A \qquad \begin{array}{c} A \\ | \\ B - C_2 - B \\ | \\ A \end{array} \quad \begin{array}{c} A \\ | \\ \\ | \\ A \end{array}$	(12, 10)
16		$\begin{array}{c} A \\ | \\ B - B \\ | \\ A \end{array} \quad \begin{array}{c} A \\ | \\ B \\ \\ B \\ | \\ A \end{array} \quad \begin{array}{c} A \\ | \\ B - B \\ | \\ A \end{array}$	(12, 12)
17		$A - C_2 - A \quad \begin{array}{c} A \\ | \\ B \\ \\ B \\ | \\ A \end{array} \quad A - C_2 - A$	(12, 10)

A. A. OSHEMKOV

FIGURE 1

(a)

(b)

(c)

(d)

FIGURE 2

FIGURE 3

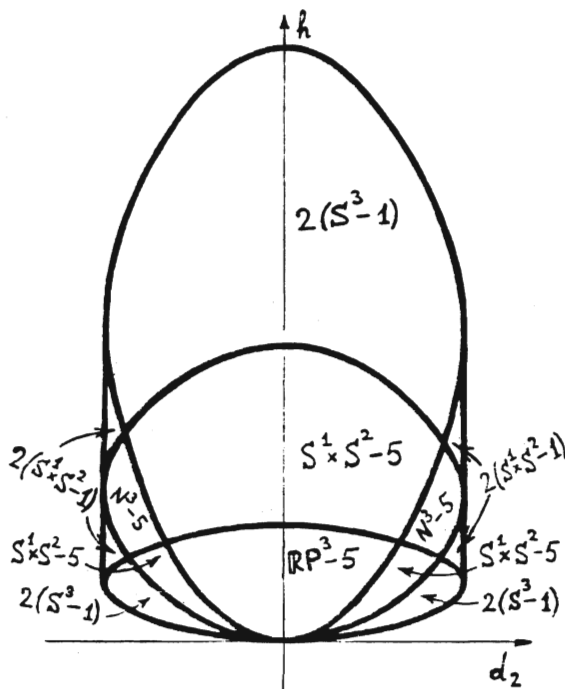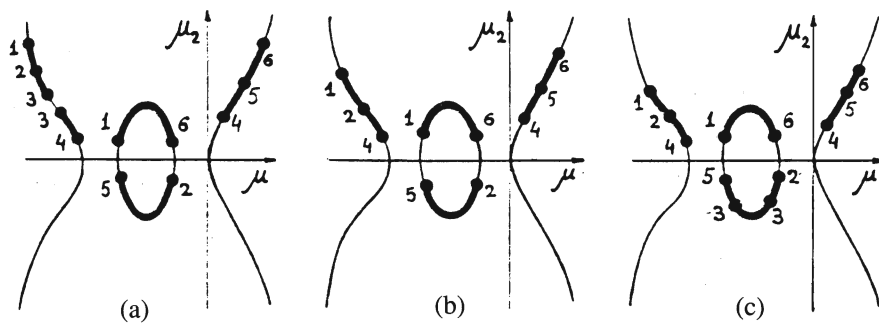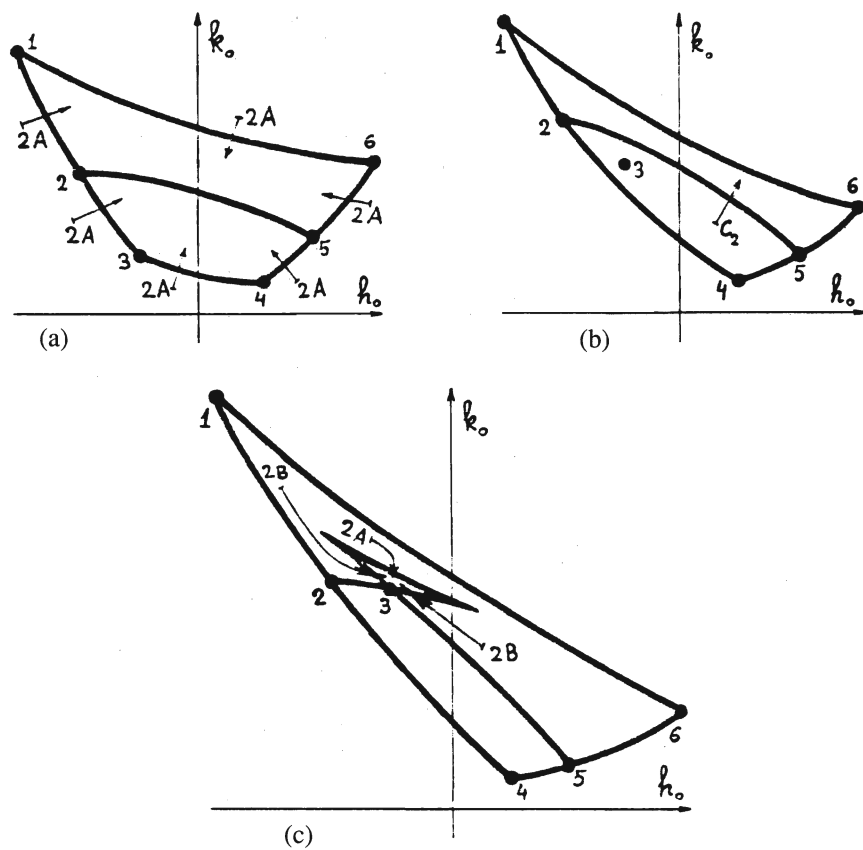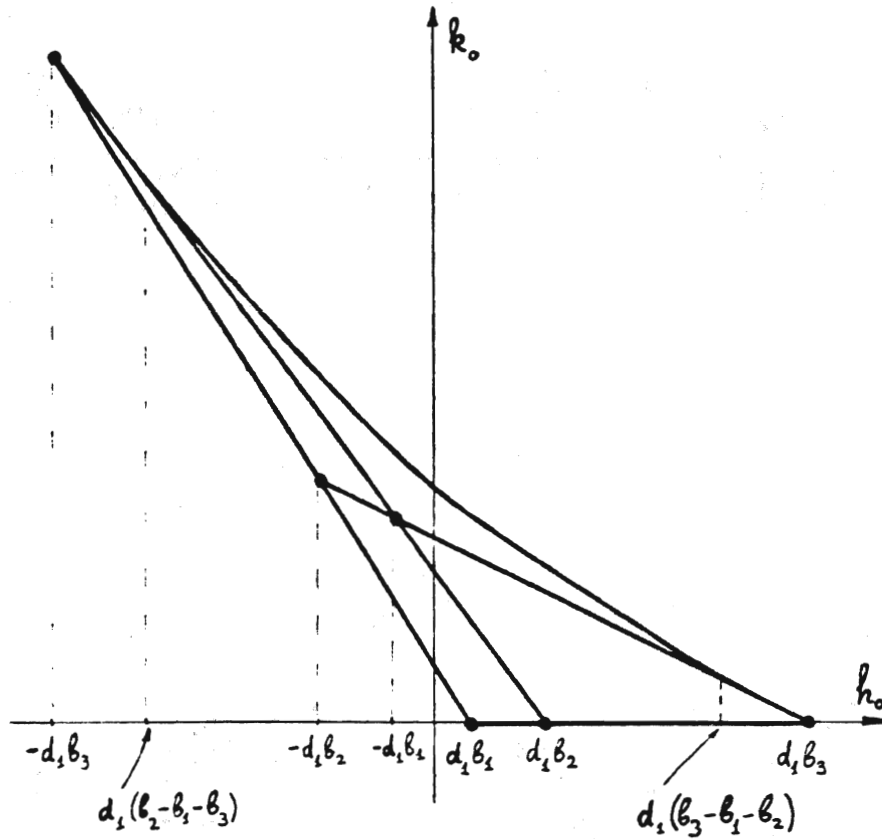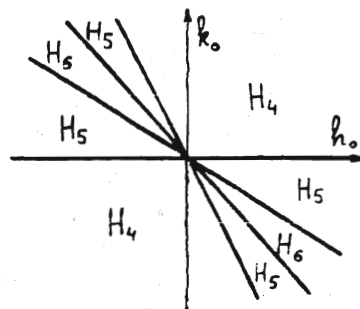FIGURE 4
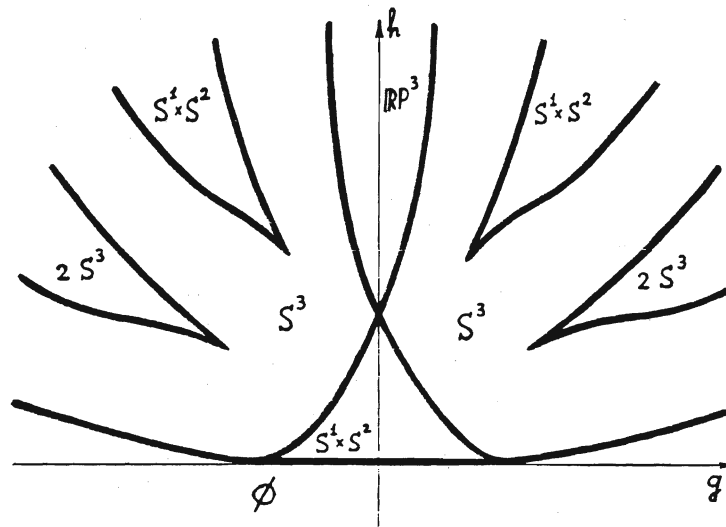
FIGURE 5
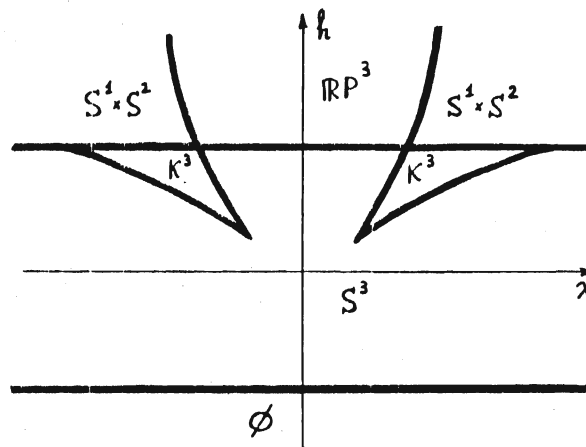
FIGURE 6
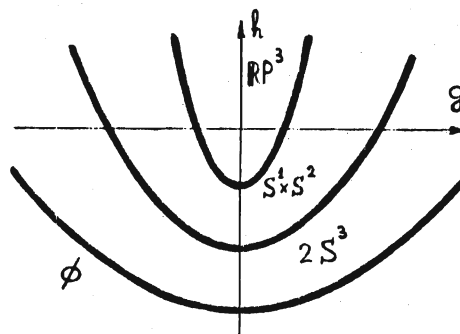
FIGURE 7
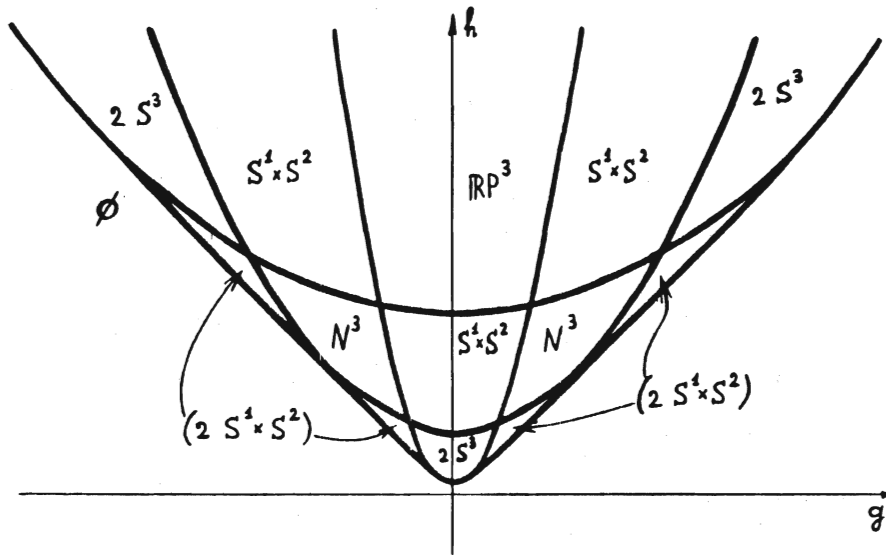
FIGURE 8
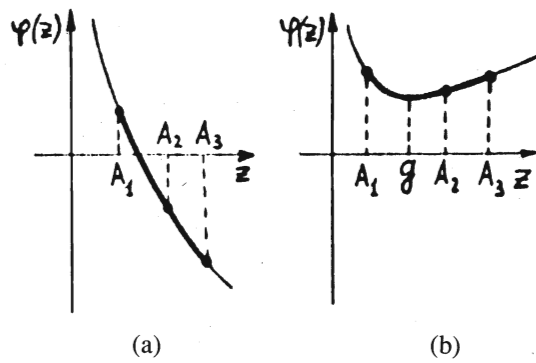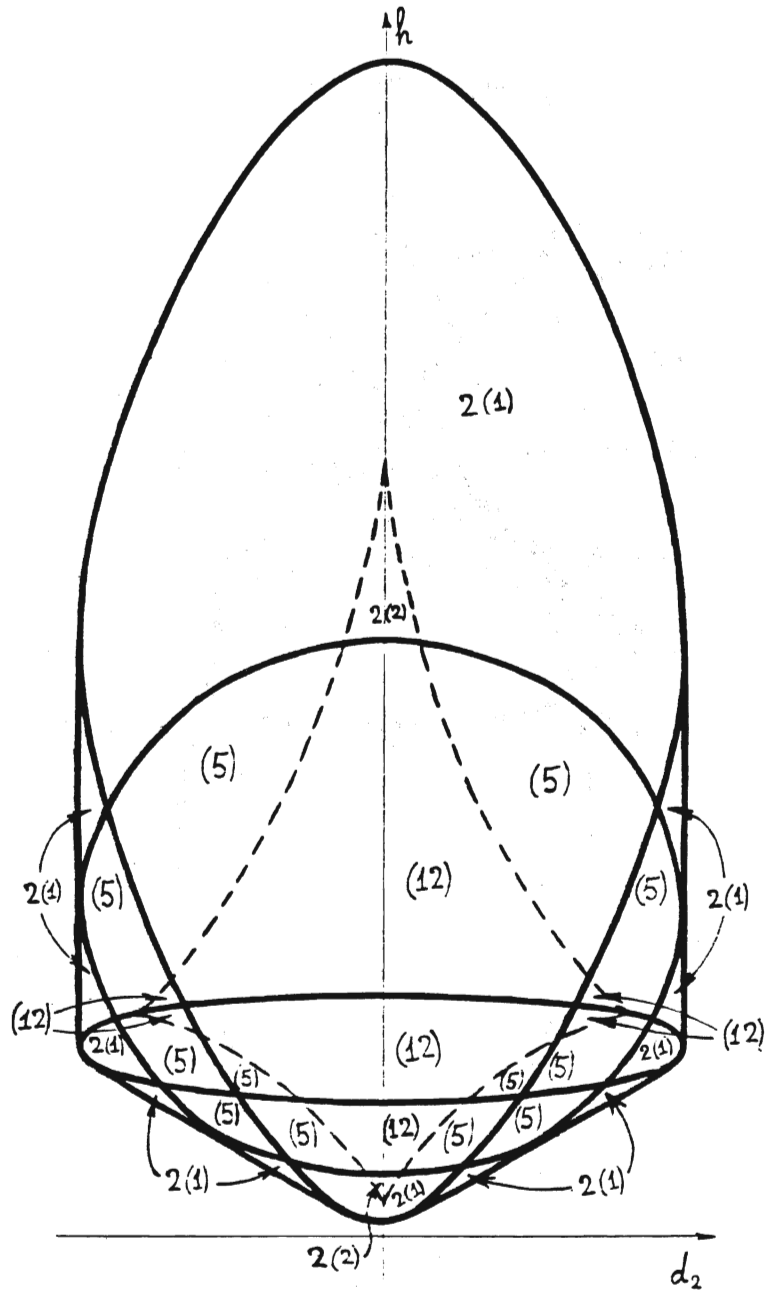

FIGURE 9
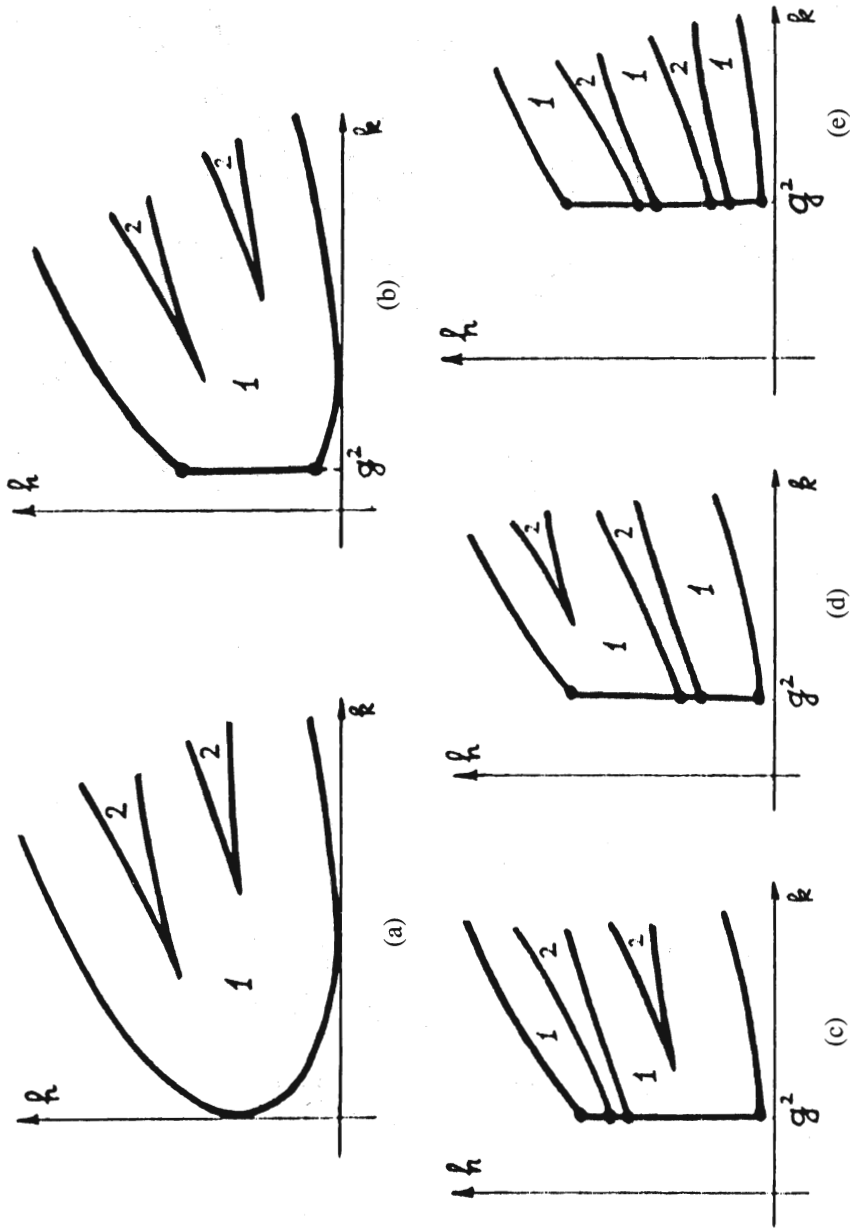
FIGURE 10
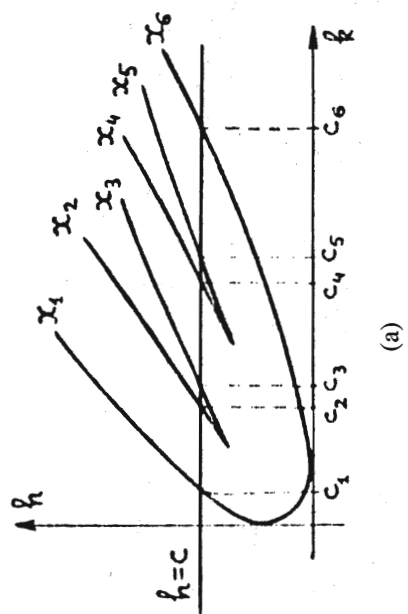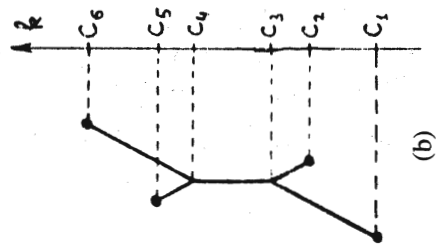
FIGURE 11
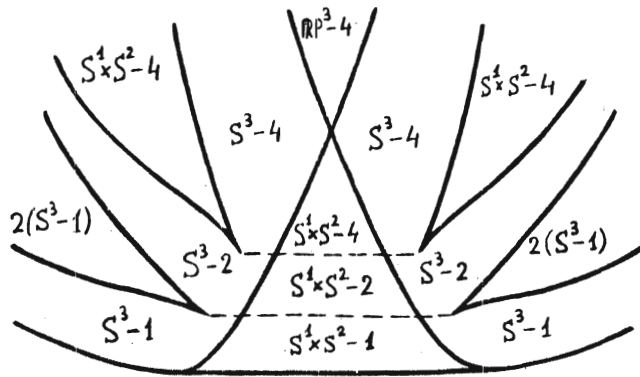
(a)
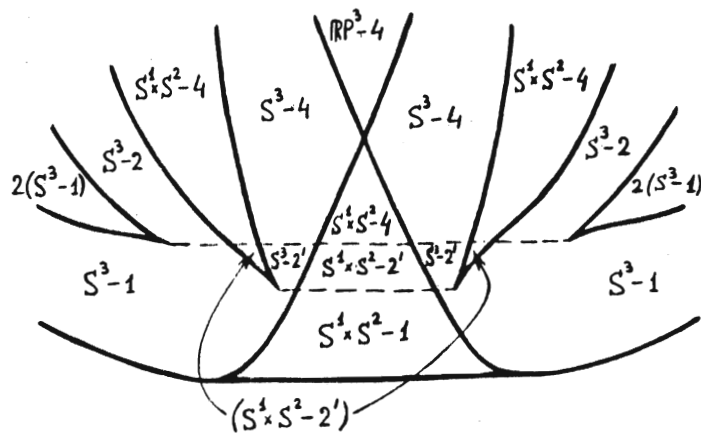
(b)
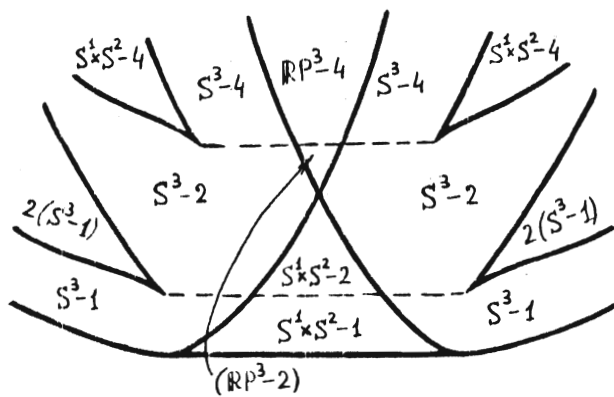
(c)
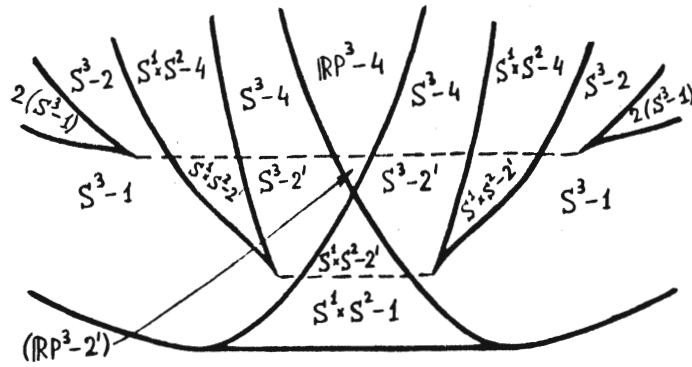
(d)
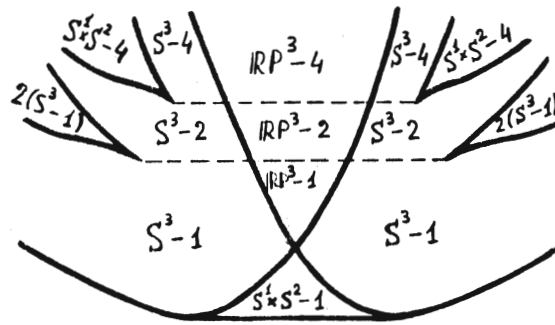
(e)
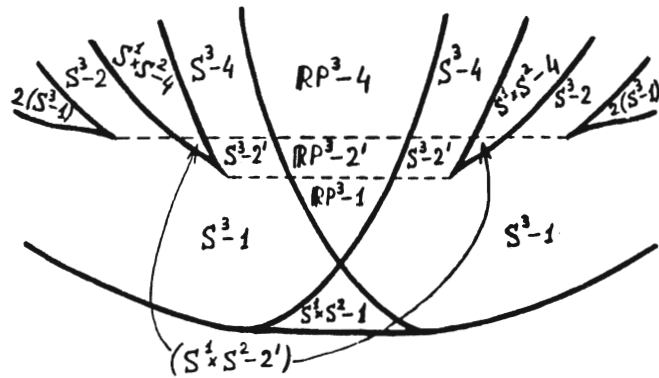
(f)

FIGURE 12
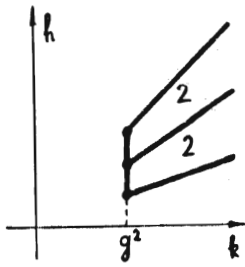
FIGURE 13
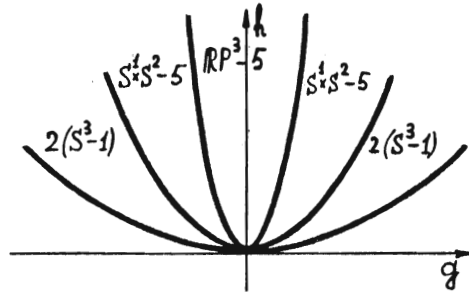
FIGURE 14
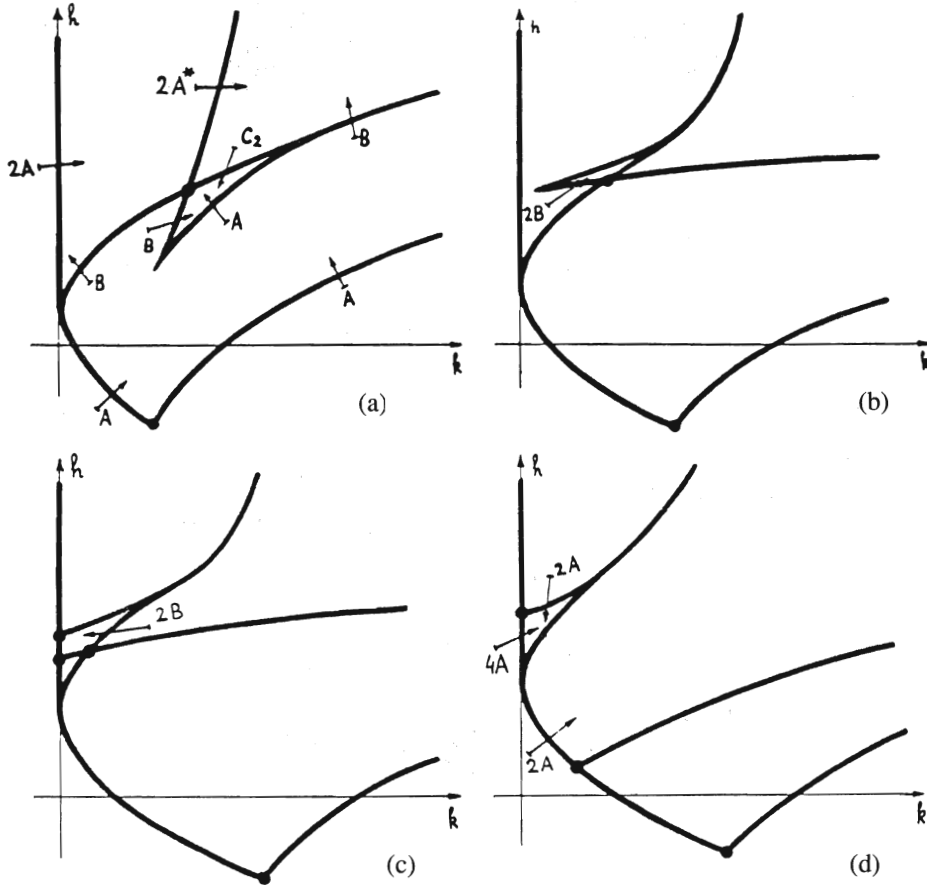
FIGURE 15

FIGURE 16

(a)

(b)

(c)

(d)
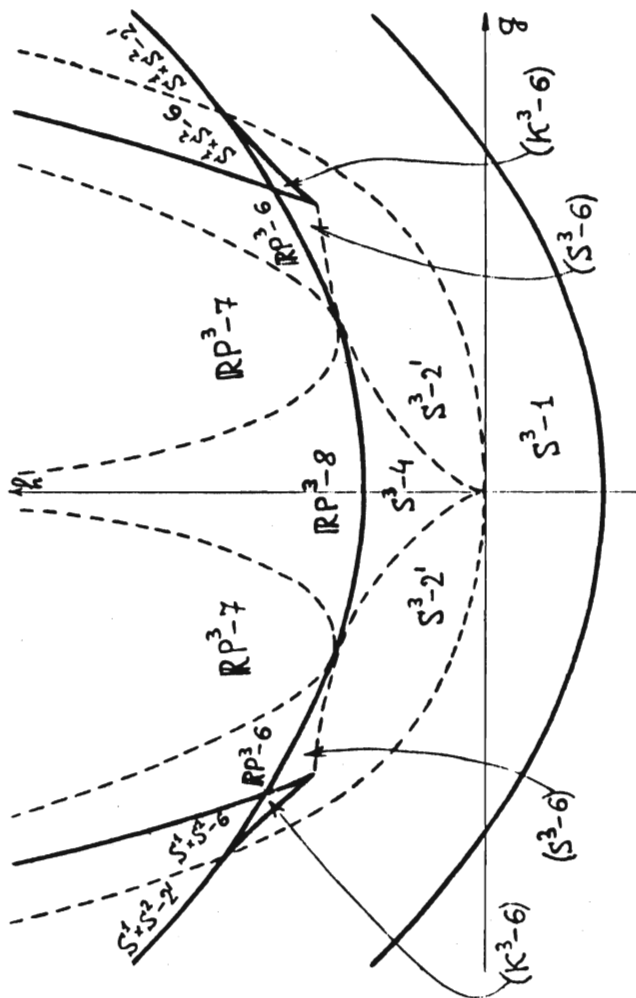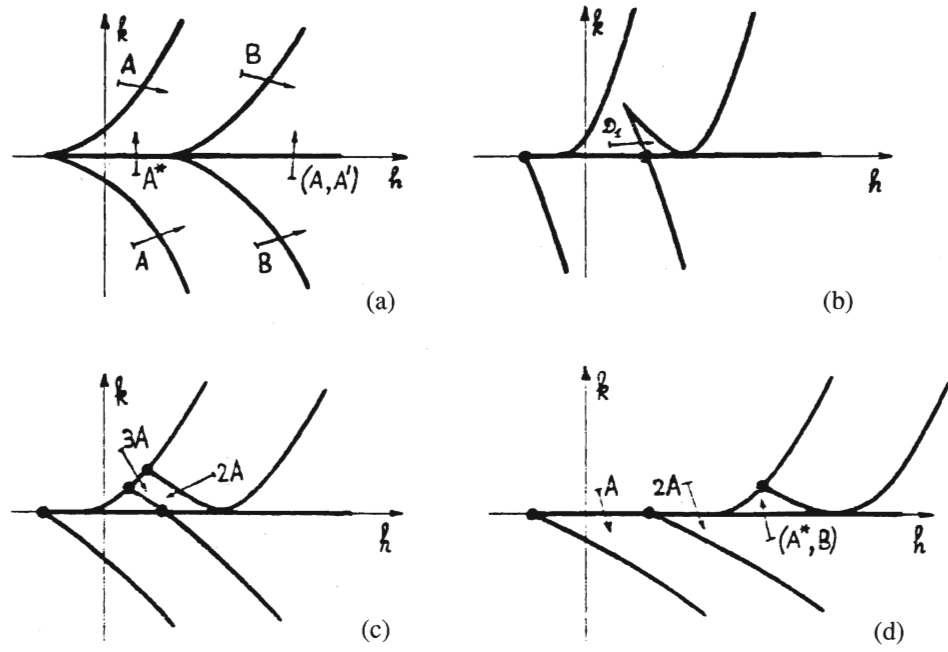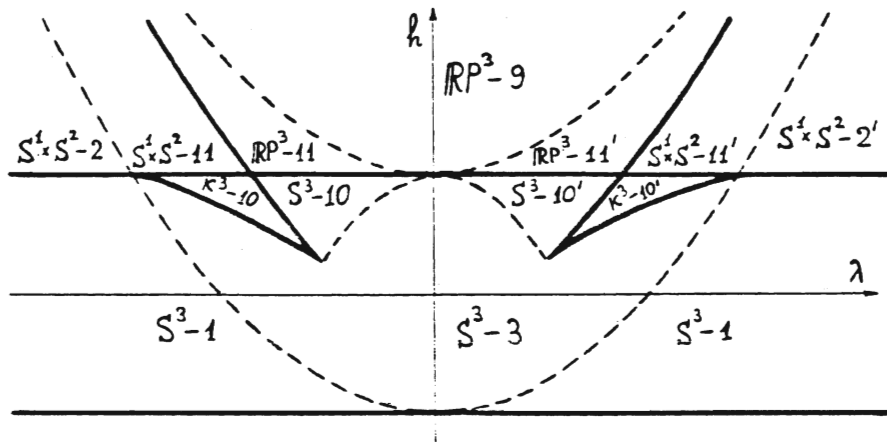
FIGURE 17

FIGURE 18
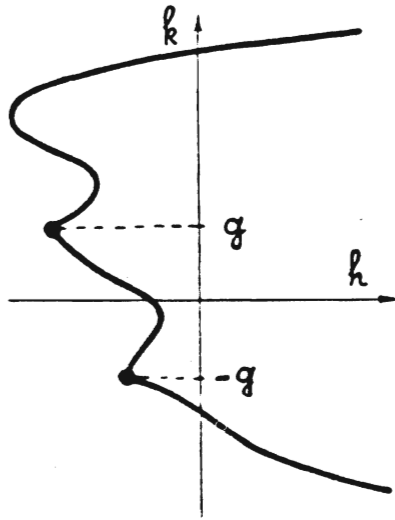
FIGURE 19
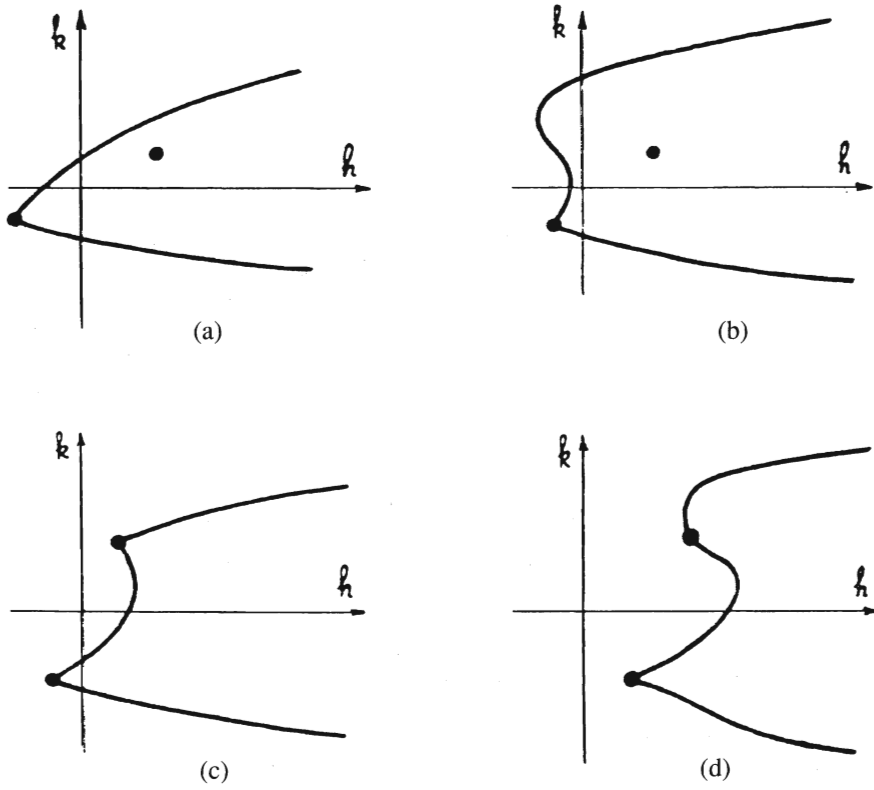
FIGURE 20

FIGURE 21

FIGURE 22

$2(S^3-1)$ $2(S^3-1)$ $\mathbb{R}P^3-5$

$S^1 \times S^2 - 5$ $S^1 \times S^2 - 5$

$2(S^3-2)$ $2(S^3-2)$
$2(S^1 \times S^2-2)$ $2(S^1 \times S^2-2)$
$2(S^1 \times S^2-1)$ $2(S^1 \times S^2-1)$

$S^1 \times S^2 - 12$ $\mathbb{R}P^3-12$ $S^1 \times S^2-12$

N^3-12

N^3-5 N^3-12 N^3-5

$S^1 \times S^2 - 12$

$2(S^1 \times S^2-2)$ $2 (S^1 \times S^2-2)$

$2(S^1 \times S^2-1)$ $2(S^3-2)$ $2 (S^1 \times S^2-1)$

h g

$2(S^3-1)$

(a)

h

$\mathbb{R}P^3-5$

$\mathbb{R}P^3-12$

$S^1 \times S^2-5$ $S^1 \times S^2-5$ g

$S^1 \times S^2-12$

$2(S^3-2)$

$2(S^3-1)$

(b)

FIGURE 23

A. A. OSHEMKOV
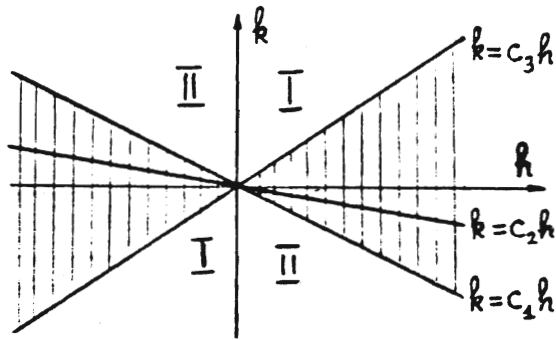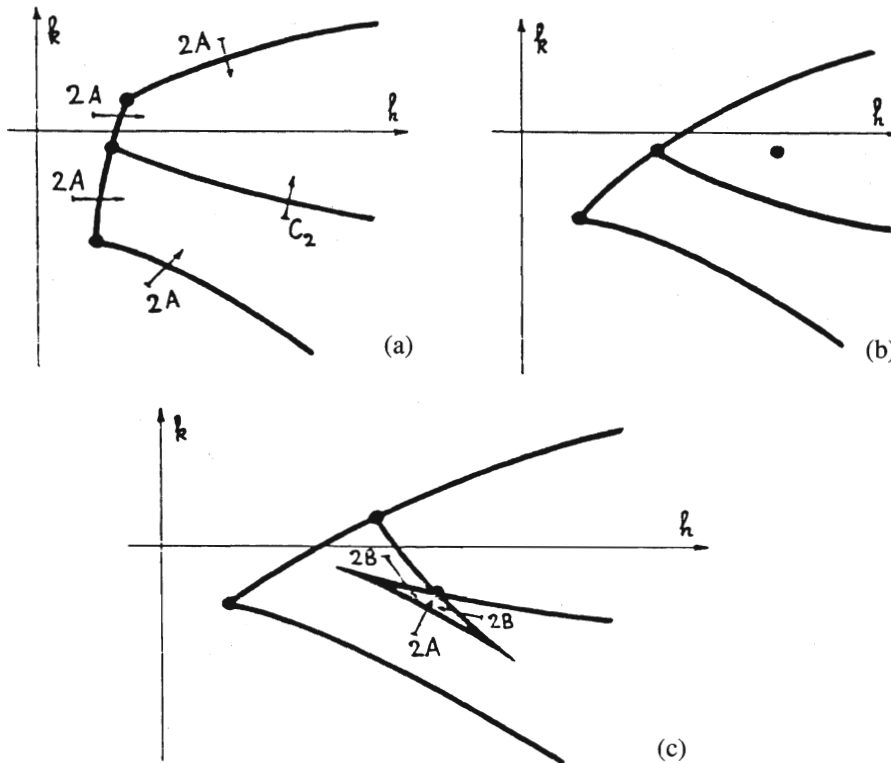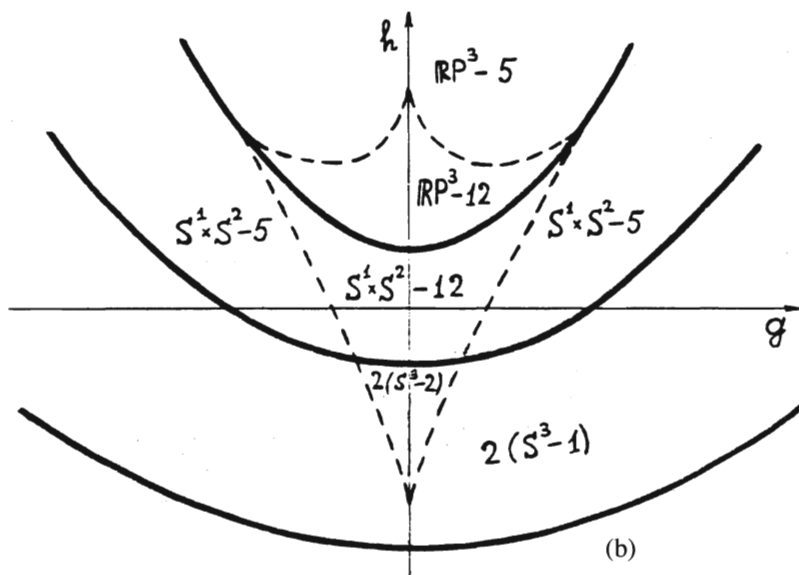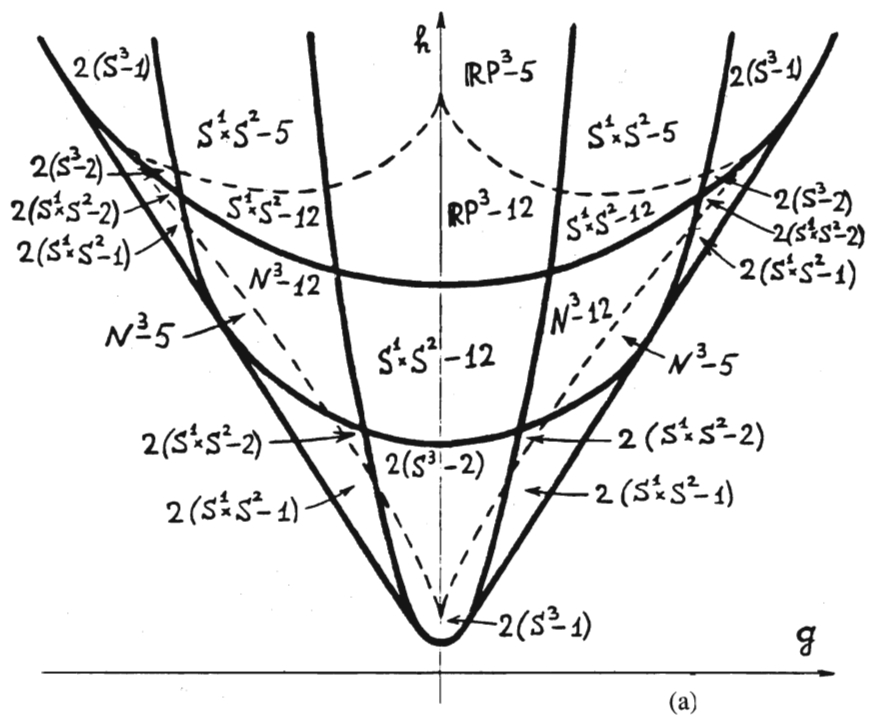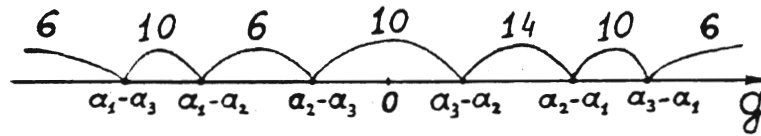
FIGURE 24

FIGURE 25

(a)

(b)
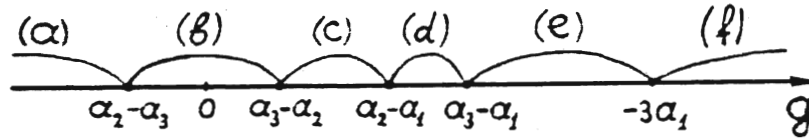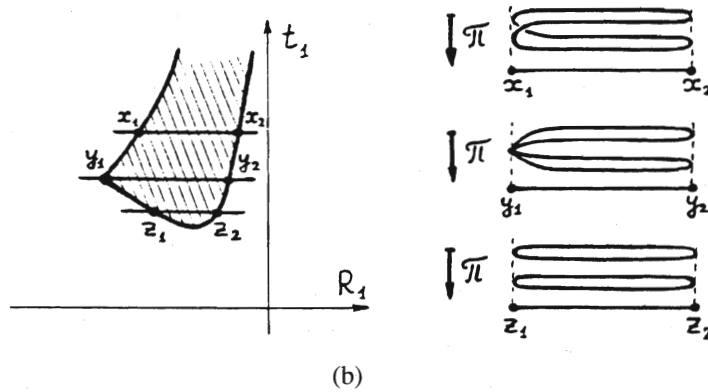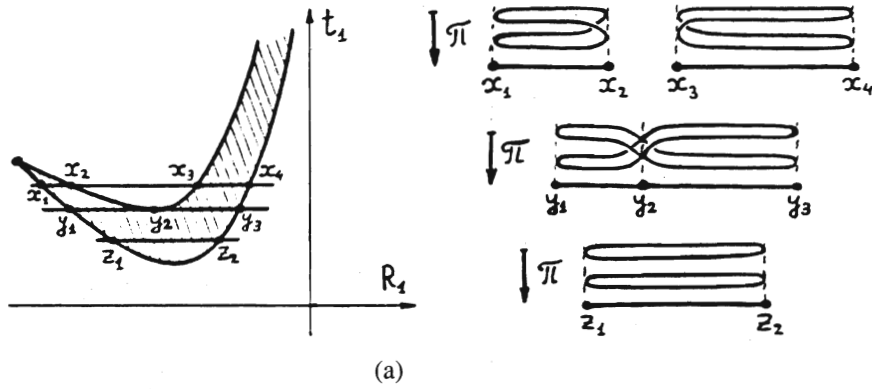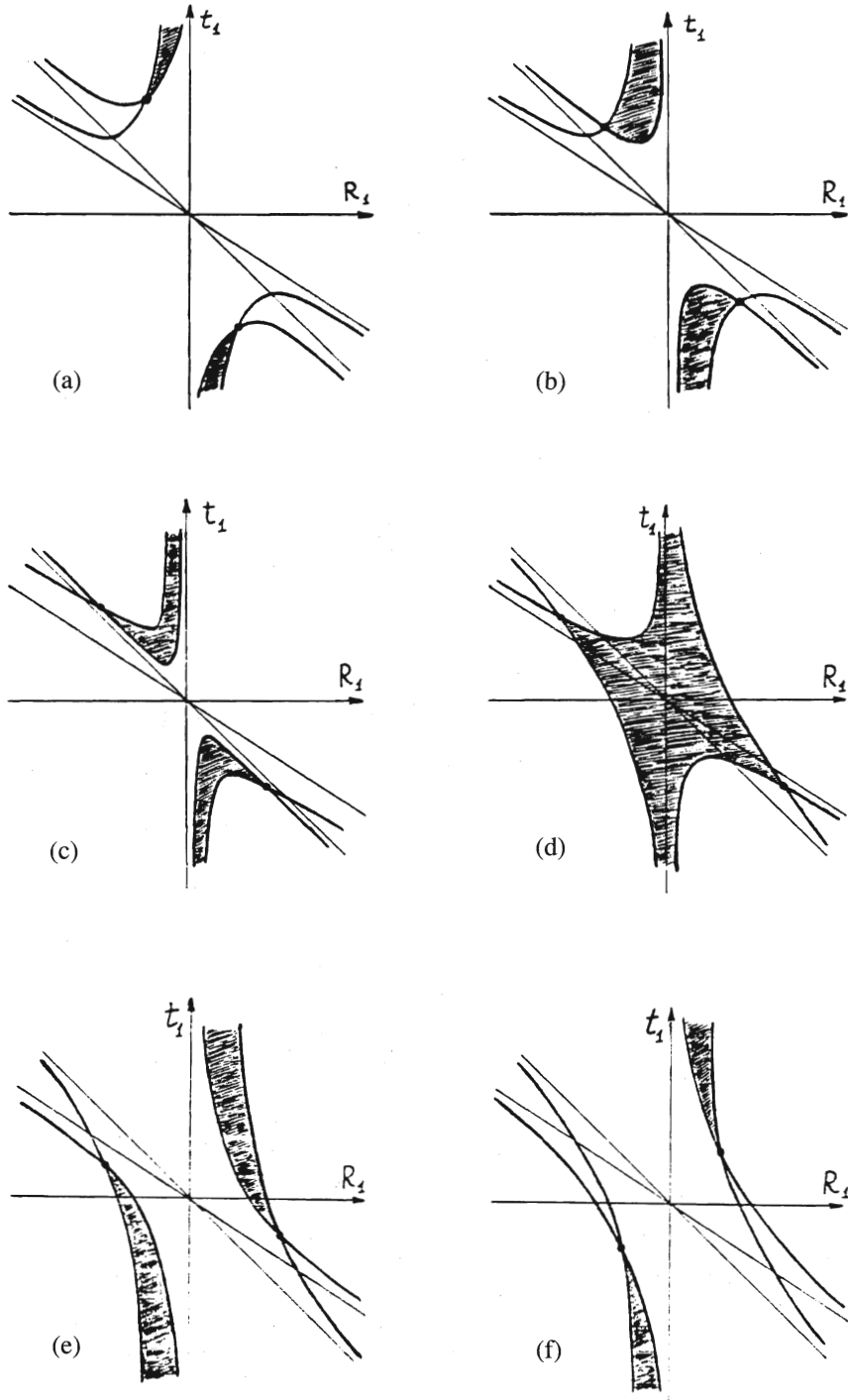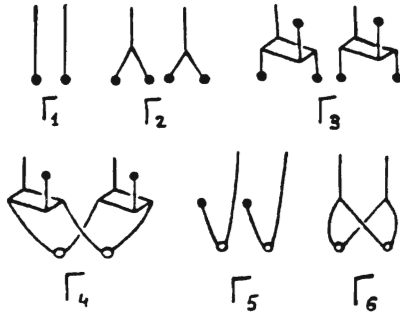
FIGURE 26

FIGURE 27

FIGURE 28
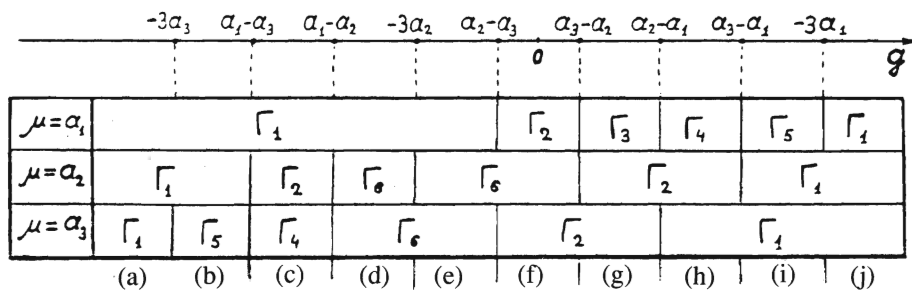
FIGURE 29
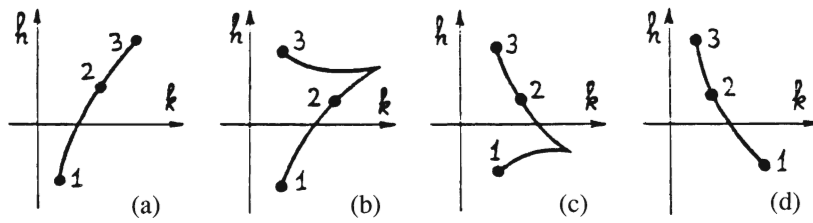
FIGURE 30

FIGURE 31

A. A. OSHEMKOV
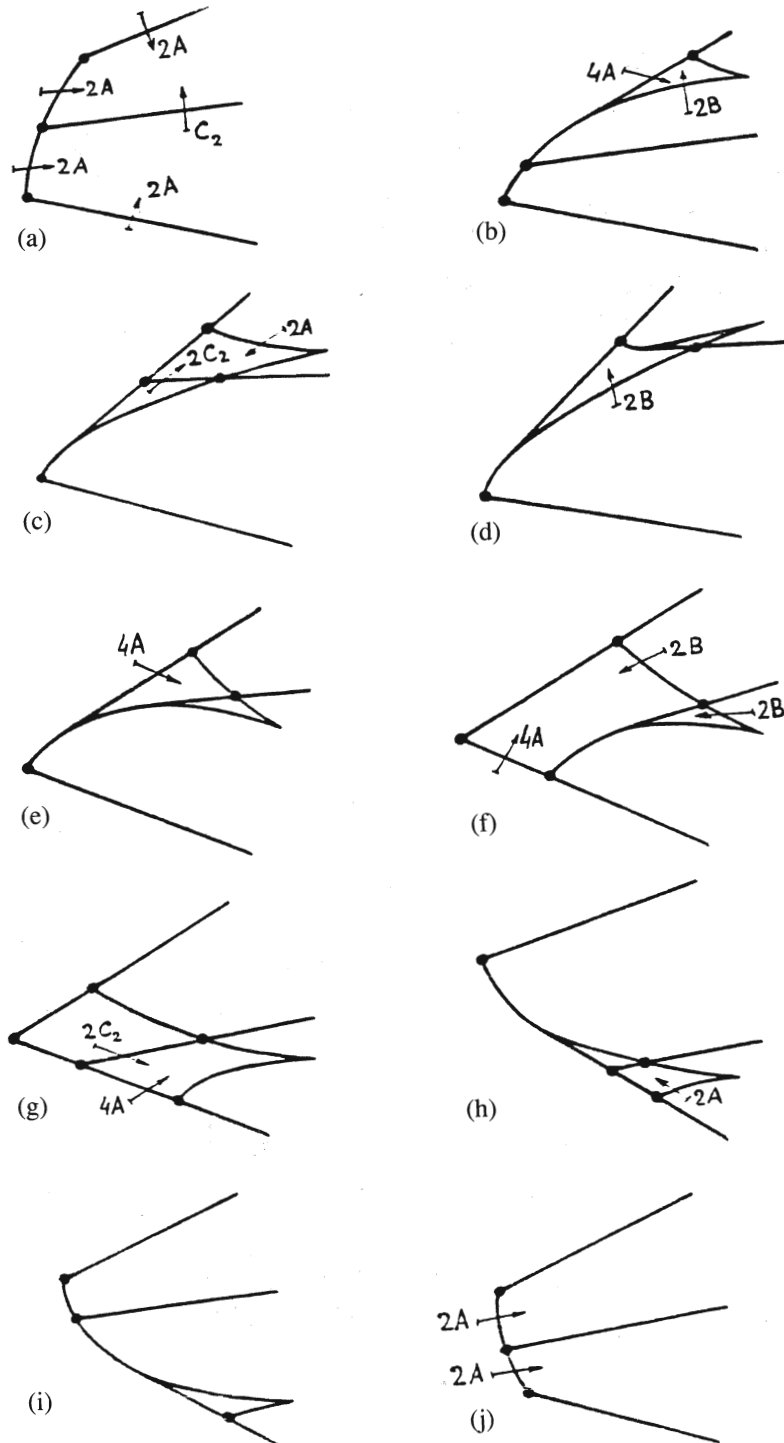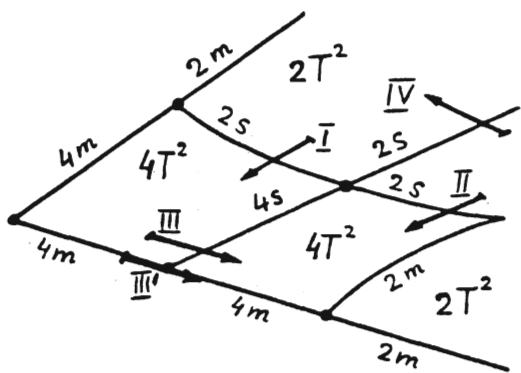
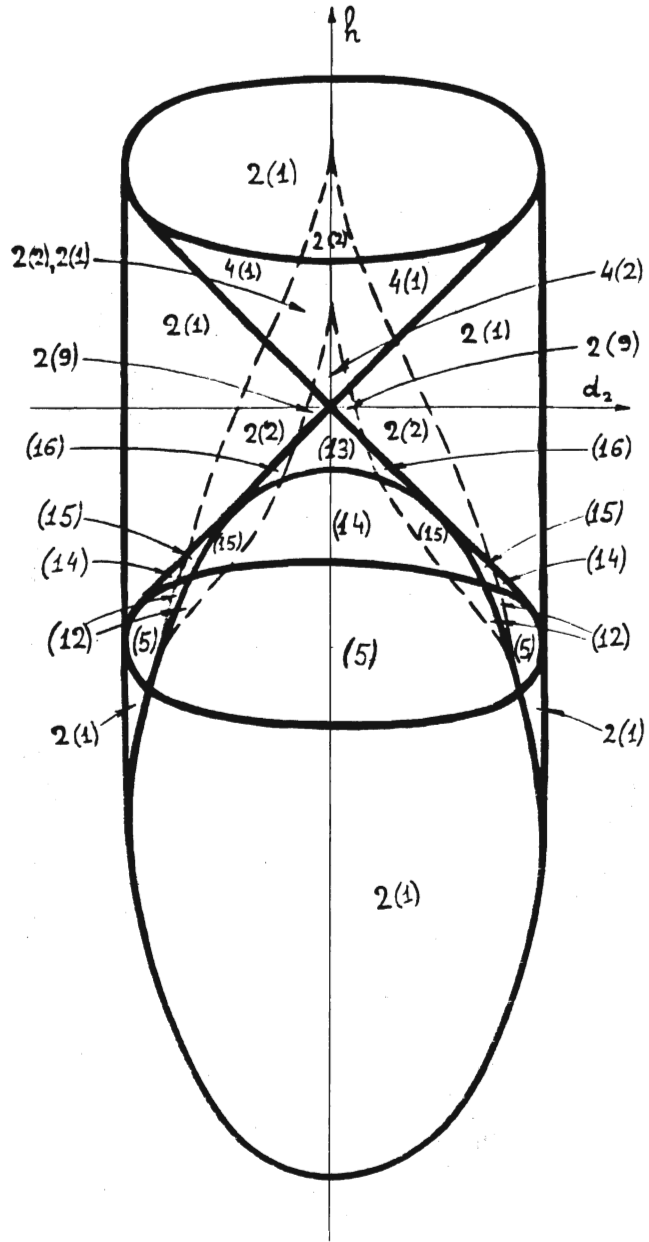FIGURE 32

FIGURE 33

FIGURE 34
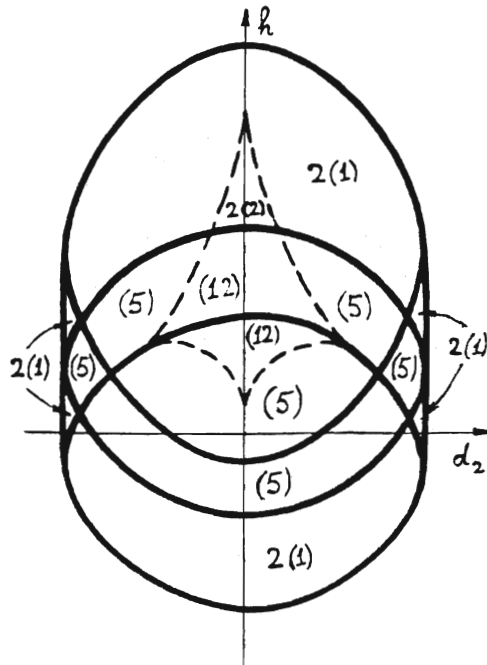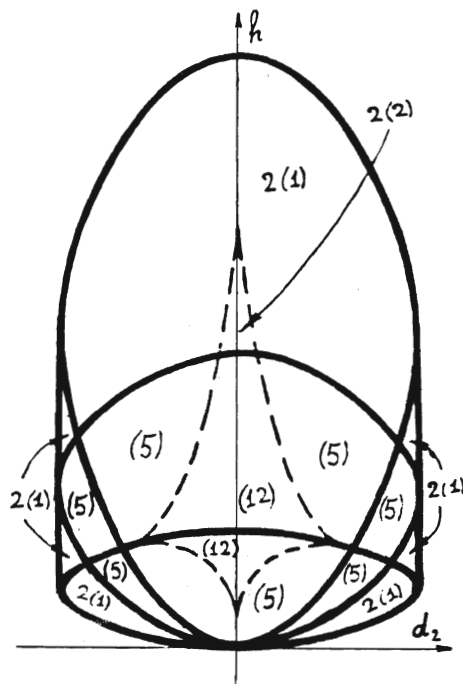
FIGURE 35

FIGURE 36

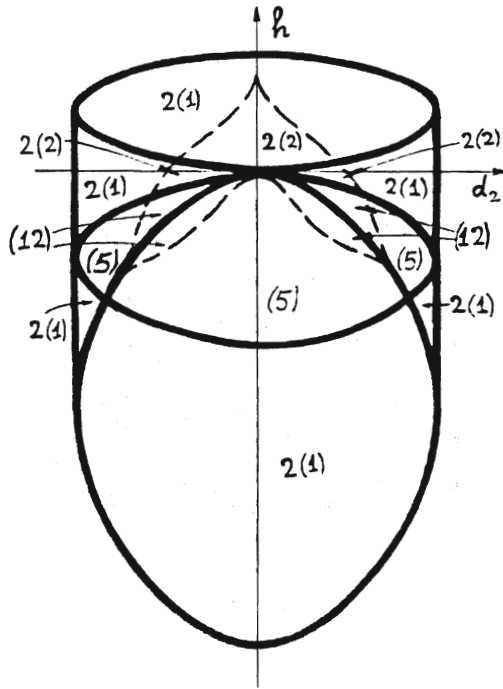FIGURE 37

FIGURE 38
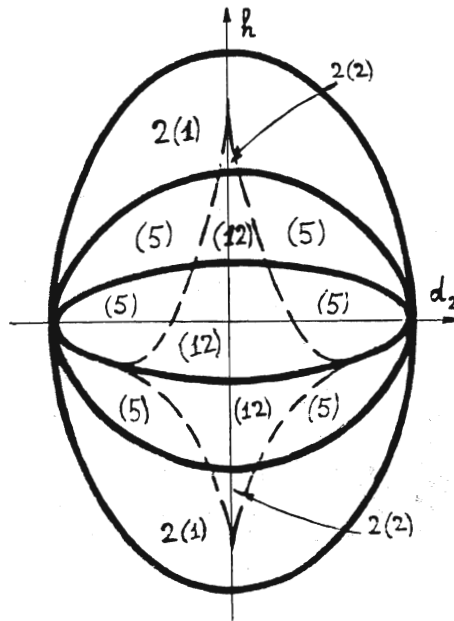
FIGURE 39 (a)

FIGURE 39 (b)

FIGURE 39 (c)

FIGURE 39 (d)

FIGURE 39 (e)

FIGURE 39 (f)